Electronic Thesis and Dissertation Repository

10-23-2023 11:00 AM

Investigation of the growth, motility, and optical properties of microorganisms in active fluids

Zahra Samadi,

Supervisor: Hassan Peerhossaini, *The University of Western Ontario*
Joint Supervisor: Christopher Thomas DeGroot, *The University of Western Ontario*
A thesis submitted in partial fulfillment of the requirements for the Doctor of Philosophy degree in Civil and Environmental Engineering
© Zahra Samadi 2023

Follow this and additional works at: https://ir.lib.uwo.ca/etd

Recommended Citation

Abstract

To have better control over photobioreactors at various operating conditions, it is necessary to characterize microorganisms' motion, optimize light distribution, and investigate efficient mixing methods in photobioreactors.

The second chapter of this thesis aims to develop a theoretical model for the calculation of microorganisms' optical characteristics. Modeling light transfer in photobioreactors needs accurate input data to solve Maxwell's equations. Here, input data include absorption properties of the microorganism's pigment, pigment-content measurement, and the details of the shape and size of the microorganism cells. These input data predicted the optical characteristics of microorganism cells with homogeneous, coated, and heterogeneous geometries.

The third chapter reports on experiments that were carried out to investigate the effect of two mixing methods, turbulent stirring and orbitally shaking, on the growth metrics of *Synechocystis* sp. CPCC 534, and compare them with stationary cultures. The study revealed that stirring *Synechocystis* cultures can enhance the growth rate, doubling per day, yield, and Chl_a production in contrast to cultures without any mixing.

In the fourth chapter, the motility of wild-type *Synechocystis* sp. CPCC 534 was investigated to establish a correlation between the evolution of cell motility and cell growth phases during the complete growth cycle of 78 days. Average cell velocity, mean squared displacement (MSD), diffusion coefficient, and displacement probability density function (PDF) were calculated to assess the dynamics of *Synechocystis* sp. CPCC 534 during the growth period. The obtained results indicate that the age of microorganisms has a notable influence on different aspects of cell motility. Consequently, this can affect the transport characteristics of active suspension.

In the final chapter of this thesis, we aimed to examine the transport characteristics of active fluids and passive fluids in a bifurcated microchannel with a rectangular cross-section. A PDMS microchannel was designed and fabricated to investigate the behavior of two fluids in the bifurcated microchannel. Finally, our investigation revealed that passive fluids exhibit

higher velocity than active fluids. This difference arises due to the minimal movement of active fluids caused by their run-and-tumble motion.

Keywords

Photobioreactors, Optical characteristics, Mixing, Cell motility, Mean squared displacement (MSD), Diffusion coefficient, Active fluid, Passive fluid.

Summary for Lay Audience

An active fluid is a type of fluid that contains tiny living elements such as bacteria, algae, and sperm cells, which can move around. Active fluids have unique behaviors that distinguish them from regular fluids (passive fluids). Unlike regular fluids (passive fluids), which require gradients of pressure, velocity, or temperature to create flow, the motion of active fluids is driven by the microorganisms'cells. Microorganisms cells convert chemical energy from nutrients into mechanical energy to move around. Understanding the motion of microorganisms is crucial due to their significant impact on human life, and the environment, and their widespread applications in various fields, including industry, medicine, food, and energy.

In the second chapter of this thesis, theoretical methods were used to assess the suitability of various sphere geometries (homogenous-sphere, coated-sphere, and heterogenous sphere) in simulating the optical properties of photosynthetic microorganism (*Chlamydomonas reinhardtii*). This was completed using the finite difference time domain (FDTD) method and a precise geometric model. These results showed that more accurate input data were required to correctly determine the optical properties of *Chlamydomonas reinhardtii*, including the absorption properties of pigments, the real part of refractive indices of each cell component, and the shape of the cells.

The third chapter focuses on the experiments, that were conducted on the impact of different mixing modes on the cultivation of the cyanobacterium *Synechocystis* sp. CPCC 534, and compared with simple molecular diffusion (motionless mode). The study showed that applying mixing in the culture can enhance both the growth rate and biomass yield production in comparison to relying solely on molecular diffusion (motionless mode).

In the fourth chapter, experiments were performed on how microbial growth and aging affect microorganism movement. The focus is on studying the motility behavior of *Synechocystis* sp. CPCC 534 and its relationship with aging in a closed microfluidic chip. The findings of the study explained a clear connection between the cell growth phase and cell motility. Specifically, the motility of cells increased steadily during the exponential linear growth phases and declined during the stationary phase until it reached a constant value.

In the final chapter, an experimental investigation was carried out to study the flows of suspension fluids containing live (active fluid) and dead (passive fluid) *Synechocystis* sp. bacteria in a bifurcating microchannel at different flow rates. Analyzing the average flow velocities of active and passive fluids, showed that the passive fluid's average velocity exceeded that of the active fluid at various flow rates. This difference can be attributed to the tiny movement of active fluids caused by their run-and-tumble motion.

Co-Authorship Statement

The present doctoral thesis has been compiled by the guidelines set forth by the School of Graduate and Postdoctoral Studies (SGPS) of the University of Western Ontario, using an integrated article format. Within this format, the thesis incorporates articles that have been co-authored, with each author's specific contribution outlined below.

Chapter 2: Modelling Optical Properties of Algae Using the Finite-Difference Time-Domain Method

Zahra Samadi carried out the numerical simulations, who also analyzed the results, and played a role in writing the paper. Dr. Eric Johlin was involved in the research simulation and analysis. Dr. Christopher DeGroot and Dr. Hassan Peerhossaini oversaw the research and contributed to writing the paper.

Status: Published in FEDSM2021-66314, V003T05A016; 8 pages
https://doi.org/10.1115/FEDSM2021-66314

Chapter 3: Effects of Turbulent Mixing and Orbitally Shaking on Cell Growth and Biomass Production in Active Fluids

The experiments were conducted by Zahra Samadi, under the guidance of Drs. Hassan Peerhossaini, Christopher DeGroot, and Malihe Mehdizadeh Allaf. Zahra Samadi completed the literature review and data analysis with the collaboration of Drs. Hassan Peerhossaini and Malihe Mehdizadeh Allaf. The research design was proposed jointly by Zahra Samadi, Drs. Hassan Peerhossaini, Malihe Mehdizadeh Allaf, Christopher DeGroot, and Reza Saifi (graduate student). Zahra Samadi drafted the initial version of the paper, which was later revised by Dr. Hassan Peerhossaini, Malihe Mehdizadeh Allaf, Christopher DeGroot, and Reza Saifi.

Status: Published in American Journal of Biomedical Science & Research 2022 15, 396-404. https://doi.org/10.34297/AJBSR.2022.15.002129

Chapter 4: Investigation of *Synechocystis* sp. CPCC 534 Motility During Different Stages of The Growth Period in Active Fluids

Zahra Samadi accomplished the experiments under the leadership of Drs. Hassan Peerhossaini, Christopher DeGroot, and Malihe Mehdizadeh Allaf. Zahra Samadi completed the literature review and collaborated with Drs. Hassan Peerhossaini, Christopher DeGroot, Malihe Mehdizadeh Allaf, and Thomas Vourc'h on data analysis by MATLAB. Zahra Samadi prepared the first draft of the manuscript and then reviewed and revised it by Drs. Hassan Peerhossaini, Christopher DeGroot, Malihe Mehdizadeh Allaf, and Thomas Vourc'h

Status: Published in Processes 2023, 11(5), 1492; https://doi.org/10.3390/pr11051492

Chapter 5: The Investigation of Active Fluids' Behavior in the Y-Shaped Microchannel

The experiments were performed collaboratively by Drs. Hassan Peerhossaini, Christopher DeGroot, Malihe Mehdizadeh Allaf, Mohammad Z. Hossain, and Reza Saifi (graduate student). Zahra Samadi completed the literature review and completed data analysis with Drs. Hassan Peerhossaini, Mohammad Z. Hossain, and Reza Saifi. The first draft was prepared by Zahra Samadi and was edited by Drs. Hassan Peerhossaini, Christopher DeGroot, Malihe Mehdizadeh Allaf, Mohammad Z. Hossain, and Reza Saifi.

Status: Accepted at ASME Conference, 2023

Acknowledgments

I would like to extend my sincere gratitude to my Ph.D. supervisors, Prof. Hassan Peerhossaini and Prof. Christopher DeGroot, for their unwavering support and guidance throughout my doctoral studies. They imparted invaluable knowledge about performing experiments, numerical analysis, and research skills, making me a better researcher. It was a pleasure working with them. I would also like to express my appreciation to my advisory committee members, Prof. Lars Rehmann, Prof. Eric Johlin, and Prof. Mohammad Reza Najafi, for their guidance and contribution toward the success of my work.

I greatly appreciate Dr. Malihe Mehdizadeh Allaf for her unwavering support and guidance. It was truly an enriching experience to work with her during my doctoral research.

I would also like to express my gratitude towards my family for their steady support and valuable advice throughout my journey. I am also deeply grateful for the support I received from my mother, brothers, and sisters.

I would also like to thank my laboratory colleagues, Dr. Mohammad Z. Hossain, and Reza Saifi, for their invaluable input and constructive feedback during discussions about my work. Their recommendations have significantly improved the quality of my research, which I enjoyed. The vast fluid dynamic insight of Dr. Hossain was a great help in interpreting some results of the last chapter of this thesis.

Table of Contents

List of Tables

List of Figures

List of Abbreviation

FDTD	Finite-Difference Time-Domain
PBR	Photo Bioreactor
PML	Perfectly matched layer
Chl_a	Chlorophyll a
Chl_b	Chlorophyll b
PPC	Photo protective carotenoid
PC	Phycocyanin
TS	Turbulent Stirring
MD	Molecular Diffusion
OS	Orbitally Shaking
OD	Optical Density
D	Day
D	Diffusion coefficient
EPS	Exopolysaccharide
PDF	Probability density function
MSD	Mean squared displacement
PDMS	Polydimethylsiloxane
Q	Flow rate
dft	Discrete Fourier transform

List of Nomenclature

H	Magnetic fields
E	Electric fields
D	Displacement field
ε	Dielectric constant
J	Current density of electric charge
J_B	Magnetic-charge current density
B	Magnetic flux density
μ	Magnetic permeability
σ_B	Frequency-independent magnetic
σ_D	Electric conductivities
S_s	Poynting vector
μ_0	Permeability of the free space
m_λ	Complex refractive index
n_λ	Real part of complex refractive index
k_λ	Imaginary part of complex refractive index
λ	Wavelength
C_i	Concentration of pigment i
ω_i	Mass fraction
ρ_{dm}	Density of dry mass

$Ea_{i,\lambda}(\lambda)$	Specific spectral absorption coefficients,
x_ω	Water volume fractions of the cell.
N_0	Number of microorganism cells
N_t	Microorganism cells number at the end of the time period,
Δt	Duration of the time period $(t_t - t_0)$.
R	Specific growth rate
K	Doubling per day
$C_{biomass}$	Biomass concentration
V_p	Average cell velocity
n_p	Number of motile *Synechocystis* cells present
δ	Time elapsed between two successive values of t
Δ	Time interval

Chapter 1

1   Introduction

1.1 Overview

Active fluids contain self-propelled microstructural elements suspended in a viscous fluid. These microelements are typically biological microorganisms such as bacteria, algae, or sperm cells. The recent interest in these active systems has been motivated by a variety of factors. The microorganisms embedded in the active fluid can develop complex spontaneous fluid motions and exhibit remarkable physical manifestations over a wide range of scales, from microscopic diffusion and motility to large-scale colonization. Understanding these complex collective dynamics and spontaneous organization might yield a better understanding of fundamental processes in biophysics, from the transport and spreading of bacterial colonies, to the biomechanics of individual cells or subcellular units. Therefore, it is essential to investigate active fluids due to their effects on human lives, on the environment and their vast applications in industrial, medical, food, domestic energy supply and carbon sequestration [1]. This knowledge can also facilitate the engineering of active suspensions suitable for a wide range of technological applications, from fluid mixing and pumping to the directed transport of materials on the microscale, for instance, in lab-on-a-chip devices or for drug delivery [2].

There are a wide range of microorganisms available to constitute an active fluid. Here we focus our attention on photosynthetic microorganisms such as photosynthetic cyanobacteria and green algae, due to their major role in the earth's ecosystem in producing around half of the atmospheric oxygen through photosynthesis. Microalgae and photosynthetic bacteria are utilized in a wide range of industries. Due to the efficient conversion rate of CO_2 to organic compounds, microalgae and cyanobacteria play a significant role in carbon capture and storage [3]. In addition, their biomass is used as a potential feedstock for biofuel production [4]. In the wastewater treatment industry, photosynthetic microorganisms can be used to remove pollutants from water by using CO_2 and consequently mitigating the environmental impacts [3]. Furthermore, they are great

resources to produce high-value materials in industries like bioplastics, pharmaceuticals, nutritional supplements, cosmetics, animal feed and human food supplements [4].

1.2 Photosynthetic Microorganisms

Photosynthetic microorganisms have become a focal point of interest for their potential in generating high-value products and bioenergy in a sustainable manner. These organisms are characterized by their rapid growth rate, high biomass productivity, and reliance on sunlight as their primary energy source [5].

Microalgae are a type of phytoplankton that can be grown photosynthetically in various environmental conditions such as freshwater, marine ecosystems, deserts, and even in Antarctica [6]. The size of microalgae can vary greatly, ranging from picoplankton with dimensions of 0.2 to 2 μm to filamentous forms that can be 100 μm or larger [7]. They are described as the atmospheric oxygen producer by photosynthesis process, which converts water and carbon dioxide into oxygen using solar energy [8].

Another oxygenic photosynthetic microorganism is cyanobacteria, which is one of the species studied in this research. Cyanobacteria are characterized as a diverse group of Gram-negative prokaryotes with a wide range of morphological structures (including unicellular, colonial, and filamentous forms) and developmental characteristics. Cyanobacteria's capacity to harness sunlight as an energy source and CO_2 as a carbon source, along with their accelerated growth rates when compared to plants, has rendered them an ideal selection for numerous biotechnological purposes. Cyanobacteria can be found in a wide range of environmental temperatures from cold Antarctica to hot springs. However, the suitable cultivation temperature is between 20 °C and 35 °C, while this temperature can be expanded to 45 °C. Cyanobacteria are compatible with diverse salinity ranges and can be found in both marine and freshwater ecosystems [9].

In the next section, we present a brief overview of the two model microorganisms: one green microalgal and the other cyanobacteria, that are used in this research.

1.2.1 *Chlamydomonas reinhardtii*

Chlamydomonas reinhardtii is a green alga that is unicellular and has a diameter of 10 micrometers. It swims by means of two flagella. It can be found in soil or fresh water. Because of its easy cultivation and ability to manipulate its genetics, *Chlamydomonas reinhardtii* has been used in most studies on the behavior of microorganisms. This kind of green algae can grow in phototrophic, heterotrophic or mixotrophic regimes [10].

Chlamydomonas reinhardtii is a microalga that has a cell wall and several intracellular structures, including the cytoplasm, chloroplast, nucleus, and mitochondria. Furthermore, the microalga produces metabolites like lipid and starch bodies that could potentially form new compartments within the cell during nitrogen starvation [11]. *Chlamydomonas reinhardtii* has a rudimentary visual system known as the eyespot apparatus, which enables it to detect the light direction and intensity of light. The eyespot apparatus in *Chlamydomonas reinhardtii* consists of two layers of highly organized carotenoid-rich lipid globuli that are located at the chloroplast's edge [12, 13].

1.2.2 *Synechocystis* sp.

The other microorganism that is studied in this research is *Synechocystis* sp. It is a unicellular, spherical, non-nitrogen-fixing, freshwater cyanobacteria with approximately 2-3 μm in diameter [14]. In *Synechocystis* sp.'s cell, the thylakoid membranes are predominantly arranged in three or more concentric layers around the periphery of the cell, with the central cytoplasmic region mostly. Photosynthesis takes place within the thylakoid membranes [15]. The cytoplasm contains several detectable components such as ribosomes, carboxysomes, lipid bodies, polyphosphate bodies, and cyanophycin granules [16].

Cyanobacteria is a phylum of bacteria that obtains its metabolic energy through photosynthesis. *Synechocystis* sp. can have both phototrophic growth, by oxygenic photosynthesis during light periods, and heterotrophic growth [17, 18]. *Synechocystis* sp. is an ideal model organism for exploring various areas such as photosynthesis, lipid metabolism, stress responses, molecular biology, genetic systems, pili system, biofilm

formation, etc., owing to its brief generation periods, ease of genetic manipulation, and the limited size of its genome and proteome [16].

1.3 Cultivation Process:

The photosynthetic microorganisms that we studied in this research were cultivated in photobioreactors (PBRs) under artificial light (indoor) or sunlight (outdoor) [19]. To achieve maximum microalgal productivity in a cost-effective way, it is essential to carefully choose a mode of microalgae cultivation. Three major modes of microalgae cultivation are available, which include phototrophic, heterotrophic and and mixotrophic modes (i.e., phototrophic, and heterotrophic simultaneously) [20]. Environmental conditions, such as energy and carbon sources, determine which metabolism is dominant for the cultivation of photosynthetic microorganisms [21]. Metabolism is schematically shown in Figure 1-1.
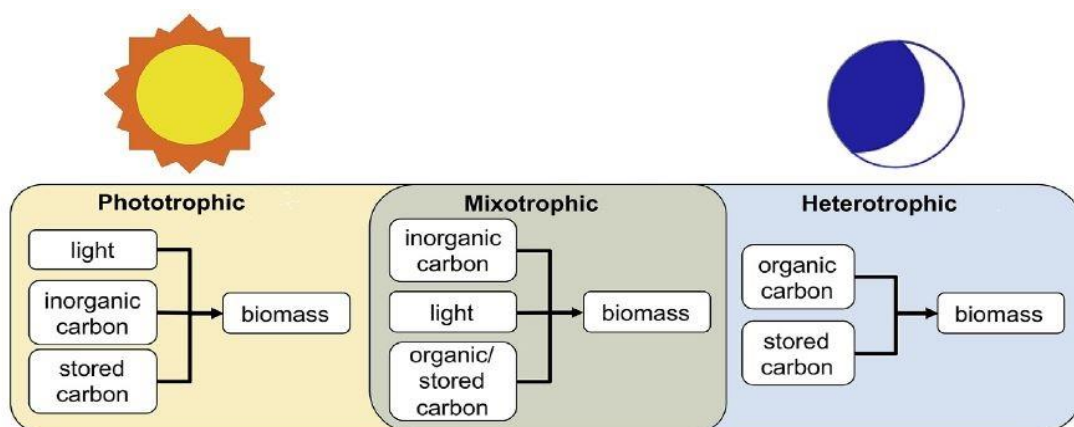
Figure 1-1: Energy and carbon sources that are used by microorganisms in each of the three metabolisms [21]

In phototrophic cultivation mode, microorganisms utilize light energy and CO_2 to grow and build organic molecules from carbon dioxide via photosynthesis [22]. Phototrophic cultivation of microorganisms to produce biofuel and other value-added products is a feasible practice for CO_2 capture, and thus potentially contributes to global CO_2 reduction. Due to limitations of light distribution to the cells in phototrophic growth mode, there are two disadvantages associated with this kind of metabolism: low cell densities and long

growth periods. Some microorganisms are heterotrophic, utilizing organic sources for cultivation; therefore, they do not need light as an energy source. Heterotrophic growth does not require any light source for cultivation and then higher cell densities can be achieved. However, the preparation of organic carbon necessary for this cultivation mode constrains the industrial production of heterotrophic microorganisms because of the high economic and environmental cost [23].

In mixotrophic cultivation, microorganisms simultaneously consume inorganic and organic carbon sources in the presence of light therefore, phototrophic, and heterotrophic growth occur simultaneously. CO_2 is fixed through photosynthesis, which is influenced by illumination, while organic compounds are assimilated through aerobic respiration, which is affected by the availability of organic carbon [20]. Under mixotrophic cultivation, photosynthetic microorganisms have the characteristics of both phototrophic and heterotrophic growth with higher growth rates and biomass yield. In addition, mixotrophic growth requires lower energy in comparison with heterotrophic growth [21].

1.4 Optical Properties of Microorganisms

The important factors for photosynthetic microorganisms' growth are light, CO_2, mixing, temperature, and pH [24]. However, among those parameters, the optical properties of photosynthetic microorganisms and the consequent interaction mechanisms with light are of special importance in the photosynthetic process. It is difficult to create homogenous light distribution in PBRs due to the absorption and scattering of light by the microorganism's cells [19]. Under low light intensity, cell respiration consumes the high-carbon compounds at a higher rate than what is produced in photosynthesis and no new biomass is accumulated. On the other hand, under high light intensity, the photoinhibition process occurs in the photosystem and consequently results in damaging or death of the cell [3]. Therefore, in the design and optimization of PBRs for high efficiency and productivity, it is vital to provide relatively uniform illumination in the microorganism culture [19].

To control biomass culture in PBRs and maximize their efficiency in the production of high-value products, experimental studies have been carried out to investigate the optical

properties of photosynthetic microorganisms. Experimental methods have been devised and adapted to different shapes of photosynthetic microorganisms, their structure, and their heterogeneous nature [25]. Berberoglu et al [26] experimentally measured the optical properties of two hydrogen-producing microorganisms: filamentous cyanobacteria *Anabaena variabilis* ATCC 29413-U and the unicellular purple bacteria *Rhodobacter sphaeroides* ATCC 49419. By using a spectrophotometer without and with an integrating sphere, they measured the extinction and absorption coefficients in the spectral range from 300 to 1300 nm respectively. A nephelometer was designed and constructed to measure the scattering phase function of the microorganisms at 632.8 nm.

However, the experimental setup and preparation of initial materials can be costly, and the experimental procedure is time consuming. Moreover, measurements are valid only for specific growth conditions and are not applicable to other growth conditions [25].

Theoretical methods for predicting the radiation characteristics of photosynthetic microorganisms are relatively straightforward and accurate and could be applied to simulate microorganisms' growth under various operating conditions. Theoretical predictions of the radiation properties of microorganisms are based on solving Maxwell's equations of electromagnetic wave theory depending on the cell's shapes, size distribution and complex refractive index [27]. To solve Maxwell's equations for the prediction of optical properties of microorganisms, the most common methods include Lorenz–Mie, T-Matrix, and finite difference time domain (FDTD) [28]. Most theoretical methods estimate the radiation characteristics of microorganisms as volume-equivalent spheres and are based on Lorenz–Mie theory [25]. Lorenz–Mie theory is applicable to homogeneous and spherical particles, homogeneous concentric spheres, or coated spheres [28]. Lee et al [29] calculated the complex refractive index of biofuel producing photosynthetic microalgae between 400 and 750 nm by experimental measurements of average absorption cross-sections (the absorbed power divided by the incident intensity) and scattering cross-sections (the scattered power divided by the incident intensity). The unicellular green algae *Chlamydomonas reinhardti*i strain CC125 and its truncated chlorophyll antenna transformants tla1, tlaX, and tla1-CW+ as well as *Botryococcus braunii*, *Chlorella sp.*, and *Chlorococcum littorale* were studied. Lorentz–Mie theory, as the forward method and

genetic algorithm, were used to calculate the complex refractive index of microorganisms. Such radiative properties can be applied in various areas like biofuel production and photobiological carbon dioxide mitigation.

The T-matrix is also a solution to Maxwell's equations, which can be applied to the models with a more detailed description of the cell [3]. Unlike Mie theory, it can be used for a variety of geometries including spheroids, cylinders, etc. but in practice, at least one axial symmetry is required to achieve efficient computation. In addition, particles with a much larger size than the light wavelength or highly aspherical leading to accumulating more rounding error that prevents convergence. The method uses an infinite expansion of vector spherical wave functions that are evaluated numerically and then truncated when converged to enough accuracy. The resulting matrix is a complete solution to Maxwell's equations over the entire scatterer geometry [30].

The FDTD method can compute the optical properties of microorganisms with multiple heterogeneous organelles and provides greater geometric flexibility than Mie theory and T-matrix solutions. It can be applied to a single sphere, coated sphere, or cell models containing numerous organelles and intricate dielectric structures. FDTD solution is a time-domain method, which can be applied in a wide frequency range with a single simulation run and treat nonlinear material properties in a natural way. Drezek et al [31] predicted the light scattering properties of biological cells over a range of wavelengths by the finite-difference time-domain method. By using the two-dimensional FDTD mode, they found that the selection of geometry and dimension have significant effects on scattering properties.

1.5 The Effect of Mixing on the Cell Growth

Mixing is the main feature in creating a homogenized environment for microorganisms' growth and improving cellular contact with chemical nutrients. In high-cell-density microorganisms' cultures, the transmission of light will be decreased, and the culture temperature will be increased. Therefore, mixing is an important factor to consider in the design of photobioreactors. The mixing of the culture systems enhances the efficiency of biomass productivity by 1) preventing microorganism sedimentation; 2) increasing the

availability of light, carbon source-CO_2 and nutrients for the microorganism cells; 3) improving the heat transfer and gas exchange between the culture medium and the air phase [32, 33]. However, excessive mixing beyond a certain amount of mixing rate inhibits the efficiency and growth of microorganism cells, and shear forces may damage microorganisms' cells and alter their functions. In addition, it can cause dead zones in media and consequently decrease the mass transfer in the growth environment [34]. In laboratory or industrial photobioreactors, mixing can be accomplished by various methods including mechanical agitation, bubbling, aeration, and pumping or a combination of these modes [33]. Turbulent stirring (TS) and orbitally shaking (OS) are the major mixing modes which are used widely in chemical and biochemical industries. On a laboratory scale, turbulent stirring (TS) and orbitally shaking (OS) can be achieved by using a magnetic bar spinning under the effect of an external rotating magnetic field and the orbital displacement of a vessel, respectively [35].

Light distribution, fluid dynamics, and microorganism metabolism are the most critical factors for the cultivation of microorganisms. These three factors influence each other and the turbulent mixing process in photobioreactors plays an important role in the connection of the three factors [36]. Mehdizadeh Allaf et al. [37] carried out experiments to evaluate the turbulent mixing on the response of biological, rheological, and physical properties of an active fluid (suspensions of the cyanobacterium *Synechocystis* sp. CPCC 534). Experiments were conducted at three various mixing rates in the experimental flask, and the results revealed that the growth, biomass, total chlorophyll, and carotenoid production of *Synechocystis sp.* under different stirring conditions were enhanced significantly, and the yield was approximately doubled.

Hu et al. [38] conducted a study using fundamental rheological analysis to establish a feasible technical justification for selecting the agitation speed in suspensions containing *Porphyridium cruentum*, a red micro-alga. The results of the study indicated that biomass growth and the formation of high-value chemicals in photobioreactors were influenced by the agitation speed in PBRs. They investigated five agitation speeds for *P. cruentum* cultivation: 0, 150, 300, 450 and 600 rpm during 16 days. An agitation speed of 150 rpm was found to be optimal for cultivating *P. cruentum*, resulting in a 19-57%

increase in biomass concentration compared to microalgae grown under different agitation speeds.

The orbital shaking mode provides low shear stress in a microbiological environment and prevents cell damage in active fluid suspension. It can be utilized in a wide range of applications including drug production, animal cell cultivation and bacterial biofilm [39]. Monteil et al [40] experimentally investigated the cultivation of mammalian cells in suspension at different scales of operation in a shaking bioreactor. High gas transfer, high level of homogeneity in media, and low specific power consumption were revealed in this study. The optimal operating growth condition was observed at shaking frequencies of 180–220 rpm and working volumes of 300–500 mL. In a study by Ojo et al [41], microalgae cultivation was investigated in the orbitally shaken photobioreactor. Their results showed that orbital shaking provides rapid mixing and a relatively constant light intensity and improves effective gas mass transfer inside the media.

1.6 Hydrodynamics of Microorganisms

Motility is defined as a tool to respond the environmental changes by some kind of self-propulsion [42]. The investigation among 40 bacterial species from 18 different genera indicates that microorganisms have six various modes of motility: swimming, swarming, gliding, twitching, sliding and darting. Except for swimming, all other kinds are associated with the presence of a solid surface. Swimming at or near a surface is actuated through one or more flagella [43]. Friction drag is the main physical reason which does not allow microorganisms to swim like a fish [44].

Swimming is the most familiar form of bacterial motility; bacteria have developed flagella (originally from secretory systems), whose movements in viscous surroundings drive the cells forward and swim at very low Reynolds numbers [45]. Swarming is the multicellular movement of bacteria on a surface by flagella. Under the proper conditions, some microorganisms experience a phenotypic change, and their movement is described by spatial and temporal correlations that consist of billions of individuals [46, 47]. Twitching motility of bacteria on the solid surface is actuated by the extension and retraction of pili [43]. These pili are the main virulence aspect of *Pseudomonas aeruginosa*, and their

twitching motion allows the opportunistic infection of wounds [48]. Gliding is a surface-related motion that does not require flagella or pili, but utilizes macromolecular structures, identified as focal adhesion complexes, that attach the cellular surface to external molecules or surfaces [36]. Spreading/sliding is a form of passive translocation [43]. Darting is a form of passive mobility, which happens when the bacteria are supposed to make clusters of cells on a surface and then grow [49].

Gliding and twitching motility are commonly detected and observed among cyanobacteria. In this study, it is concentrated mainly on the hydrodynamic properties of *Synechocystis*. The model cyanobacterium *Synechocystis* displays twitching motility by type IV pili (TFP), in response to favorable environmental stimuli such as light/nutrition or getting away from unfavorable conditions. Molecular attitudes maintain the function of the pili in motility, metal acquisition, biofilm formation, cell adhesion, and natural transformation (NT) in *Synechocystis* [50]. Type IV pili consist of intricate multi-protein structures composed of pilin subunits that are 15-20 kDa. These pili are remarkably slender, with a diameter of 6-9 nm, and can exceed a length of 1 micron. Additionally, they can aggregate together to form bundles (figure 1-2) [51, 52].
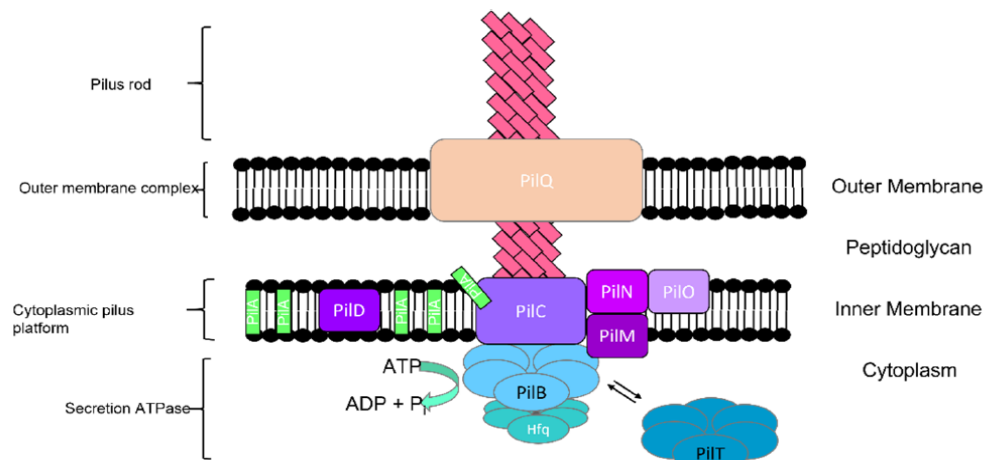
Figure 1-2:Type IV pilus and four distinctive subcomplexes in cyanobacteria [16, 51].

The physics of swimming at the micrometer scale is different from the macroscopic scale, a low 'Reynolds number' governs the microorganism motion, where inertia has a little role and viscous force is dominant [44]. Low-Reynolds number hydrodynamics is at the center

of the ability of flagella which creates propulsion at the microscale [53]. Bacterial motion in a uniform chemical environment is a random-walk pattern, with mobile "run" periods broken by immobile "tumble" periods [1, 54].

Bacterial motility is a key part of the pathogenesis of bacteria and has been widely investigated [55, 56]. Bacterial motility demonstrates how bacteria respond to different environmental conditions or interact with various environmental factors, which leads to enhance local colonization and survival [57]. For example, some motile microorganisms move towards or away from a stimulus of light (known as phototaxis). Most motile bacteria, such as *Escherichia coli*, move toward nutrient-rich locations or get away from unfavorable ones (known as chemotaxis process) [58, 59].

Whether the non-uniform lighting in the PBR has any effect on the bacterial motility, Vourc'h et al. [1] focused on the effect of the light perturbation on the diffusion coefficient of bacterial suspensions by tracking bacterial response to light stimuli under isotropic and non-isotropic conditions. They investigated the influence of illumination on the intermittent motility and found that the probability to be in the run state increases just after a rise in light intensity; this feature disappears after about 1 hour, and the initial probability of motility was recovered. With higher light intensity, bacteria have a greater propensity to be in a run mode during which they perform longer displacements and therefore increase their diffusion coefficient. Under directional light flux, the authors observed that *Synehcocystis* cells had phototactic motility and moved toward the light source (phototaxis). This phototaxis phenomenon enables the controlling of microorganisms by light intensity and light direction.

Desai and Ardakani [60] investigated the interaction between hydrodynamics and chemotaxis and its impact on the colonization of nutrient sources by microorganisms. An individual-based model was used and performed probabilistic simulations to determine the effects of essential environmental and motility properties on the spatial distribution of microorganisms over a spherical nutrient resource. Generally, four distinct regimes were revealed based on the distribution of the microorganisms: 1) solid superficial colonization, 2) rotary-diffusion-made "off-surface" accumulation, 3) a reduction zone in the spatial

distribution, and 4) no considerable accumulation. More specifically, they represented that the amount of surface colonization first enhanced, then levelled off, and ultimately declined as the nutrient availability increased. Finally, they also demonstrated that surface colonization decreased monotonically when the mean run duration of the chemotactic microorganisms improved.

Chau et al [61] studied the phototactic response of *Synechocystis* sp. PCC6803 to the complex light source. They measured the single-cell motility properties in different wavelengths and light intensities. Their results showed that red and green light impacted motility bias, whereas blue light prevented motility. Active fluid revealed the phototactic response along the vector sum of the light directions to the light signals from different directions simultaneously; it indicated microorganism cells have the ability to recognize and bring together multiple signals into a combined motility response.

Vourc'h et al [14] studied the surface diffusion of *Synechocystis* sp. PCC 6803 during the initial phases of cell contact with a glass surface in the active fluid. Their results indicated a twitching motility with alternating low-motility "tumble" and high-motility "run" periods, leading to a normal diffusion explained by a continuous time random walk with a diffusion coefficient D and remarkably, D decreased by passing time. Polysaccharide production by cyanobacterial cells is the main reason for this observation.

Motility has a vital role in the life cycle of bacteria and is critical for biofilm formation, and biofilm dispersion [62]. In addition, bacterial motility has been inferred mostly as an adaptive characteristic that permits bacteria to achieve nutrient and optimal growth conditions in a heterogeneous environment [63]. The structure of a biofilm can be influenced by various factors such as nutrient gradient, cell differentiation, quorum sensing, bacterial motion, and their interplay with the surrounding environment [43]. Once the bacteria meet a solid surface, microcolonies may begin to form [64]. After the biofilm has developed and matured, certain cells secrete chemical molecules that facilitate their dispersion into the surrounding environment [65].

For *Synechocystis*, it has been observed that biofilm initiation is primarily dependent on the cell motility, then it is influenced by the physicochemical and electrostatic interactions

between the surface and the microorganism's envelope, and microorganism cells together [16]. Concentrating on the dynamics at the cellular level, the interplay between nucleation-division and diffusion-aggregation processes plays a critical role in the emergence of microcolonies. For instance, the role of motility is significant as it can promote bacterial aggregation by facilitating cell-to-cell contact, while it can inhibit localized aggregates by increasing dispersion [43, 66, 69]. The study by Vourc'h et al. [68] investigated the growth of *Synechocystis* microcolonies on surfaces with varying degrees of hardness. The findings revealed that soft surfaces facilitate greater amounts of motile bacteria p_m compared to hard surfaces, and the number of cell clusters decreased over time as a function of p_m. Therefore, it was proposed that motility lets the bacteria evade clustering, whereas non-motile bacteria become trapped. This study emphasizes that it is necessary to account for subpopulations of changed dynamics among a particular strain for a sufficient explanation of the microcolonies' formation.

1.7 Flow Behavior of Active Fluids in a Bifurcating Microchannel

The behaviors of active fluids have been extensively investigated in different situations such as surface diffusion during initial periods of bacterial colonization near glass surfaces [14], microorganism motility in the presence of external periodic static fields [69], the motion of a Brownian circle swimmer in circular confinement with Petri dish- and ring-like geometries [70] etc. Of special importance is the study of active fluids' hydrodynamics in microfluidic devices that are related to observing microorganism movement in confined geometries. Transport properties of active particles via thin channels have a great potential for the development of microfluidic tools that can monitor and sort motile cells [71].

The swimming properties of biological microorganisms are mostly dependent on the traits of the micro-swimmer, their shape and flow field. Bacterial motion is influenced by fluid flow, for example, motile bacteria become confined near flat surfaces in a straight microfluidic channel [72]; in shallow microfluidic channels, bacterial accumulation occurs behind obstacles and after constrictions [73] or downstream of corners in curved channels, leading to the formation of biofilm [74, 75].

The confinement and walls essentially modify the swimming properties of microorganisms [76]. Binz et al [77] studied the motility of *Serratia marcescens*, a rod-shaped bacterium, in micro-channel systems. They found that bacteria were able to move through narrow microchannels and bacteria's hydrodynamic behaviors such as their swimming paths, velocity and modes were affected by the channel width and its complexity. These results demonstrated that the microfluidic environment as a simple tool can be utilized to detect and measure the navigation and movement properties of bacteria via geometrically heterogeneous environments.

Recently, microfabrication and microfluidics have been found to be especially useful in the study of the behavior of active fluids. Microfabrication can be utilized to generate complex conditions at the micrometer-scale and so allow the analysis of behavior of microorganism cells and handle fluids flowing in miniature channels. The small size of the microchannels and precise control over the dimensions and flow provide the prospects for scientists to make simple and relatively low-cost devices for the production of active fluids from organic and inorganic materials in a variety of shapes and sizes. In addition, microfluidics provide better manipulation to create accurate and stable gradients of stimuli such as light, chemical nutrients, pH, and temperature which in sequence lets more accurate analyses into microorganism taxis. Also, microfluidics facilitates easier studies of more than one stimulus such as temperature and chemical gradients simultaneously [78].

Microfluidic devices have been extensively used in different applications such as in micrometer-sized channels for medical diagnostics, cell separation, drug screening, detection and sorting, and single-cell genomics and in the study of the motility of microorganisms [79]. Before, microfluid devices were fabricated by glass and silicon, nevertheless, the opacity of silicon and fragility and high cost of both glass and silicon make their usage limited. Since the 1990s, polydimethylsiloxane (PDMS) has been utilized commonly and offers some advantages such as its suitability for studies of living cells, optical transparency, biocompatibility, gas permeability, flexibility, non-toxic, oxygen permeable, inexpensive, and chemically inertness [80, 77].

Tokárováa et al. [79] conducted a study on the motility of five bacterial species with various dimensions and morphologies, namely *Vibrio natriegens*, *Magnetococcus marinus*, *Pseudomonas putida*, *Vibrio fischeri*, and *Escherichia coli*, in microfluidic environments made of polydimethylsiloxane (PDMS) with several levels of confinement and complexity. The study was performed in the absence of external flow and concentration gradients. The results indicated that when the confinement was normal, such as in quasi-open spaces with only one limiting wall and in wide channels, the motility properties of the complex flagellated bacteria followed the hydrodynamics-based predictions for simple monotrichous bacteria. Particularly, *V. natriegens* and *V. fischeri* moved parallel to the wall, while *P. putida* and *E. coli* moved parallel to the wall with occasional wall escape events. On the other hand, *M. marinus* frequently flipped between wall accumulator and wall escaper regimes. In tighter confining environments, motility was dominated by steric interactions between bacteria and the surrounding walls. In mesoscale regions where the effects of hydrodynamics and steric interactions overlain, these mechanisms could either drive bacteria in the same path, resulting in smooth bacterial motion in linear channels, or be opposite, generating chaotic motion and bacterial trapping in mesoscale-sized meandered channels. The report offers a framework for designing microfluidic tools for single-cell genomic screening.

1.8 Literature Gap

The literature gap in this thesis can be summarized as follows:

- Many numerical methods focused on optical geometries associated with spherical or cylindrical shapes. No specific numerical method exists for precisely calculating the optical characteristics of heterogeneous geometries of microorganism cells.
- The scarcity of prior research or studies dedicated to evaluating laboratory-scale (turbulent stirring and orbitally shaking) mixing techniques for microorganism cultivation highlights the need for this investigation to determine the most efficient method.

- The limited availability of similar long-term studies of microorganism motility throughout an entire growth cycle for different microorganism species and cultures emphasis the more novel contribution to the literature and covers the entire growth cycle, going far beyond the exponential and stationary growth phases. More research on the long-term dynamics of microorganism motility and its correlation with growth phases could enhance our understanding of bioprocess behavior.

- The need for more comprehensive investigations of the interplay between fluid dynamics and microorganisms' motility in the y-type microchannel, especially concerning different microorganism types and microchannel geometries. Research that delves deeper into how the motility of microorganisms influences fluid dynamics within confined spaces could have broader applications in biotechnology.

1.9 Thesis Objectives

To have better control over photobioreactors at various operating conditions, it is necessary to optimize light distribution in photobioreactors, choose the suitable mixing mode for the growth of microorganisms, and characterize microorganisms' trajectory and movement. The overall goal of this work is to investigate the behavior of active fluids in photobioreactors under various situations and enhance the living conditions for their optimal growth. To attain this overall goal, the following objectives are defined:

i. To develop a generic numerical method for computation of light-scattering properties of photosynthetic microorganisms within the visible spectrum to analyze the light transfer in photobioreactors.

ii. To investigate the efficiency of various mixing techniques such as turbulent stirring (TS) and orbitally shaking (OS) mixings versus a molecular diffusion (MD, no mixing) mode on the growth of cyanobacterium *Synechocystis* sp. CPCC 534.

iii. To study the possible correlation between the cell's age and their motility. Since biofilm formation has been shown to be dependent on the cell motility, the question rises as weather old cells are more susceptible to initiate biofilm on solid surfaces.

iv. In the flow of active fluids two driving forces act simultaneously: the pressure gradient and the cell motility. The first one is deterministic as it follows the general Navier-Stokes equations while, the cell motility is stochastic. Given the predominance of pressure gradient in this combination it is crucial to carry out experiments in very low Reynolds number regimes to better capture the effects of cell motiliy on flow regime. For this purpose we conduct experiments in microfluidic devices.

1.10 Thesis Organization

The thesis is organized into four articles that discuss the optical properties of microorganisms, mixing modes, motility of self-propelled particles and the behavior of active fluid in a bifurcating microchannel.

- *Chapter 2:* The FDTD method has been applied to calculate the optical properties of microorganisms with heterogeneous cells. By the numerical method, optical characteristics were predicted with homogeneous, heterogenous, and coated spheres under mixing growth conditions. Modelling was performed for *Chlamydomonas reinhardtii* CPCC 243 within the visible spectrum to analyze the light transfer in photobioreactors.

- *Chapter 3:* This study examined the effects of two mixing techniques (turbulent stirring and orbitally shaking) on the growth characteristics of *Synechocystis* sp. CPCC 534 and compared them to stationary cultures. The findings demonstrated that mixing *Synechocystis* cultures can enhance growth rate, doubling per day, yield, and Chl_a production compared to cultures without mixing.

- *Chapter 4:* The study employed *Synechocystis* sp. CPCC 534 as a model organism to investigate the effects of cell age on motility over long periods (up to 78 days), extending beyond the exponential and stationary growth phases. To achieve this objective, the study computed cell transport parameters, including cell velocity, mean squared displacement (MSD), time-dependent diffusion coefficient D(t), and displacement probability density function (PDF).

- *Chapter 5:* In this chapter, the behavior of the cyanobacterium *Synechocystis* sp. was studied CPCC 534 in a bifurcated microchannel with a rectangular cross-section to measure the motility and velocity profile.

- *Chapter 6:* The present study's summary and primary contribution are presented, alongside suggestions for future research.

1.11   References

[1]   Vourc'h, T., Léopoldès, J., & Peerhossaini, H. (2020). Light control of the diffusion coefficient of active fluids. Journal of Fluids Engineering, 142(3).

[2]   Saintillan, D. (2018). Rheology of active fluids. Annual Review of Fluid Mechanics, 50, 563-592.

[3]   Lehmuskero, A., Chauton, M. S., & Boström, T. (2018). Light and photosynthetic microalgae: A review of cellular-and molecular-scale optical processes. Progress in oceanography, 168, 43-56.

[4]   Wang, S. K., Stiles, A. R., Guo, C., & Liu, C. Z. (2014). Microalgae cultivation in photobioreactors: An overview of light characteristics. Engineering in Life Sciences, 14(6), 550-559.

[5]   Touloupakis, E. (2023). Photosynthetic Microorganisms: Cultivation and Application. Symmetry, 15(3), 742.

[6]   Bule, M. H., Ahmed, I., Maqbool, F., Bilal, M., & Iqbal, H. M. (2018). Microalgae as a source of high-value bioactive compounds. Front. Biosci, 10(2), 197-216.

[7]   Balasubramani, R., Gupta, S. K., Cho, W., Kim, J., Lee, S., Jeong, K., ... & Choi, H. (2016). Microalgae potential and multiple roles-current progress and future prospects-an overview. Sustainability, 8(12).

[8]   Tan, J. S., Lee, S. Y., Chew, K. W., Lam, M. K., Lim, J. W., Ho, S. H., & Show, P. L. (2020). A review on microalgae cultivation and harvesting, and their biomass extraction processing using ionic liquids. Bioengineered, 11(1), 116-129.

[9]   Waterbury, J. B. (2006). The cyanobacteria—isolation, purification and identification. The prokaryotes, 4, 1053-1073.

[10]   Merchant, S. S., Prochnik, S. E., Vallon, O., Harris, E. H., Karpowicz, S. J., Witman, G. B., ... & Grossman, A. R. (2007). The *Chlamydomonas* genome reveals the evolution of key animal and plant functions. Science, 318(5848), 245-250.

[11]   Bhowmik, A., & Pilon, L. (2016). Can spherical eukaryotic microalgae cells be treated as optically homogeneous?. JOSA A, 33(8), 1495-1503.

[12]   Wagner, V., Ullmann, K., Mollwo, A., Kaminski, M., Mittag, M., & Kreimer, G. (2008). The phosphoproteome of a *Chlamydomonas reinhardtii* eyespot fraction includes key proteins of the light signaling pathway. Plant physiology, 146(2), 772.

[13]   Ramakrishnan, G. S., Kamath, M. M., & Niranjan, V. (2014). Increasing Microbial Biofuel Production by In-silico Comparative Genomic Studies. International Journal of Bioscience, Biochemistry and Bioinformatics, 4(5), 386.

[14]   Vourc'h, T., Peerhossaini, H., Léopoldès, J., Méjean, A., Chauvat, F., & Cassier-Chauvat, C. (2018). Slowdown of surface diffusion during early stages of bacterial colonization. Physical Review E, 97(3), 032407.

[15]   Collins, A. M., Liberton, M., Jones, H. D., Garcia, O. F., Pakrasi, H. B., & Timlin, J. A. (2012). Photosynthetic pigment localization and thylakoid membrane morphology are altered in *Synechocystis* 6803 phycobilisome mutants. Plant physiology, 158(4), 1600-1609.

[16]   Mehdizadeh Allaf, M., & Peerhossaini, H. (2022). Cyanobacteria: Model microorganisms and beyond. Microorganisms, 10(4), 696.

[17]   Heidorn, T., Camsund, D., Huang, H. H., Lindberg, P., Oliveira, P., Stensjö, K., & Lindblad, P. (2011). Synthetic biology in cyanobacteria: engineering and analyzing novel functions. In Methods in enzymology (Vol. 497, pp. 539-579). Academic Press.

[18]   Heng, R. L., Sy, K. C., & Pilon, L. (2015). Absorption and scattering by bispheres, quadspheres, and circular rings of spheres and their equivalent coated spheres. JOSA A, 32(1), 46-60.

[19]   Pilon, L., Berberoğlu, H., & Kandilian, R. (2011). Radiation transfer in photobiological carbon dioxide fixation and fuel production by microalgae. Journal of Quantitative Spectroscopy and Radiative Transfer, 112(17), 2639-2660.

[20]   Perez-Garcia, O., & Bashan, Y. (2015). Microalgal heterotrophic and mixotrophic culturing for bio-refining: from metabolic routes to techno-economics. Algal Biorefineries: Volume 2: Products and Refinery Design, 61-131.

[21]   Shoener, B. D., Schramm, S. M., Béline, F., Bernard, O., Martínez, C., Plósz, B. G., ... & Guest, J. S. (2019). Microalgae and cyanobacteria modeling in water resource recovery facilities: A critical review. Water research X, 2, 100024.

[22]   Baroukh, C., Turon, V., & Bernard, O. (2017). Dynamic metabolic modeling of heterotrophic and mixotrophic microalgal growth on fermentative wastes. PLoS computational biology, 13(6), e1005590.

[23] Abreu, A. P., Fernandes, B., Vicente, A. A., Teixeira, J., & Dragone, G. (2012). Mixotrophic cultivation of Chlorella vulgaris using industrial dairy waste as organic carbon source. Bioresource technology, 118, 61-66.

[24] Bitog, J. P., Lee, I. B., Lee, C. G., Kim, K. S., Hwang, H. S., Hong, S. W., ... & Mostafa, E. (2011). Application of computational fluid dynamics for modeling and designing photobioreactors for microalgae production: A review. Computers and electronics in agriculture, 76(2), 131-147.

[25] Kandilian, R., Pruvost, J., Artu, A., Lemasson, C., Legrand, J., & Pilon, L. (2016). Comparison of experimentally and theoretically determined radiation characteristics of photosynthetic microorganisms. Journal of Quantitative Spectroscopy and Radiative Transfer, 175, 30-45.

[26] Berberoglu, H., & Pilon, L. (2007). Experimental measurements of the radiation characteristics of Anabaena variabilis ATCC 29413-U and Rhodobacter sphaeroides ATCC 49419. International Journal of Hydrogen Energy, 32(18), 4772-4785.

[27] Mie, G. (1908). Beiträge zur Optik trüber Medien, speziell kolloidaler Metallösungen. Annalen der physik, 330(3), 377-445.

[28] Charon, J., Blanco, S., Cornet, J. F., Dauchet, J., El Hafi, M., Fournier, R., ... & Weitz, S. (2016). Monte Carlo implementation of Schiff's approximation for estimating radiative properties of homogeneous, simple-shaped and optically soft particles: Application to photosynthetic micro-organisms. Journal of Quantitative Spectroscopy and Radiative Transfer, 172, 3-23.

[29] Lee, E., Heng, R. L., & Pilon, L. (2013). Spectral optical properties of selected photosynthetic microalgae producing biofuels. Journal of Quantitative Spectroscopy and Radiative Transfer, 114, 122-135.

[30] Giacomelli, M. G., Chalut, K. J., Ostrander, J. H., & Wax, A. (2008). Application of the T-matrix method to determine the structure of spheroidal cell nuclei with angle-resolved light scattering. Optics letters, 33(21), 2452-2454.

[31] Drezek, R., Dunn, A., & Richards-Kortum, R. (2000). A pulsed finite-difference time-domain (FDTD) method for calculating light scattering from biological cells over broad wavelength ranges. Optics Express, 6(7), 147-157.

[32] Ajala, S. O., & Alexander, M. L. (2022). Evaluating the effects of agitation by shaking, stirring and air sparging on growth and accumulation of biochemical compounds in microalgae cells. Biofuels, 13(3), 371-381.

[33] Wang, B., Lan, C. Q., & Horsman, M. (2012). Closed photobioreactors for production of microalgal biomasses. Biotechnology advances, 30(4), 904-912.

[34] Toma, M. K., Ruklisha, M. P., Vanags, J. J., Zeltina, M. O., Lelte, M. P., Galinine, N. I., ... & Tengerdy, R. P. (1991). Inhibition of microbial growth and metabolism by excess turbulence. Biotechnology and bioengineering, 38(5), 552-556.

[35] Reclari, M., Dreyer, M., Tissot, S., Obreschkow, D., Wurm, F. M., & Farhat, M. (2014). Surface wave dynamics in orbital shaken cylindrical containers. Physics of Fluids, 26(5), 052104.

[36] Yang, Z., Del Ninno, M., Wen, Z., & Hu, H. (2014). An experimental investigation on the multiphase flows and turbulent mixing in a flat-panel photobioreactor for algae cultivation. Journal of applied phycology, 26, 2097-2107.

[37] Mehdizadeh Allaf, M., Habib, Z., de Bruyn, J. R., DeGroot, C. T., & Peerhossaini, H. (2022). Rheological and Biophysical Properties of Living Fluids Under Shear: Active Suspensions of Synechocystis sp. CPCC 534. Journal of Fluids Engineering, 144(2).

[38] Hu, H., Wang, H. F., Li, J. Y., Ma, L. L., Shen, X. F., & Zeng, R. J. (2019). Evaluation of the effect of agitation speed on the growth and high-value LC-PUFA formation of Porphyridium cruentum based on basic rheological analysis. Journal of Chemical Technology & Biotechnology, 94(7), 2158-2166.

[39] Alpresa, P., Sherwin, S., Weinberg, P., & van Reeuwijk, M. (2018). Orbitally shaken shallow fluid layers. I. Regime classification. Physics of Fluids, 30(3), 032107.

[40] Monteil, D. T., Tontodonati, G., Ghimire, S., Baldi, L., Hacker, D. L., Bürki, C. A., & Wurm, F. M. (2013). Disposable 600-mL orbitally shaken bioreactor for mammalian cell cultivation in suspension. Biochemical engineering journal, 76, 6-12.

[41]   Ojo, E. O., Auta, H., Baganz, F., & Lye, G. J. (2014). Engineering characterisation of a shaken, single use photobioreactor for early stage microalgae cultivation using Chlorella sorokiniana. Bioresource technology, 173, 367-375.

[42]   Palma, V., Gutiérrez, M. S., Vargas, O., Parthasarathy, R., & Navarrete, P. (2022). Methods to evaluate bacterial motility and its role in bacterial–host interactions. Microorganisms, 10(3), 563.

[43]   Mazza, M. G. (2016). The physics of biofilms—an introduction. Journal of Physics D: Applied Physics, 49(20), 203001.

[44]   Lauga, E., & Powers, T. R. (2009). The hydrodynamics of swimming microorganisms. Reports on progress in physics, 72(9), 096601.

[45]   Bray, D. (2000). Cell movements: from molecules to motility. Garland Science. New York.

[46]   Kearns, D. B. (2010). A field guide to bacterial swarming motility. Nature Reviews Microbiology, 8(9), 634-644.

[47]   Darnton, N. C., Turner, L., Rojevsky, S., & Berg, H. C. (2010). Dynamics of bacterial swarming. Biophysical journal, 98(10), 2082-2090.

[48]   Hahn, H. P. (1997). The type-4 pilus is the major virulence-associated adhesin of Pseudomonas aeruginosa–a review. Gene, 192(1), 99-108.

[49]   Pollitt, E. J., & Diggle, S. P. (2017). Defining motility in the Staphylococci. Cellular and Molecular Life Sciences, 74, 2943-2958.

[50]   Chen, Z., Li, X., Tan, X., Zhang, Y., & Wang, B. (2020). Recent advances in biological functions of thick pili in the cyanobacterium *Synechocystis* sp. PCC 6803. Frontiers in Plant Science, 11, 241.

[51]   Schuergers, N., & Wilde, A. (2015). Appendages of the cyanobacterial cell. Life, 5(1), 700-715.

[52]   Tokárová, V., Sudalaiyadum Perumal, A., Nayak, M., Shum, H., Kašpar, O., Rajendran, K., ... & Nicolau, D. V. (2021). Patterns of bacterial motility in microfluidics-confining environments. Proceedings of the National Academy of Sciences, 118(17), e2013925118.

[53]   Lauga, E. (2016). Bacterial hydrodynamics. Annual Review of Fluid Mechanics, 48, 105-130.

[54]   Worthington, R. J., Richards, J. J., & Melander, C. (2012). Small molecule control of bacterial biofilms. Organic & biomolecular chemistry, 10(37), 7457-7474.

[55]   Frymier, P. D., Ford, R. M., Berg, H. C., & Cummings, P. T. (1995). Three-dimensional tracking of motile bacteria near a solid planar surface. Proceedings of the National Academy of Sciences, 92(13), 6195-6199.

[56]   Berg, H. (2000). Motile behavior of bacteria. Physics today.

[57]   Alexandre, G., Greer-Phillips, S., & Zhulin, I. B. (2004). Ecological role of energy taxis in microorganisms. FEMS microbiology reviews, 28(1), 113-126.

[58]   Long, T., & Ford, R. M. (2009). Enhanced transverse migration of bacteria by chemotaxis in a porous T-sensor. Environmental science & technology, 43(5), 1546-1552.

[59]   Zonia, L., & Bray, D. (2009). Swimming patterns and dynamics of simulated Escherichia coli bacteria. Journal of the Royal Society Interface, 6(40), 1035-1046.

[60]   Desai, N., & Ardekani, A. M. (2018). The combined influence of hydrodynamics and chemotaxis in the distribution of microorganisms around spherical nutrient sources. Physical Review E, 98(1), 012419.

[61]   Chau, R. M. W., Bhaya, D., & Huang, K. C. (2017). Emergent phototactic responses of cyanobacteria under complex light regimes. MBio, 8(2), e02330-16.

[62]   Vater, S. M., Weiße, S., Maleschlijski, S., Lotz, C., Koschitzki, F., Schwartz, T., ... & Rosenhahn, A. (2014). Swimming behavior of Pseudomonas aeruginosa studied by holographic 3D tracking. PloS one, 9(1), e87765.

[63]   Matz, C., & Jürgens, K. (2005). High motility reduces grazing mortality of planktonic bacteria. Applied and Environmental Microbiology, 71(2), 921-929.

[64]   Taktikos, J., Lin, Y. T., Stark, H., Biais, N., & Zaburdaev, V. (2015). Pili-induced clustering of N. gonorrhoeae bacteria. *PLoS One*, *10*(9), e0137661.

[65]   Vlamakis, H., Chai, Y., Beauregard, P., Losick, R., & Kolter, R. (2013). Sticking together: building a biofilm the Bacillus subtilis way. Nature Reviews Microbiology, 11(3), 157-168.

[66]   Bell, G. I. (1978). Models for the specific adhesion of cells to cells: a theoretical framework for adhesion mediated by reversible bonds between cell surface molecules. Science, 200(4342), 618-627.

[67]   Berne, C., Ducret, A., Hardy, G. G., & Brun, Y. V. (2015). Adhesins involved in attachment to abiotic surfaces by Gram-negative bacteria. Microbial biofilms, 163-199.

[68]   Vourc'h, T., Léopoldès, J., & Peerhossaini, H. (2020). Clustering of bacteria with heterogeneous motility. Physical Review E, 101(2), 022612.

[69]   Angelani, L., Costanzo, A., & Di Leonardo, R. (2011). Active ratchets. Europhysics Letters, 96(6), 68002.

[70]   van Teeffelen, S., Zimmermann, U., & Löwen, H. (2009). Clockwise-directional circle swimmer moves counter-clockwise in Petri dish-and ring-like confinements. Soft Matter, 5(22), 4510-4519.

[71]   Costanzo, A., Di Leonardo, R., Ruocco, G., & Angelani, L. (2012). Transport of self-propelling bacteria in micro-channel flow. Journal of Physics: Condensed Matter, 24(6), 065101.

[72]   Rusconi, R., Guasto, J. S., & Stocker, R. (2014). Bacterial transport suppressed by fluid shear. Nature physics, 10(3), 212-217.

[73]   Ezhilan, B., & Saintillan, D. (2015). Transport of a dilute active suspension in pressure-driven channel flow. Journal of Fluid Mechanics, 777, 482-522.

[74]   Miño, G. L., Baabour, M. D., Chertcoff, R. H., Gutkind, G. O., Clément, E., Auradou, H., & Ippolito, I. P. (2018). E coli accumulation behind an obstacle.

[75]   Altshuler, E., Mino, G., Pérez-Penichet, C., Del Río, L., Lindner, A., Rousselet, A., & Clément, E. (2013). Flow-controlled densification and anomalous dispersion of E. coli through a constriction. Soft Matter, 9(6), 1864-1870.

[76]   Qi, K., Annepu, H., Gompper, G., & Winkler, R. G. (2020). Rheotaxis of spheroidal squirmers in microchannel flow: Interplay of shape, hydrodynamics, active stress, and thermal fluctuations. Physical Review Research, 2(3), 033275.

[77]   Binz, M., Lee, A. P., Edwards, C., & Nicolau, D. V. (2010). Motility of bacteria in microfluidic structures. Microelectronic Engineering, 87(5-8), 810-813.

[78]   Gurung, J. P., Gel, M., & Baker, M. A. (2020). Microfluidic techniques for separation of bacterial cells via taxis. Microbial Cell, 7(3), 66.

[79]   Tokárová, V., Sudalaiyadum Perumal, A., Nayak, M., Shum, H., Kašpar, O., Rajendran, K., ... & Nicolau, D. V. (2021). Patterns of bacterial motility in

microfluidics-confining environments. Proceedings of the National Academy of Sciences, 118(17), e2013925118.

[80]   Pérez-Rodríguez, S., García-Aznar, J. M., & Gonzalo-Asensio, J. (2022). Microfluidic devices for studying bacterial taxis, drug testing and biofilm formation. Microbial Biotechnology, 15(2), 395-414.

Chapter 2

2 Modelling Optical Properties of Algae Using the Finite-Difference Time Domain Method [1]

Photosynthetic microorganisms are important to the Earth's ecosystem, since about half of the atmospheric oxygen is produced by photosynthesis. To have better control over photobioreactors under various operating conditions, it is necessary to accurately characterize the propagation of light in the reactor. Theoretical methods calculate the radiation properties of microorganisms through solving Maxwell's equations of electromagnetic wave theory. To solve Maxwell's equations for prediction of optical characteristics of microorganisms, various methods can be used including Lorenz-Mie, T-Matrix, Finite Difference Time Domain (FDTD), and Volume Integral methods. Most theoretical methods predict the optical properties of microorganisms by Lorenz-Mie theory. Lorenz–Mie theory is applicable for homogeneous and spherical particles, homogeneous concentric spheres, or coated spheres.

This work seeks to determine the suitability of the commonly used homogenous-sphere, coated-sphere, and heterogenous-sphere approximation by simulating the optical behavior of photosynthetic microorganism (*Chlamydomonas reinhardtii*) using the FDTD and an accurate geometric model. Here, each of the key cell organelles will be included in the model with the appropriate optical properties specified. These results allow for a more accurate optical model to be developed while studying the effects of different growth regimes.

2.1 Introduction

Due to the efficient conversion rate of CO_2 to organic compounds, microalgae and cyanobacteria have significant applications for carbon capture and storage. They are used as a feedstock for biofuel production and in wastewater treatment operations. In wastewater

---

[1] Published in FEDSM2021-66314, V003T05A016; 8 pages

treatment, photosynthetic microorganisms can be used to remove pollutants from water by using CO_2 and consequently mitigate environmental impacts [1]. Furthermore, algal biomass is an excellent feedstock for production of high-value materials in industry like bioplastics, pharmaceuticals, nutritional supplements, cosmetics, and animal feed [2].

Photosynthetic microorganisms can be cultivated in photobioreactors (PBRs) by two main light sources: artificial light or sunlight [3]. The appropriate choice of cultivation mode plays an important role in ensuring cost-effective operation [4]. Microalgae and cyanobacteria can grow autotrophically, heterotrophically, or mixotrophically (i.e., autotrophic, and heterotrophic simultaneously). Environmental conditions, such as energy and carbon sources determine which metabolism is dominant for cultivation of photosynthetic microorganisms [5]. In autotrophic cultivation mode, microorganisms convert light energy into chemical energy by photosynthesis, producing organic sources from inorganic carbon source [6]. Photoautotrophic cultivation of microorganisms to produce biofuel and other value-added products is a feasible practice for CO_2 capture, and thus potentially contributes to global CO_2 reduction. Due to the limitation of light distribution to the cells in photoautotrophic growth mode, there are two disadvantages associated with this kind of metabolism: low cell densities and long growth periods. Some microorganisms are heterotrophic, utilizing organic sources for cultivation; hence, there is no need to light source in this kind of cultivation. Heterotrophic growth does not require any light source for cultivation and higher cell densities can be achieved. However, preparation of organic carbon necessary for this cultivation mode constrains the industrial production of heterotrophic microorganisms because of the high economic and environmental cost [7].

In mixotrophic cultivation, in the presence of light, inorganic and organic carbon sources are consumed by microorganisms thus, photoautotrophic, and heterotrophic growth occur simultaneously [8]. Under mixotrophic cultivation, photosynthetic microorganisms have the characteristics of both phototrophic and heterotrophic growth with higher growth rates and biomass yield. In addition, mixotrophic growth requires lower energy in comparison with heterotrophic growth [5].

Some of the important factors for microorganism growth include light, CO_2, nutrients, temperature, and pH [9]. Efficient light distribution is critical for photosynthetic processes. It is difficult to create a homogenous light distribution in PBRs [3]. Under low light intensity, carbon sources are used by cell respiration at a higher rate than its production in photosynthesis, therefore no new biomass is produced. On the other hand, under high light intensity, the photoinhibition process occurs in the photosystem and consequently results in cell death or damage [1]. Therefore, in design, control, and optimization of PBRs for high efficiency and productivity, it is vital to provide relatively uniform illumination in the microorganism culture [3]. To control biomass culture in PBRs and maximize their efficiency in production of high-value products, experimental studies have been conducted to investigate the optical properties of photosynthetic microorganisms. However, experimental setups can be expensive and time consuming. It is also extremely difficult to observe a small number of cells in an experiment. Moreover, the results are specific to a particular cultivation method and are not directly applicable to other growth conditions [10]. Theoretical methods for calculation of the optical properties of photosynthetic microorganisms are rather fast, accurate, and can be applied for simulation of microorganism's growth in different operating conditions. Theoretical predictions of the light characteristics of microorganisms, including their absorption efficiency and scattering efficiency, are based on solving Maxwell's equations of electromagnetic wave theory, which has the dependency on the size, geometry, and complex refractive index of microorganism cell [11].

2.2 Materials and Methods

2.2.1 Theoretical Approaches

The FDTD approach is used to model optical properties of the photosynthetic microorganism: *Chlamydomonas reinhardtii*. The FDTD method originates from Yee's algorithm in 1966 [12] and has received more attention since 1996. The current work utilizes the Meep open-source software package to solve the FDTD system. FDTD model has some superiority to Mie theory for its application to asymmetrical cell shapes and heterogenous microorganisms [13]. The FDTD method calculates the scattering and absorption characteristics of microorganisms in the time and spatial domain by

discretization of Maxwell equations, which explain the interactions of magnetic (H) and electric (E) fields with each other and with sources and matter. The equations for the time development of the fields are:

$$\frac{dB}{dt} = -\nabla \times E - J_B - \sigma_B B \tag{1}$$

$$B = \mu H \tag{2}$$

$$\frac{dD}{dt} = \nabla \times H - J - \sigma_D \tag{3}$$

$$D = \varepsilon E \tag{4}$$

where D, ε, J and J_B are the displacement field, the dielectric constant, the current density of electric charge and the magnetic-charge current density respectively. B, μ and H are defined as the magnetic flux density, the magnetic permeability, and the magnetic field respectively. Frequency-independent magnetic is σ_B and electric conductivities is σ_D. The divergence equations are explained as below:

$$\nabla . B = - \int_0^t \nabla . (J_B \, (t') + \sigma_B B) dt' \tag{5}$$

$$\nabla . D = - \int_0^t \nabla . (J \, (t') + \sigma_D D) dt' \; \equiv \rho \tag{6}$$

ε depends on frequency, position, and the field electric E.

In this method, the split-field perfectly matched layer (PML) absorbing boundary condition (ABC) is applied to decrease the computational field [14]. The dielectric medium is considered for geometry, which is in the divided volume with a PML layer and the edges padded [15].

2.2.2 Total Scatter Field

Measurements of full vectors of fluctuating electric and magnetic fields allow us to calculate the spectral density of the modulus of the Poynting vector S_s using the spectral matrices 6×6:

$$S_{S1} = \frac{1}{\mu_0}(\Re S_{E2B3} - \Re S_{E3B2}) \qquad (7)$$

$$S_{S2} = \frac{1}{\mu_0}(\Re S_{E3B1} - \Re S_{E1B3}) \qquad (8)$$

$$S_{S3} = \frac{1}{\mu_0}(\Re S_{E1B2} - \Re S_{E2B1}) \qquad (9)$$

$$S_S = \sqrt{S_{S1}^2 + S_{S2}^2 + S_{S3}^2} \qquad (10)$$

where $\Re S_{EiBj}$, S_{SK} and μ_0 are real parts of the cross-power spectra between components of the electric and magnetic fields, spectral densities of the effective values of components of the Poynting vector (i, j, k=1…3), and the permeability of the free space respectively [16].

2.2.3 Calculation of Scattering Efficiency

To calculate the scattered power of any object, two numerical simulations need to be performed: first the total field should be calculated from the source, and then the incident fields should be subtracted. The ratio of the scattered power to the incident intensity is defined as the scattering cross section and the division of scattering cross section to the cross-sectional area of the sphere is considered as the definition of scattering efficiency. For calculation, the microorganism cell is considered as a lossy dielectric object with wavelength-dependent complex refractive index. To predict accurately the light characteristics of microorganisms, it is necessary to develop theoretical models by considering cell non-sphericity and heterogeneity. In this section, we investigate homogenous, coated and heterogenous microorganism cells by considering each cell compartment's shape and size associated with its spectral refractive index. A microorganism cell is characterized as a homogenous cell when considering a complex refractive index for the molecular medium of microorganism cell. However, for the heterogeneous molecular medium of microorganism, each component of cell has a special

complex refractive index [1]. By subpixel smoothing, accuracy of simulations at low resolutions can be improved.

Regarding boundary conditions, first, a PML thickness is selected equal to half of the largest wavelength in the simulations, if it does not work, PML thickness should be repeatedly doubled until the simulation is converged.

2.2.4 Angular Dependency of Scattering

To measure the scattered fields in different angles to the source, first the total field and the incident field should be calculated. In this way, the incident field can be removed from the total field to get the scattered field. Through Poynting vector, finally the scattering field in different angular positions can be calculated.

2.2.5 Scattered Fields Map

Two numerical simulations are required to draw the spatial map of the scattered fields: (1) simulation should be carried out without an object and (2) simulation includes the object and then finally subtraction of two runs to get the scattered field at the interest frequency.

2.3 Results and Discussion

2.3.1 Scattering Contour

Based on the method reported by Bhowmik et al [17], first the cell geometry is created and then scattering contour is calculated as was explained in section 2.5. for the homogenous cell with and without metabolites. *Chlamydomonas reinhardtii*, used as model cell in this work, is composed of a cell wall and various internal organelles, consisting of the cytoplasm, chloroplast, nucleus, mitochondria, and lipid bodies. Under the non-metabolic condition, the lipids volumes are zero, while they are nonzero under the metabolic condition. One of the purposes of this study is to compare the effect of lipid bodies on the light characteristics of microorganism cells. The volume A schematic of the two-dimensional cross section at $z=0$ of the three-dimensional computational cell is drawn in figure 2-1. The Discrete Fourier transform (dft)-flux box calculates the power of the fields in each region. In the schematic of the simulation figure 2-1, the line source, PMLs, dft-

flux box and dft-fields surface are indicated by the red line, green hatched region, solid blue contour line, and blue hatched region respectively.

Figure 2-1:Schematic of the 2d cross-section at z=0 of the 3d computational cell for a homogenous microorganism cell

Scattering fields contour is shown in figure 2-2, which explains most of the scattering happens in a small area close to the microorganism cell's back surface.

(a)   (b)
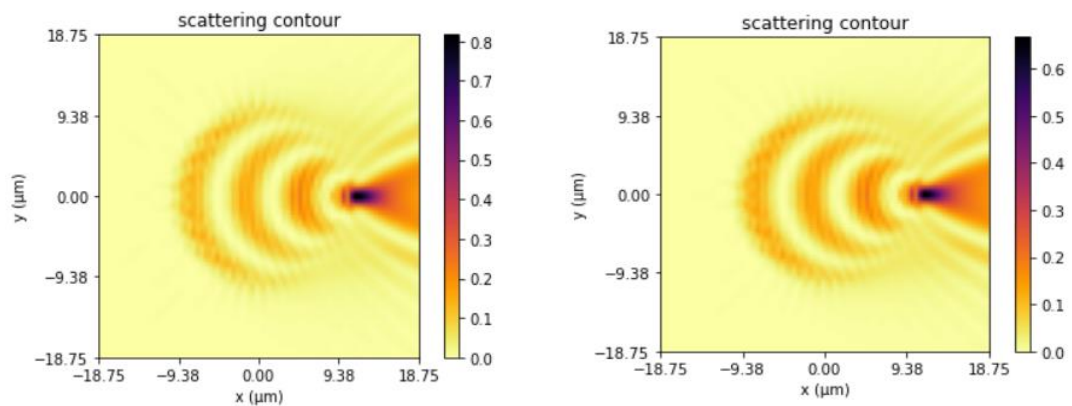
Figure 2-2:Scattering contour of the homogenous microorganism cell (a) without metabolism and (b) with metabolism

The geometry and contour for coated cells [14] are shown in Figures 2-3 and 2-4. The coated model consists of two sections: the outer layer of the microorganism cell as the coated layer, and all the intracellular compartments as the core of coated model. Different parts of the model are shown separately in figure 2-3:

(a)   (b)
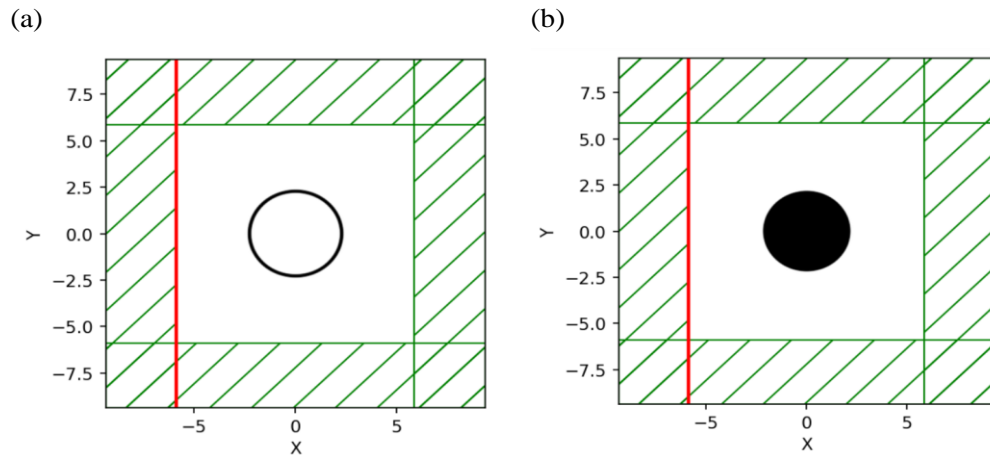
Figure 2-3:Schematic of the 2D cross-section at z=0 of the 3D computational cell for a coated microorganism cell. (a) outer layer. (b) inner core.

(a)   (b)
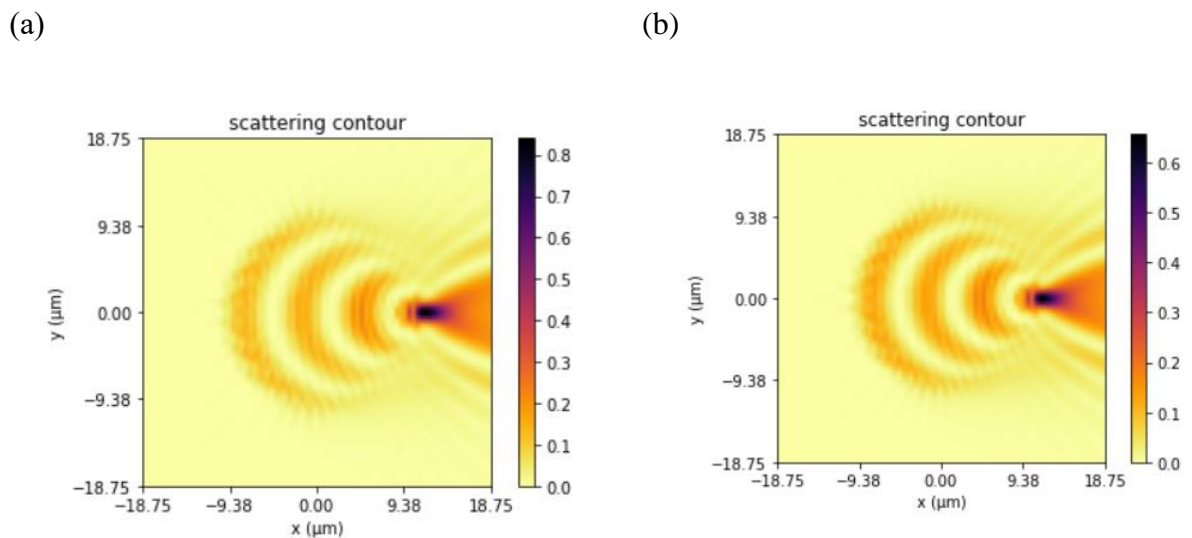
Figure 2-4:Scattering contour of the coated microorganism cell (a) without metabolism and (b) with metabolism

The geometry and contour for heterogenous cells without metabolism [16] are shown in figures 2-5 and 2-6, and with metabolites in figures 2-7 and 2-8. All parts of microorganism cells are considered in this model.
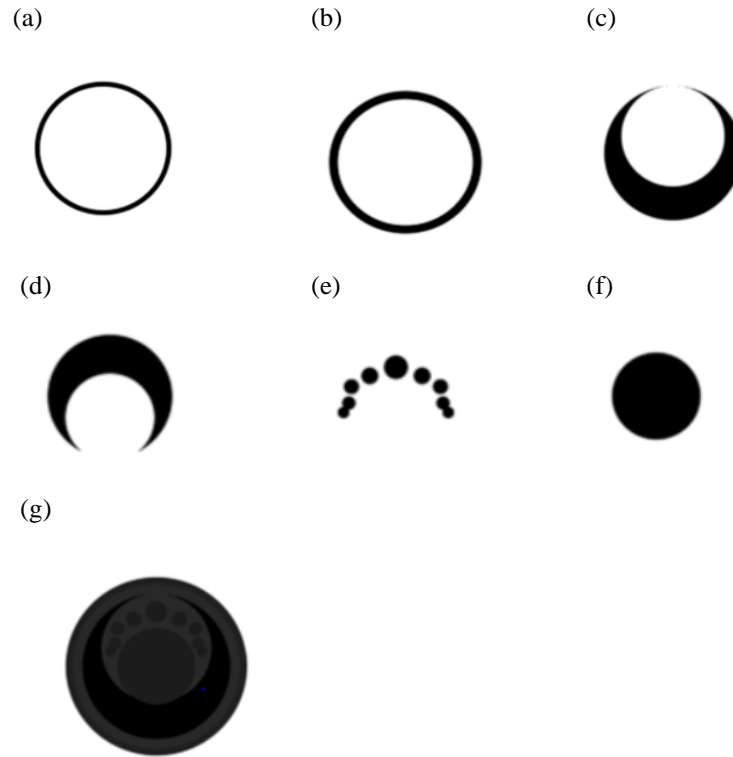
Figure 2-5:Schematic of the 2D cross-section at z=0 of the 3D computational cell for a heterogenous microorganism cell. (a) cell wall. (b, d) cytoplasm. (c) chloroplast, (e) mitochondria, (f) nucleus, (g) total microorganism cell.

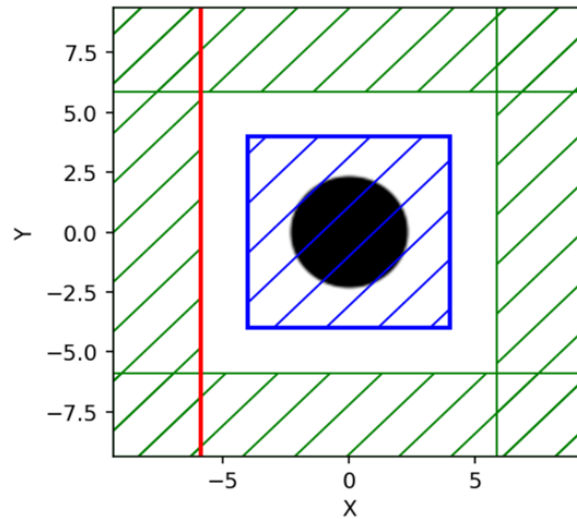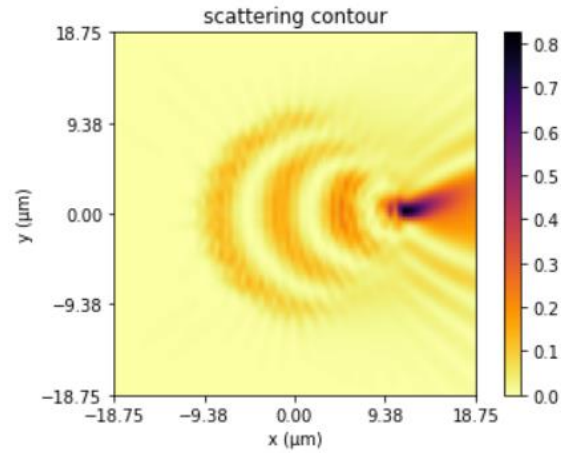Figure 2-6:Scattering contour of the heterogenous microorganism cell without metabolism
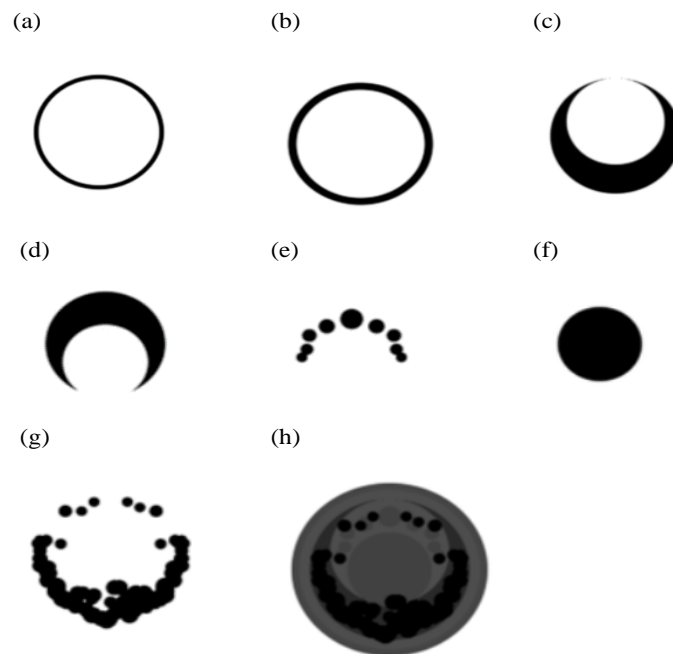
Figure 2-7:Schematic of the 2D cross-section at z=0 of the 3D computational cell for a heterogenous microorganism cell. (a) cell wall. (b, d) cytoplasm. (c) chloroplast, (e) mitochondria, (f) nucleus, (g) lipid Bodies. (h) total microorganism cell.

scattering contour
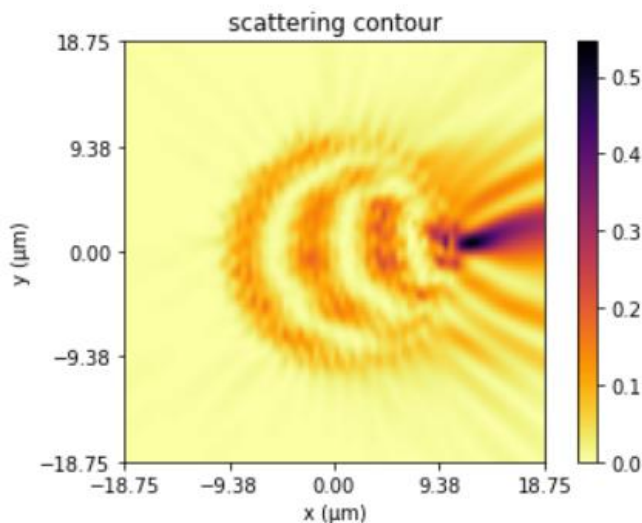
Figure 2-8:Scattering contour of the heterogenous microorganism cell with metabolism

2.3.2 Scattering Efficiency Results

To calculate the optical properties of *Chlamydomonas reinhardtii*, the finite-difference time-domain (FDTD) method is applied over the wavelength range of 400 -750 nm. The FDTD method provides greater geometric flexibility than Mie- theory solutions to compute the light characteristics of microorganism consisting of various heterogeneous organelles. In this section, we calculate the scattering efficiency patterns for common homogeneous, coated and heterogenous models of microorganism cells. First, scattering efficiency is shown in figures 2-9 and 2-10 for the homogenous sphere model of *Chlamydomonas reinhardtii* for both theoretical and Meep methods with metabolism and without metabolism. Theoretical method and Meep method are based on Mie theory and FDTD method respectively.
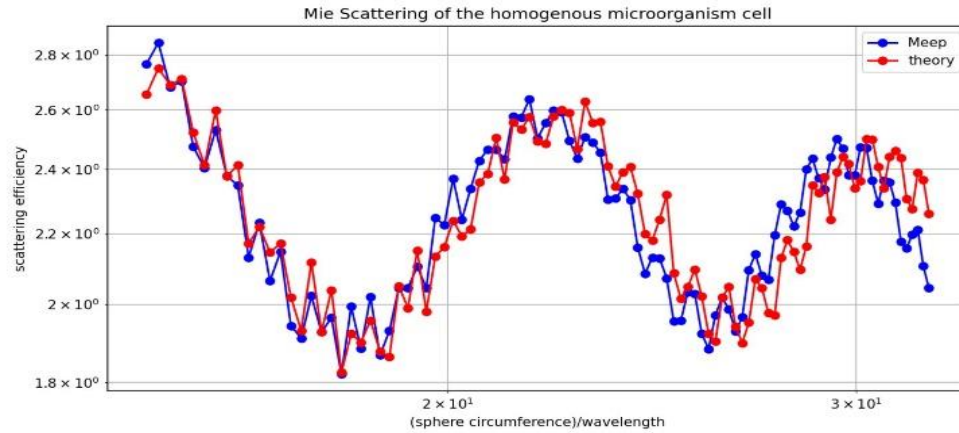
Figure 2-9:Scattering efficiency of the homogeneous microorganism cell without metabolism
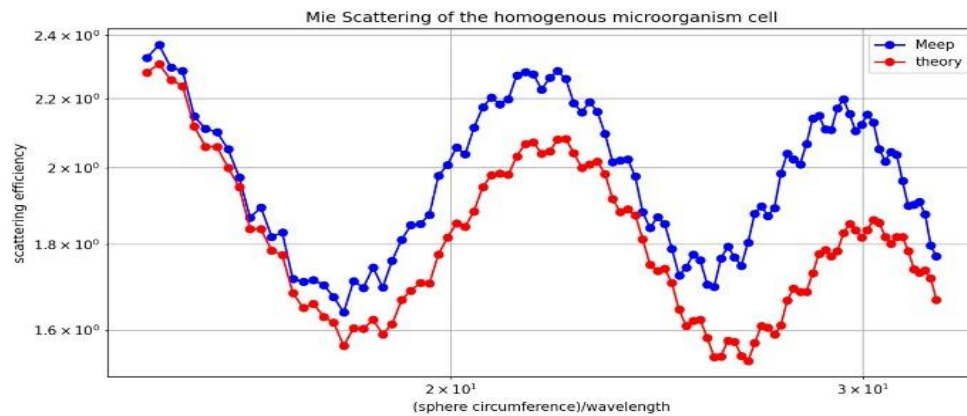
Figure 2-10:Scattering efficiency of the homogeneous microorganism cell with metabolism

The coated sphere cell was also considered to compute the scattering efficiency with two sections: outer layer of microorganism cell as the coated layer and all the intracellular compartments as the core of coated model; each section has its own specific refractive index. The results are shown in followings figures:
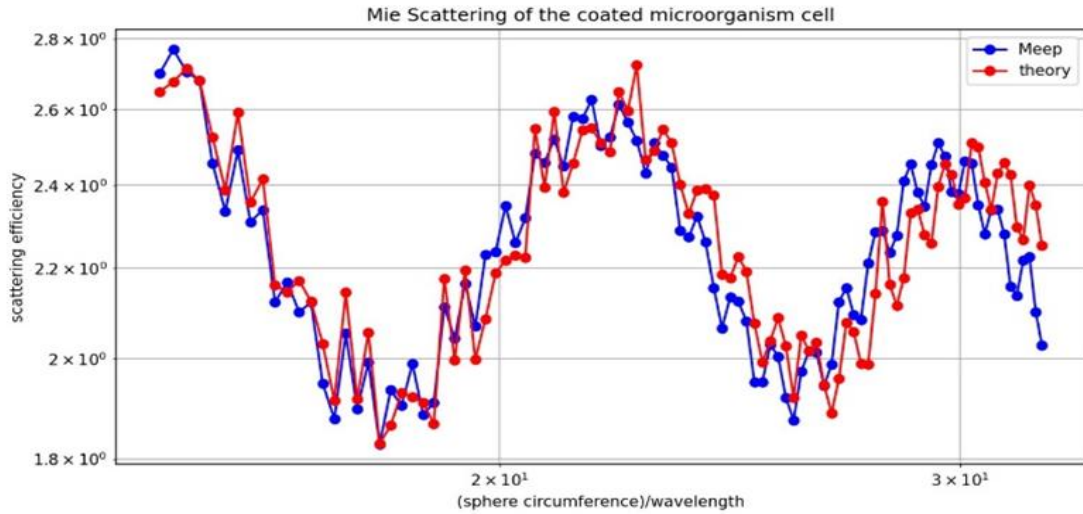
Figure 2-11:Scattering efficiency of the coated microorganism cell without metabolism
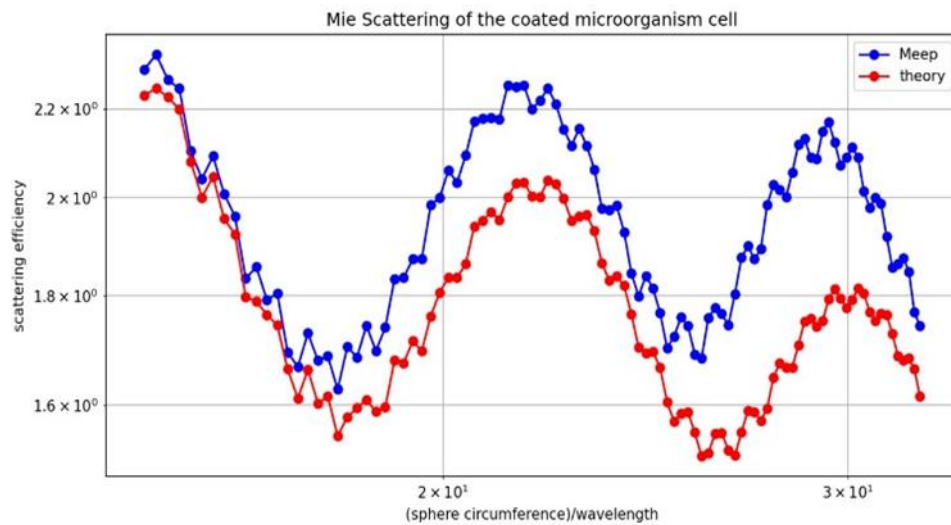
Figure 2-12:Scattering efficiency of the coated microorganism cell with metabolism

In the heterogeneous model, each component of the microorganism cell with different refractive index and spherical geometry is considered separately. The equation of complex refractive index is $m_\lambda = n_\lambda + i k_\lambda$, in which n_λ and k_λ are the real and imaginary part respectively, their value for different cell components is presented in table 1:

Table 2-1: Values of the real and imaginary part of cell's components.

Compartments	J	$n_{j,\lambda}$	$k_{j,\lambda}$
Nucleus	1	1.38	0
Mitochondria	2	1.38	0
Cytoplasm	3	1.36	0
Cell (including cell wall)	4	1.375	0
Chloroplast	5	1.42	Equation (11)
Lipid bodies	6	1.49	0

All parts of the microorganism cell are non-absorbing except for chloroplast (i.e., $k_{j,\lambda} = 0$ for j 1, 2,3, 4, 6). We calculate $k_{5,\lambda}$ from the following equation:

$$k_{5,\lambda} = \frac{\lambda}{4\pi} \sum_{i=1}^{M} Ea_{i,\lambda}(\lambda)C_i = \frac{\lambda}{4\pi} \rho_{dm} \frac{1 - x_\omega}{x_\omega} \sum_{i=1}^{M} Ea_{i,\lambda}(\lambda)\omega_i \quad (11)$$

where the index i denotes the different pigments present in the chloroplast. The concentration C_i of pigment i can be presented in terms of its mass fraction ω_i, and its density of dry mass ρ_{dm} (kg/m³). $Ea_{i,\lambda}(\lambda)$ (m²/kg) refers to the specific spectral absorption coefficients, and x_ω i the water volume fractions the cell. $Ea_{i,\gamma}(\lambda)$ is the specific spectral absorption coefficient of pigment i consisting of chlorophyll a (Chl$_a$), chlorophyll b (Chl$_b$), and photoprotective carotenoid (PPC), as was reported in [18].

In this simulation method, each compartment is defined in a complex manner, which determines how each part of the microorganism cell contributes to the scattering efficiency.
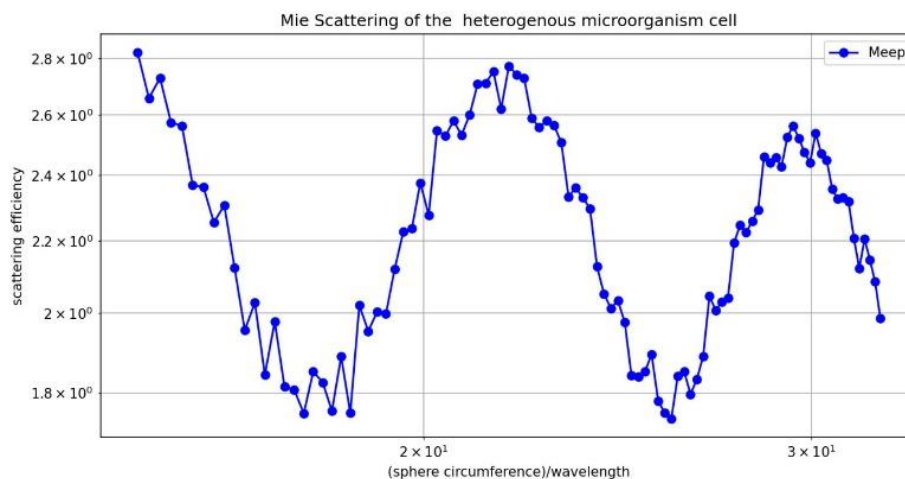
Figure 2-13:Scattering efficiency of the heterogeneous microorganism cell without metabolism
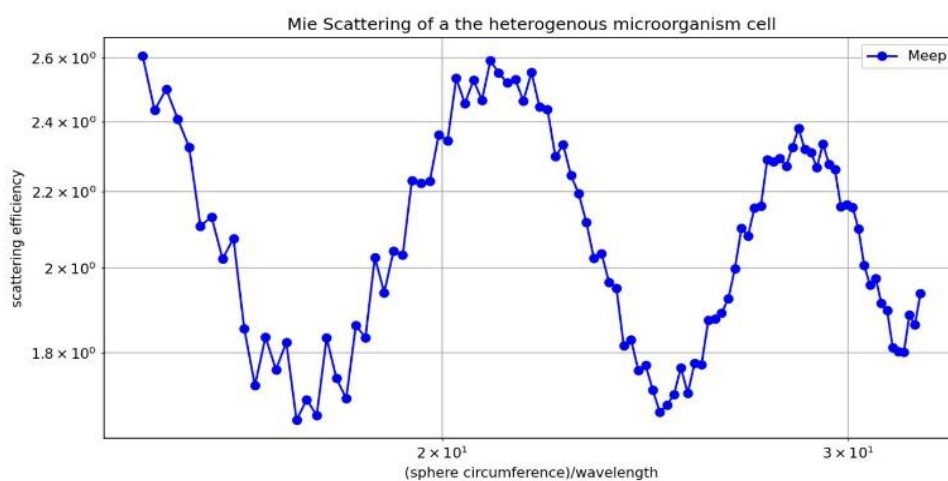
Figure 2-14:Scattering efficiency of the heterogeneous microorganism cell with metabolism

Figure 2-12 shows a satisfactory agreement between Meep and theoretical method for non-metabolic case. The amount of Chl_a, Chl_b and PPC is zero for non-metabolic conditions while they are nonzero for metabolic conditions. Therefore, to obtain accurate results for scattering efficiency in the metabolic case, it is essential to have accurate measurements of the refractive index and the volume fractions of Chl_a, Chl_b and PPC. The theoretical method was not calculated for heterogenous cell because it is not possible to consider all microorganism components in this method.

2.3.3 Angular Dependency of Scattering

Finally, the scattering field in different angular positions can be calculated and shown as following figures with and without metabolism for *Chlamydomonas reinhardtii*.
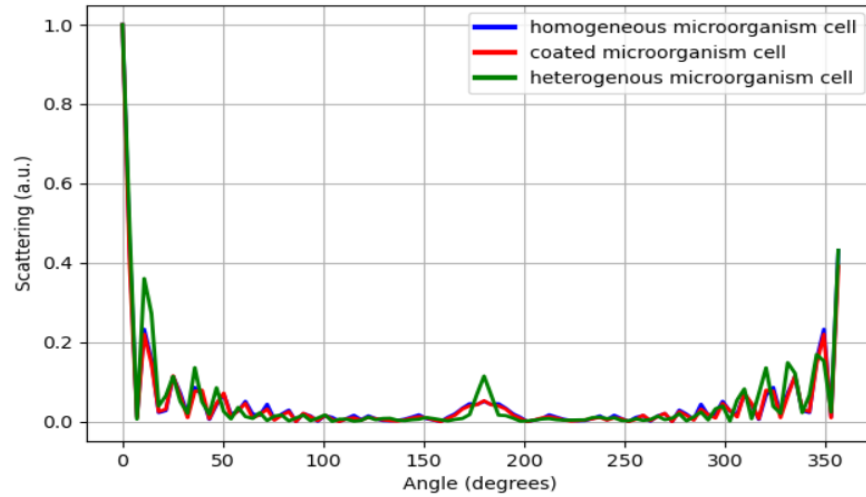
Figure 2-15:Angular scattering dependency of the microorganism cell without metabolites for three geometry models
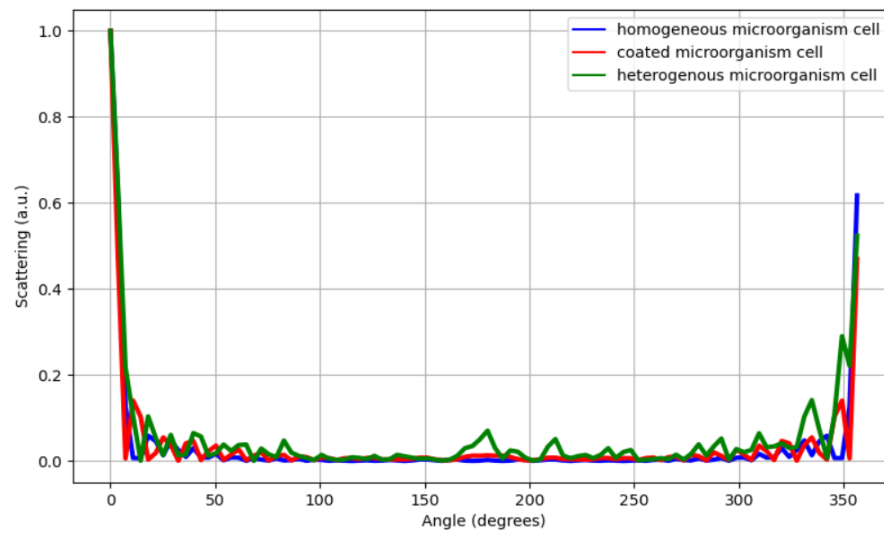
Figure 2-16:Angular scattering dependency of the microorganism cell with metabolites for three geometry models

In Figure 2-15, a small difference is observed between the light scattering of the three geometries. To estimate accurately the value of scattering, it is essential to consider the refractive index and volume fraction of each part of the microorganism cell separately. This can be obtained by direct measurement or from general databases. In the metabolic case, lipid bodies have an important role in light scattering in heterogenous microorganism cells, as can be seen in Figure 2-16. In this case, small organelles play an important role in light scattering from the cell.

2.4 Conclusions

The FDTD method has been used to compute the optical properties of microorganisms with heterogeneous cells. This method offers greater geometric flexibility than Mie theory and T-matrix solutions. However, to attain more accurate results for the light properties of microorganisms, the absorption properties of pigments, the real part of refractive indices, and the shape of the cells need more studies and investigations.

2.5 References

[1] Lehmuskero, A., Chauton, M. S., & Boström, T. (2018). Light and photosynthetic microalgae: A review of cellular-and molecular-scale optical processes. Progress in Oceanography, 168, 43-56.

[2] Wang, S. K., Stiles, A. R., Guo, C., & Liu, C. Z. (2014). Microalgae cultivation in photobioreactors: An overview of light characteristics. Engineering in Life Sciences, 14(6), 550-559.

[3] Pilon, L., Berberoğlu, H., & Kandilian, R. (2011). Radiation transfer in photobiological carbon dioxide fixation and fuel production by microalgae. Journal of Quantitative Spectroscopy and Radiative Transfer, 112(17), 2639-2660.

[4] Perez-Garcia, O., & Bashan, Y. (2015). Microalgal heterotrophic and mixotrophic culturing for bio-refining: from metabolic routes to techno-economics. Algal biorefineries, 61-131.

[5]   Shoener, B. D., Schramm, S. M., Béline, F., Bernard, O., Martínez, C., Plósz, B. G., ... & Guest, J. S. (2019). Microalgae and cyanobacteria modeling in water resource recovery facilities: A critical review. Water research X, 2, 100024.

[6]   Baroukh, C., Turon, V., & Bernard, O. (2017). Dynamic metabolic modeling of heterotrophic and mixotrophic microalgal growth on fermentative wastes. PLoS computational biology, 13(6), e1005590.

[7]   Abreu, A. P., Fernandes, B., Vicente, A. A., Teixeira, J., & Dragone, G. (2012). Mixotrophic cultivation of Chlorella vulgaris using industrial dairy waste as organic carbon source. Bioresource technology, 118, 61-66.

[8]   Perez-Garcia, O., & Bashan, Y. (2015). Microalgal heterotrophic and mixotrophic culturing for bio-refining: from metabolic routes to techno-economics. *Algal biorefineries*, 61-131.

[9]   Bitog, J. P., Lee, I. B., Lee, C. G., Kim, K. S., Hwang, H. S., Hong, S. W., ... & Mostafa, E. (2011). Application of computational fluid dynamics for modeling and designing photobioreactors for microalgae production: a review. Computers and Electronics in Agriculture, 76(2), 131-147.

[10] Kandilian, R., Pruvost, J., Artu, A., Lemasson, C., Legrand, J., & Pilon, L. (2016). Comparison of experimentally and theoretically determined radiation characteristics of photosynthetic microorganisms. Journal of Quantitative Spectroscopy and Radiative Transfer, 175, 30-45.

[11] Mie, G. (1908). Beiträge zur Optik trüber Medien, speziell kolloidaler Metallösungen. Annalen der physik, 330(3), 377-445.

[12] Yee, K. (1966). Numerical solution of initial boundary value problems involving Maxwell's equations in isotropic media. IEEE Transactions on antennas and propagation, 14(3), 302-307.

[13] Tanev, S., Sun, W., Pond, J., Tuchin, V. V., & Zharov, V. P. (2009). Flow cytometry with gold nanoparticles and their clusters as scattering contrast agents:

FDTD simulation of light–cell interaction. Journal of biophotonics, 2(8-9), 505-520.

[14] Sun, W., Loeb, N. G., & Fu, Q. (2002). Finite-difference time-domain solution of light scattering and absorption by particles in an absorbing medium. Applied optics, 41(27), 5728-5743.

[15] Hall, J. M., Afshar, V. S., Henderson, M. R., François, A., Reynolds, T., Riesen, N., & Monro, T. M. (2015). Method for predicting whispering gallery mode spectra of spherical microresonators. Optics Express, 23(8), 9924-9937.

[16] Santolík, O., Pickett, J. S., Gurnett, D. A., Menietti, J. D., Tsurutani, B. T., & Verkhoglyadova, O. (2010). Survey of Poynting flux of whistler mode chorus in the outer zone. Journal of Geophysical Research: Space Physics, 115(A7).

[17] Bhowmik, A., & Pilon, L. (2016). Can spherical eukaryotic microalgae cells be treated as optically homogeneous? JOSA A, 33(8), 1495-1503.

[18] Bidigare, R. R., Ondrusek, M. E., Morrow, J. H., & Kiefer, D. A. (1990, September). In-vivo absorption properties of algal pigments. In Ocean Optics X (Vol. 1302, pp. 290-302). International Society for Optics and Photonics.

Chapter 3

3 Effects of Turbulent Mixing and Orbitally Shaking on Cell Growth and Biomass Production in Active Fluids[2]

We have previously reported the effects of mixing on bacterial growth. Mixing can be achieved with different methods and in diverse devices. However, the nature of the intimate contact (the main purpose of mixing) made between different substances in a mixing vessel is a strong function of the hydrodynamic that underlies the specific mixing method. This study aimed to compare the growth and biomass yield of cyanobacterium *Synechocystis* sp. CPCC 534 (as a microorganism model) was obtained by three different mixing methods commonly used in life science labs and in the industry, i.e., turbulent stirring (TS), orbital shaking (OS), and simple molecular diffusion (MD). The results revealed that imposing mixing on the culture significantly improved the specific growth rate as well as biomass yield production in comparison with simple molecular diffusion. Mixing obtained by turbulent stirring proved to be more efficient than the one achieved by orbitally shaking, in the production of chlorophyll$_a$ (Chl$_a$) and phycocyanin (PC). The results of this study can help in choosing the appropriate mixing method in life science research.

3.1 Introduction

Cyanobacteria, also recognized as "blue-green algae", are the oldest oxygenic photo-synthesizers on the planet Earth [1] which have a major role in the carbon and oxygen cycles using CO_2 and solar light energy [2, 3]. Cyanobacteria may range from unicellular to complicated multicellular aggregates or filamentous strains and are found in almost any ecological environment on the earth, including soil, freshwater, polar latitudes, and oceans [2,4]. Cyanobacteria are mass cultivated and used in a wide variety of industries including food, pharmaceutical, and cosmetics [5].

The major focus in the mass cultivation of cyanobacteria is the development of high-efficiency, well-controlled, and low-cost systems [6]. Therefore, various types of

---

[2] Published in American Journal of Biomedical Science & Research 2022 15, 396-404.

photobioreactors (PBRs) have been employed in the laboratory and at an industrial scale to cultivate photosynthetic microorganisms. Efficiency, design, and optimization of bioreactors are being impacted by several essential factors including availability of light and nutrients, pH, mixing, and temperature distribution [7]. Among these parameters, mixing is the core factor in creating a homogenous environment for microorganisms' growth and improving cellular contact with chemical nutrients and light. Mixing has two significant effects on the productivity of microorganisms; first, it enhances the penetration of the light in the culture environment, and second, breaks the boundary layers, which improves mass transfer between the microorganisms and the media [8]. However, excessive mixing can enhance the amount of shear stress imposed on the microorganism which may damage the microorganism cells and reduce the growth rate [9].

In laboratory or industrial photobioreactors, mixing can be achieved by various methods including mechanical agitation, bubbling, aeration, pumping, or a combination of these modes [10]. Turbulent stirring (TS) and orbitally shaking (OS) are two major mixing modes commonly used in life science laboratories and industry. Most photobioreactors, and also open ponds, work in turbulent regimes where microorganisms confront turbulent flow in bodies of water [11] or similar liquids[12]. While orbitally shaking is a more suitable mixing technique for shear-sensitive cells [13].

On the laboratory scale, turbulent stirring (TS) can be generated by using a magnetic bar spinning under the effect of an external rotating magnetic field (Figure 3-1(a)). By increasing the rotation speed of the magnetic field, a laminar vortex or an almost uniform turbulent micro-mixing field can be generated. To maintain optimal conditions including temperature and light, turbulent stirrers can be placed in controllable incubators.

The "orbital shaking", is another type of mixing created by the orbital displacement of a vessel, providing a permanent direction regarding an inertial force, along with a rotary path at a fixed angular velocity. This mixing mode is being used in a wide range of industries such as marine, drug production, and also in biological technology [14]. As a piece of equipment, an orbital shaker provides a uniform environment for the cultivation of microorganisms, in the form of a circular shaking motion (Figure 3-1(b)). Orbital shaking

is recommended for providing a low-shear stress environment, and to prevent cellular damage in active fluid suspension [15]. Recently, some models of orbital shakers have been integrated into an incubator to maintain the optimal conditions for the growth of microorganism cells. The velocity field and shear stress distribution in an orbital shaker are less uniform than in a turbulent stirrer. This difference can be expected to provide different cellular growth in these two systems.

In a recent study by Mehdizadeh Allaf, et al. [5], the response of physical and biological characteristics of suspensions of cyanobacterium *Synechocystis* sp. CPCC 534 was investigated in turbulent stirrers under various stirring rates (450, 900, and 1500 rpm). Their results showed that adding mixing, in the form of turbulent stirring, to the culture had a significant impact on the growth, biomass production, yield, and total pigments production compared to the motionless bioreactors. Most previous work had focused on a single mixing method in the laboratory or industrial devices, few studies had compared the efficiency of the two most used mixing modes; turbulent stirring and orbitally shaken, in life science applications. In one study, Fadlallah, et al. [16] carried out experiments with two photobioreactors using two different mixing methods; agitated photobioreactors (APBR) and draft tube airlift photobioreactors (DPBR). The aim was to investigate the performance of each photobioreactor on the *Synechocystis* sp. PCC 6803 specific growth rate and pigments production under different hydrodynamic shear stress rates (0 to 400 mPa). Their results indicated that limited shear stress rates (less than 30 mPa in APBR and between 80 and 180 mPa in DPBR) can break the groups of cell colonies, and therefore, improve the growth rate and pigment production. However, higher hydrodynamic shear stress did not show a more significant impact on the growth rate of cyanobacterium *Synechocystis* sp. PCC 6803.

In this study, the efficiency of turbulent stirring (TS) and orbitally shaking (OS) mixings versus a molecular diffusion (MD, no mixing) mode on the growth of cyanobacterium *Synechocystis* sp. CPCC 534 was investigated. Cell growth was used as a proxy to compare different mixing modes. To perform this study, *Synechocystis* sp. CPCC 534 was used in the working suspensions.

Among different strains of cyanobacteria, *Synechocystisis*, a unicellular, freshwater cyanobacterium, is utilized as a model microorganism for investigating photosynthesis, energy metabolism, molecular biology, biofilm formation, and environmental stress [17,18,19]. The entire genome of *Synechocystis* sp. strain PCC 6803 was sequenced, for the first time, in 1996 by Kaneko and co-workers [20]. The cellular surface of the *Synechocystis* is covered with non-flagellar appendages, known as pili or fimbriae, which assist in adhesion, motility, biofilm structure, and DNA uptake [21]. Cyanobacterium *Synechocystis* sp. can navigate toward or away from favorable or unfavorable stimuli. For performing this movement, the cells convert nutrient chemical energy into mechanical work for driving the flow [5,22]. The characteristics of "active fluids" (bacterial suspensions) are different from those of conventional or "passive" fluids. In passive fluids, pressure, velocity, or temperature gradients are driving forces for the flow, while in active fluid, cells as the microstructural elements of the fluid, use chemical nutrients or light to stimulate microorganism cells for running metabolic functions, and create the directed motions called chemotaxis and phototaxis respectively [16,19,23,24].

3.2 Materials and Methods

3.2.1 Strain and Culture Conditions

Synechocystis sp. CPCC 534 wild type was purchased from the Canadian Phycological Culture Center (Waterloo, ON, Canada), and was cultured in chemically defined liquid BG11 medium at 20 ± 1 °C. The initial cell concentration was 5×10^5 cells. mL^{-1} and the culture were carried out under the light cycle of 12/12 h and photon flux of 50 ± 5 $\mu mole.m^{-2}. s^{-1}$.

3.2.2 Mixing Modes

Cells were cultivated under controlled conditions in three different mixing modes. In the turbulent stirring (TS) mode, digitally controlled magnetic stirrers (VWR Canada) were used to create turbulent mixing inside the lab photobioreactors placed in a fully controlled PHCbi incubator. Cylindrical magnetic stirring bars with a diameter of 7.9 mm and a length of 19.8 mm were employed to mix the sample. In the Orbitally shaking (OS) mode, the photobioreactors were placed in a fully controlled Eppendorf Innova S44i incubator shaker.

In the Molecular Diffusion (MD) mode, the photobioreactors were placed standstill inside compartments in well-controlled conditions. The light intensity and temperature were set at 50 ± 5 µmole.m^{-2}. s^{-1} and 20 ± 1 °C, respectively for all three modes. The turbulent stirring and orbitally shaking mixing devices are schematically shown in Figure 3-1.
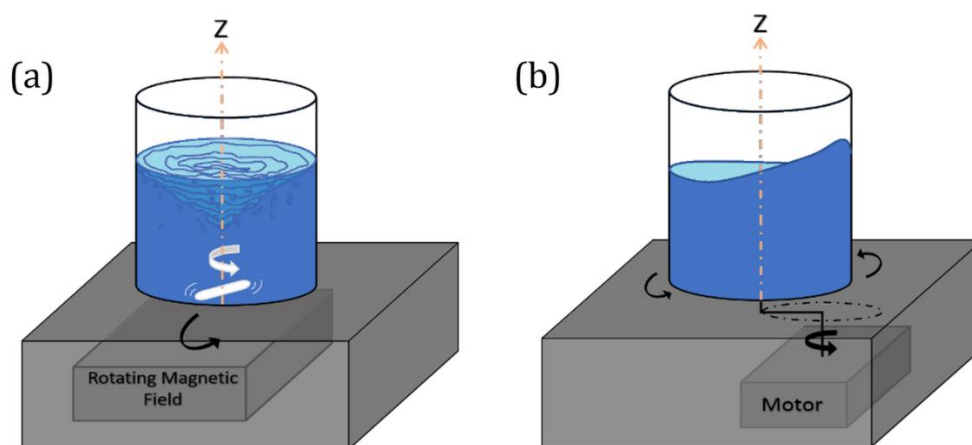
Figure 3-1:Schematic illustration of (a) a turbulent stirring (ST) mixer, and (b) an orbital shaker (OS) mixer.

3.2.3 Experimental Protocol

Each mixing mode experiment was performed in triplicates and was carried out in 125 mL Pyrex flask photobioreactors. The optical density (OD) of *Synechocystis* sp. CPCC 534, as a proxy of growth, was measured daily at 750 nm wavelength using a Spectronic 200E spectrophotometer. A calibration curve was prepared to estimate the number of cyanobacteria cells per cubic milliliter. For this purpose, a dilution series of *Synechocystis* sp. CPCC 534, all grown at the same temperature and light intensity, were prepared and the optical density and the number of cells.ml^{-1} were measured using the Spectronic 200E spectrophotometer and a Hausser Scientific hemocytometer, respectively. The calibration curve (also known as standard curves) was generated to calculate the number of cyanobacteria cells in the sample solution from the OD measurements.

3.2.4 Calculation of Cynobactrium Specific Growth Rate (r) and Doubling Time (k)

The specific growth rate (r) of the microorganism population was calculated for the exponential growth phase to assess the rate of rising in cells number per time by using equation (1) [25].

$$r = \frac{ln\ N_t - ln\ N_0}{\Delta t} \qquad (1)$$

where N_0 is the number of microorganism cells at the starting of a period, N_t is the microorganism cells number at the end of the time period, and Δt is the duration of the time period ($t_t - t_0$).

The specific growth rate (r) is used to estimate the number of cell divisions per day known as doubling per day (k), by equation (2) [25].

$$k = \frac{r}{ln2} = \frac{r}{0.6931} \qquad (2)$$

The cell yield of *Synechocystis* sp. CPCC 534 was computed by integrating the area under the growth curve from the beginning of the exponential phase up to the end of the stationary phase. A photometric scan of *Synechocystis* sp. CPCC 534 was conducted using a Spectronic 200E spectrophotometer and the absorbance peaks for Chlorophyll$_a$ (Chl$_a$) and Phycocyanin (PC) were detected at 683 nm and 630 nm, respectively. The Chlorophyll$_a$ (Chl$_a$) and Phycocyanin (PC) production were evaluated by the mean value of all data points obtained during the exponential growth phase.

3.2.5 Statistical Analysis

The significant differences in growth, doubling per day, yield, Chl$_a$, and PC production were investigated by a one-way ANOVA followed by the Tukey multiple comparison tests, and $p < 0.05$ was evaluated as significant. The relationship between the aforementioned variables was calculated by Pearson correlation (R). The correlation coefficients of 90-100 and 70-90 were considered very high and high, respectively. The statistical analyses were calculated by OriginPro 2017 (OriginLab Corporation, Northampton, MA, USA).

3.3 Results

3.3.1 Standard Curve

In the first step, a serial dilution of *Synechocystis* sp. CPCC 534 was prepared. Then, the OD of each sample was measured by the spectrophotometer and the number of *Synechocystis* sp. cells in each sample was counted by hemocytometer under Nikon microscope (Nikon ECLIPSE Ti2 inverted microscope). Then, the calibration curve was plotted, as shown in Figure 3-2. By using the obtained equation from the calibration curve, *Synechocystis* sp. CPCC 534 concentration was calculated (Figure 3-2).

The plot shows Biomass (cells.ml^{-1}) $\times 10^6$ on the y-axis (0 to 300) versus OD(750 nm) on the x-axis (0 to 10), with the equation $y = 25.757 \times 10^6 x$ and $R^2 = 0.9638$.
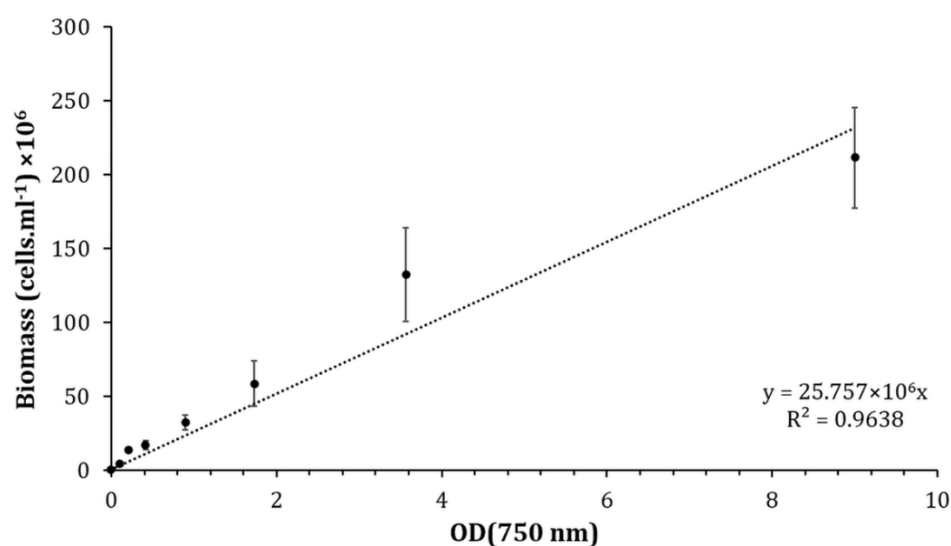
Figure 3-2:Calibration curve of *Synechocystis* sp. CPCC 534 solutions.

3.3.2 Comparison of Cell Growth Under the Three Mixing Modes

A growth curve, shown in Figure 3-3, was constructed from the experimental data to monitor the increase in the number of *Synechocystis* sp. CPCC 534 cells during a period of 20 days. In the bacterial culture, once the cells adapted themselves to the new environment, they moved from the lag phase into a logarithmic growth phase, which continued up to reaching a linear growth phase, then followed by the stationary phase. The self-shading of cells impedes the accessibility of microorganism cells to the light source. Figure 3-3 shows the *Synechocystis* cells that were grown under TS and OS mixing modes entered the logarithmic growth phase around day 4, while the motionless culture entered the

logarithmic phase around day 7. The faster start of the exponential phase in mixed cultures can be attributed to the abundance of nutrients and light available to cells due to their spatial displacement.

In the same manner, the cultures grown under TS and OS mixing modes reached stationary phase later than the cultures grown in motionless PBRs; day 15 for the former and around days 12 or 13 for the latter. Here again, efficient movement of cells inside the batches, caused by mixing, allowed the bacteria to uptake nutrients from unexplored regions and to be exposed to light more efficiently compared to the motionless cultures. A similar pattern was obtained by Fadlallah, et al. [26]. Their results showed that the biomass of *Synechocystis* sp. PCC6803 was increased considerably under turbulent stirring conditions (360 rpm) compared to motionless samples. Monteila, et al. [27] also observed cell densities improvement in the orbitally shaken bioreactor. They reported increasing the shaking rotation speed from 180 to 220 rpm could improve the cell densities from 5×10^5 to 7×10^6 cell.ml^{-1}.

Cultures grown under TS and OS mixing modes also showed a better specific growth rate (*r*) than cultures grown under motionless conditions (Figure 3-4(a)). Nevertheless, the specific growth rate for TS was slightly higher than that of OS, suggesting that turbulent stirring was more efficient in mixing the active fluid than orbitally shaking. A closer analysis of the fluid mechanics of TS and OS modes (not shown here) confirmed the superiority of TS mixing above and over that of OS mixing. However, the OS growth curve overtook the TS growth curve at the beginning of the linear phase and overlapped with it for the whole period of stationary growth. The later start of the logarithmic phase, smaller specific growth rate, and earlier start of the linear phase in motionless culture resulted in a significant lag in biomass yield, as is shown in Figure 3-5.
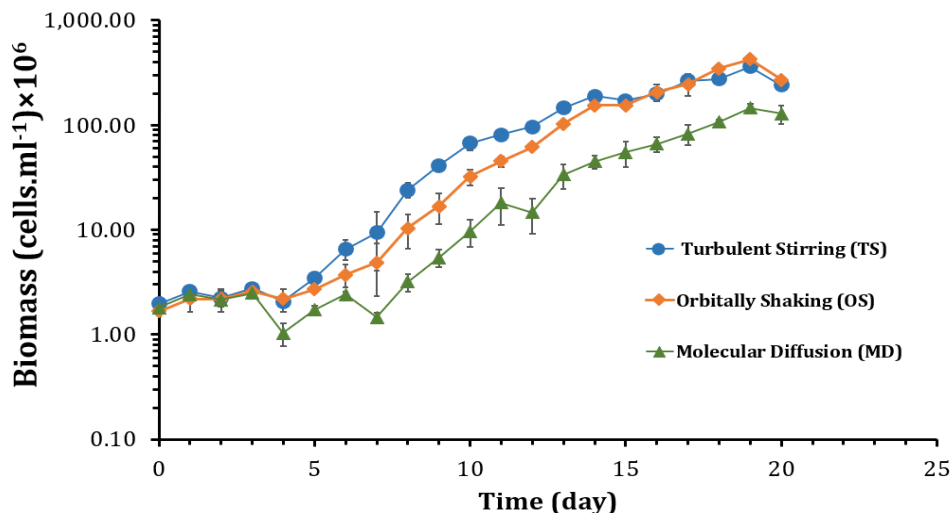
Figure 3-3:Growth curve of *Synechocystis* for three different mixing modes.

The specific growth rate and doubling per day for the three mixing modes were estimated during the exponential phase, and the results are presented in Figure 3-4. The results show that under mixing conditions, there is a significant change ($p<0.05$) in a specific growth rate and doubling per day of *Synechocystis* sp. in comparison to non-mixing (motionless) conditions. Regarding the efficiency of the two mixing modes, there was not a major difference between the turbulent stirring and orbitally shaking modes as observed by the specific growth rate and doubling per day (Figure 3-4). However, the difference is more apparent in Chl_a and PC production (Figure 3-6). Mehdizadeh Allaf, et al. [5] showed that the use of TS mixing increased the specific growth rate ($p < 0.05$) and doubling per day ($p < 0.05$) of *Synechocyctis* sp. cells significantly compared to stationary conditions, which is in the agreement with the present results. Fadlallah, et al. [16] also concluded that applying gentle turbulent stirring (TS) intensity (shear stress intensity < 30 mPa) enhanced the exponential growth rate, around 50%, compared to non-turbulent stirring cases.
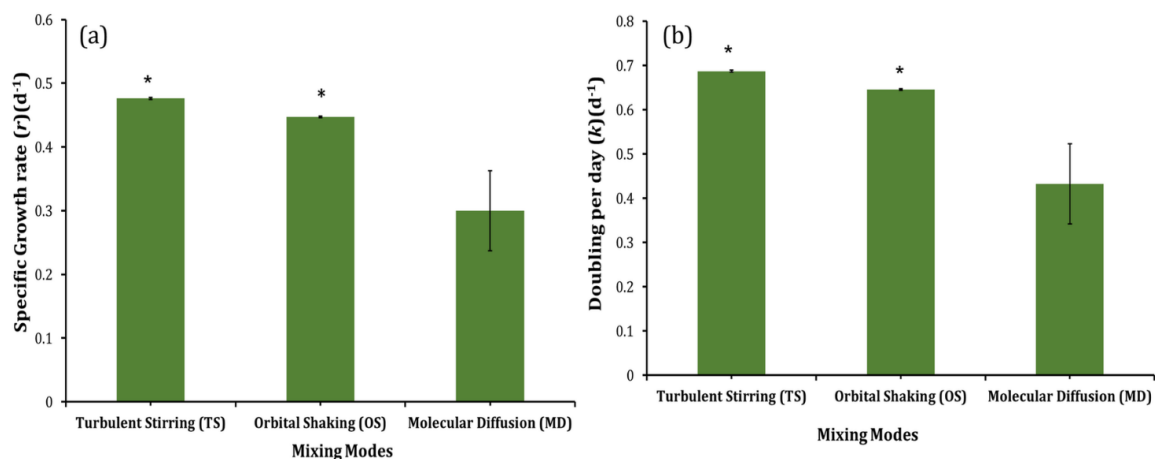
Figure 3-4: (a) Specific growth rate (*r*) and (b) Doubling per day (*k*) of *Synechocystis* sp. CPCC 534 under various mixing conditions. * indicates the significant effect at the level of 0.05 among different mixing modes.

The *Synechocystis* sp. CPCC 534 yield, under different mixing conditions, is plotted in Figure 3-5. The biomass yield production was significantly ($p < 0.05$) higher when cells were grown under mixing conditions. It showed an increase of over 213% for TS mode and 197% for OS mode compared to motionless cultures, in agreement with the findings in [5]. Mixing contributes to microorganism growth in several ways. It obviates the self-shading of microorganisms, breaks the boundary layer in the culture system, and facilitates access to CO_2, nutrients, and light.[28].

Figure 3-5:Profiles of yield for *Synechocystis* sp. CPCC 534 under different mixing modes. * indicates the significant effect at the level of 0.05 among different mixing modes.

Cyanobacteria also produce various pigments like Chlorophyll$_a$ (Chl$_a$) and Phycocyanin (PC) [29]. The mixing effect was investigated on the production of Chl$_a$ and PC and the results were plotted in Figure 3-6. Experiments under three different mixing modes showed that turbulent stirring enhanced significantly ($p < 0.05$) the production of Chl$_a$ in comparison to other modes. Under the defined mixing conditions, the production of PC was measured at the wavelength of 630 nm, and Chl$_a$ at 683 nm. Phycocyanin (PC) is recognized as a photosynthetic pigment-protein complex from the phycobiliprotein groups, which is found in most cyanobacteria and red algae [30]. From the measurement of the *Synechocystis* sp. CPCC 534 OD in the exponential phase, the average PC production was estimated and shown in Figure 3-6(b). Production of PC under turbulent stirring mode was increased significantly ($p < 0.05$) in comparison to other modes, similar to Chl$_a$ production. The effect of turbulent mixing on Chl$_a$ and PC production was more evident in comparison to orbitally shaking mode.

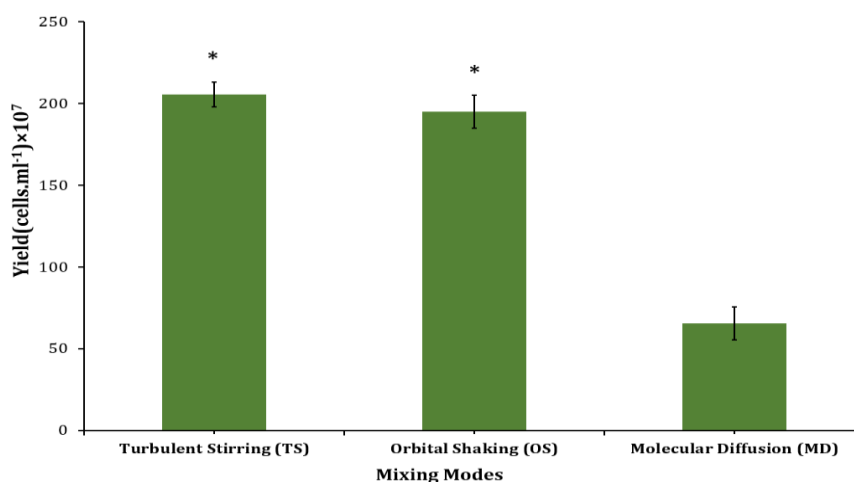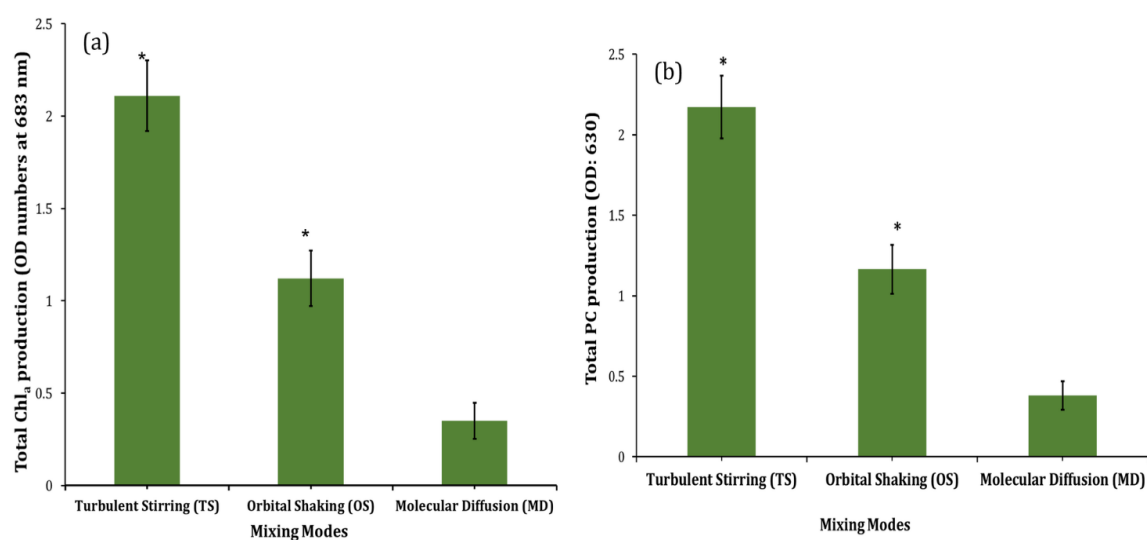Figure 3-6:(a) Profiles of Chl$_a$ production and (b) PC production of *Synechocystis* sp. CPCC 534 under various mixing conditions. * indicates the significant effect at the level of 0.05 among different mixing modes.

The correlations between yield production, Chl$_a$, PC production, and specific growth rate (*r*), were also calculated and the Pearson correlation coefficient (R) was computed; the results are plotted in Figure 3-7. Strong positive linear correlations were found between the couples of correlated parameters; including the specific growth rate and yield production

(Pearson's r: 0.996), specific growth rate and Chl_a production (Pearson's r: 0.928), specific growth rate, and PC production (Pearson's r: 0.932), and Chl_a and yield production (Pearson's r: 0.887). Overall, these findings agree with the findings reported in [31] and. [5]. Ajala, et al. [31] reported that the maximum biomass concentration and productivity were achieved under turbulent stirring (TS) mode at 1400 rpm. The data presented by Mehdizadeh Allaf, et al. [5] showed a similar trend in the selection of mixing methods to produce Chl_a, PC, and yield.
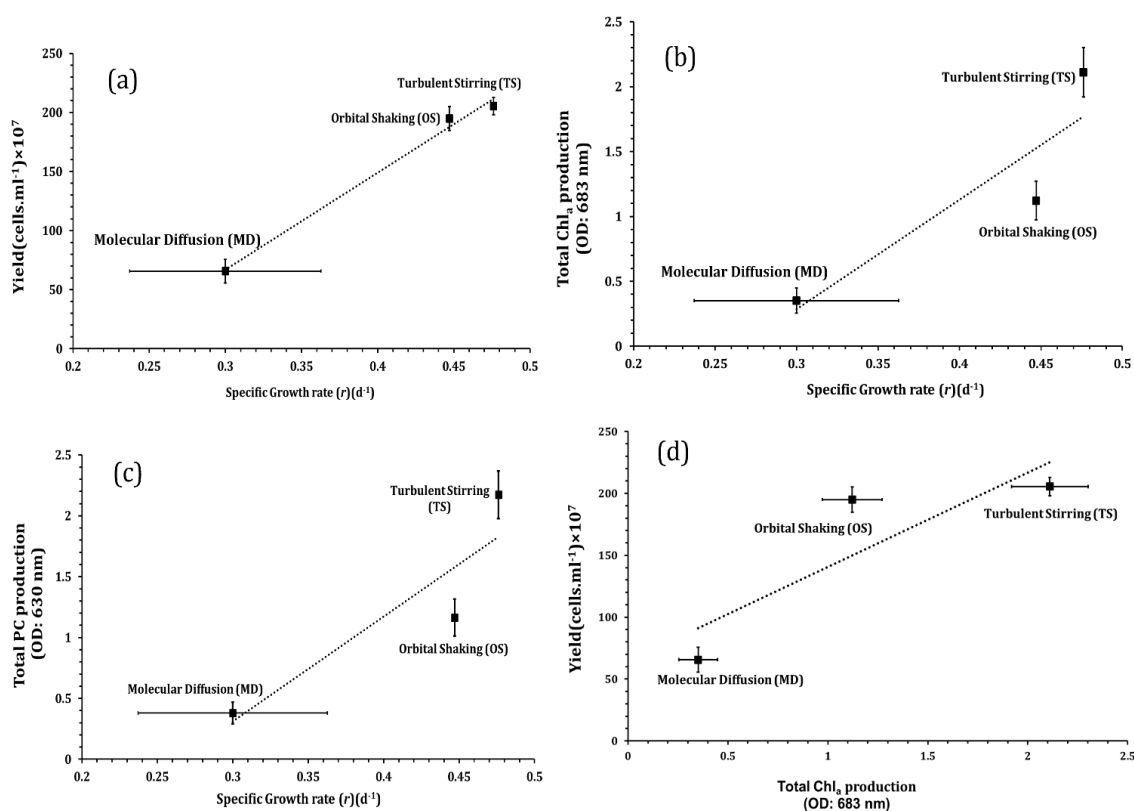
Figure 3-7:The correlation between specific growth rate and yield (a), specific growth rate and Chl_a production (b), specific growth rate and PC production (c), and Chl_a production and yield (d) for *Synechocystis* sp. CPCC 534 under different mixing mod

3.4 Discussion

The results of this study suggest that mixing by turbulent stirring is more efficient than mixing by orbitally shaking, as appears in most cell growth metrics, This difference can be attributed to the dissimilarity in the fluid motion and wall shear stress distribution between

the two mixing modes. In orbitally shaking, the fluid undergoes a solid body rotation about the central axis of the cylindrical vessel, and therefore, most of the fluid and suspended cell particles' movement is concentrated in the peripheral zone of the reactor. In solid body rotation, the fluid body is not sheared thus, the relative distance between fluid particles remains constant. Fluid particles trapped in the solid body rotation zone have a very limited chance (except by molecular diffusion) to visit other places and other fluid particles in the culture medium for nutrient uptake, especially getting close to the free surface and wall vicinity where they can be exposed to light. While this difference can affect the logarithmic growth period (shorter in TS than in OS) however, the OS growth curve catches up to this delay and reaches the TS growth curve in the stationary phase.

Comparable types of orbiting reactors, such as orbiting dishes, are used in endothelial cell studies. In this configuration, the height of the culture medium is smaller than the one considered in this study. In the endothelial cell application, one is interested in the effects of wall shear stress on the response of anchored cells exposed to culture medium flow. Nevertheless, the hydrodynamic of the problem remains similar to the one studied here.

It is expected that the rotating speed of the orbital shaker has a chief influence on the mixing efficiency with the OS method, the problem that was not addressed here. Ojo, et al. [32] evaluated the performance of microalgae cultivation (*Chlorella sorokiniana*) under orbitally shaken photobioreactors at three shaking frequencies 70, 90, and 180 rpm. They concluded that more efficient biomass production was achieved at 180 rpm. However, this study did not show whether there is a limit to this efficiency increase with rotation frequency. Ajala, et al. [31] also studied the effect of orbitally shaking mode at different frequencies on the Chl_a production from *Dunaliella salina*, *Nannochloropsis oculata*, *Oocystis minuta*, and *Neochloris conjuncta*. In all microalgae strains, their results showed that the highest Chl_a was achieved at 200 rpm.

3.5 Conclusions

In this study, the impact of two methods of mixing (turbulent stirring and orbitally shaking), on various growth metrics of *Synechocystis* sp. CPCC 534 was investigated and compared with stationary (motionless) culture. The results revealed that mixing of

Synechocystis cultures can improve growth rate, doubling per day, yield, and Chl$_a$ production in comparison with the cultures where no mixing was imposed. Mixing by turbulent stirring seems to be more efficient than mixing by orbitally shaking, as appears in most of the cell growth metrics, this difference can be attributed to the dissimilarity in the fluid motion and wall shear stress distribution between the two mixing modes. Mixing enhances the nutrient uptake as well as the homogeneity of the light and temperature distribution in the culture.

3.6 References

[1] Shevela, Dmitriy. (2011). Adventures with cyanobacteria: a personal perspective. Frontiers in plant science, 2-28.

[2] Stucken, Karina, Robin Koch, and Tal Dagan. (2013). Cyanobacterial defense mechanisms against foreign DNA transfer and their impact on genetic engineering. Biological research 46.4: 373-382.

[3] Sebesta, Jacob, Allison Werner, and Christie Ann Marie Peebles. (2019). Genetic engineering of cyanobacteria: Design, implementation, and characterization of recombinant *Synechocystis* sp. PCC 6803. Microbial Metabolic Engineering. Humana Press, New York, NY. 139-154.

[4] Conradi, Fabian D., Conrad W. Mullineaux, and Annegret Wilde. (2020). The role of the cyanobacterial type IV Pilus Machinery in finding and maintaining a favorable environment. Life 10.11: 252.

[5] Mehdizadeh Allaf, Malihe., Habib, Zahra., de Bruyn, John. R., DeGroot, Christopher. T., & Peerhossaini, Hassan. (2022). Rheological and Biophysical Properties of Living Fluids Under Shear: Active Suspensions of *Synechocystis* sp. CPCC 534. Journal of Fluids Engineering, 144(2).

[6] Wolf, J., et al. (2016). Multifactorial comparison of photobioreactor geometries in parallel microalgae cultivations. Algal Research 15: 187-201.

[7] Samadi, Zahra., Johlin, Eric., DeGroot, Christopher., & Peerhossaini, Hassan. (2021). Modelling Optical Properties of Algae Using the Finite-Difference Time-Domain Method. In Fluids Engineering Division Summer Meeting (Vol. 85307, p. V003T05A016). American Society of Mechanical Engineers, USA.

[8] Grobbelaar, Johan U. (1991). The influence of light/dark cycles in mixed algal cultures on their productivity. Bioresource technology 38.2-3: 189-194.

[9] Wang, Chinchin, and Christopher Q. Lan. (2018). Effects of shear stress on microalgae– A review. Biotechnology Advances 36.4: 986-1002.

[10] Wang, Bei, Christopher Q. Lan, and Mark Horsman. (2012). Closed photobioreactors for production of microalgal biomasses. Biotechnology advances 30.4: 904-912.

[11] Rusconi, Roberto, Melissa Garren, and Roman Stocker. (2014). Microfluidics expanding the frontiers of microbial ecology. Annual review of biophysics 43: 65-91.

[12] Wang, Chinchin, and Christopher Q. Lan. (2018). Effects of shear stress on microalgae– A review. Biotechnology Advances 36.4: 986-1002.

[13] Lehmann, Nicolai, Heiko Rischer, Dieter Eibl, and Regine Eibl. (2013). Wave-mixed and orbitally shaken single-use photobioreactors for diatom algae propagation. Chemie Ingenieur Technik 85.1-2: 197-201.

[14] Reclari, Martino, et al. (2014). Surface wave dynamics in orbital shaken cylindrical containers. Physics of Fluids 26.5: 052104.

[15] Alpresa, Paola, Spencer Sherwin, Peter Weinberg, and Maarten van Reeuwijk. (2018). Orbitally shaken shallow fluid layers. I. Regime classification. Physics of Fluids 30.3: 032107.

[16] Fadlallah, H., et al. (2019). Active Fluids: effects of hydrodynamic stress on growth of self-propelled fluid particles. Journal of Applied Fluid Mechanics 13.2: 561-570.

[17] Heidorn, Thorsten, et al. 2011. Synthetic biology in cyanobacteria: engineering and analyzing novel functions. Methods in enzymology. Vol. 497. Academic Press, 539-579.

[18] Xu, Chen, et al. (2021). Global landscape of native protein complexes in *Synechocystis* sp. PCC 6803. Genomics, proteomics & bioinformatics.

[19] Vourc'h, Thomas, et al. (2018). Slowdown of surface diffusion during early stages of bacterial colonization. Physical Review E 97.3: 032407.

[20] Kaneko, Takakazu, et al. (1995). Sequence analysis of the genome of the unicellular cyanobacterium *Synechocystis* sp. strain PCC6803. I. Sequence features in the 1 Mb region from map positions 64% to 92% of the genome. DNA research 2.4: 153-166.

[21] Schuergers, Nils, and Annegret Wilde. (2015). Appendages of the cyanobacterial cell. Life 5.1: 700-715.

[22] Saintillan, David. (2018). Rheology of active fluids. Annual Review of Fluid Mechanics 50: 563-592.

[23] Alexandre, Gladys. (2015). Chemotaxis control of transient cell aggregation. Journal of bacteriology 197.20: 3230-3237.

[24] Varuni, P., Shakti N. Menon, and Gautam I. Menon. (2017). Phototaxis as a collective phenomenon in cyanobacterial colonies. Scientific reports 7.1: 1-10.

[25] Wood, A. Michelle, R. C. Everroad, and L. M. Wingard. (2005). Measuring growth rates in microalgal cultures. Algal culturing techniques 18: 269-288.

[26] Fadlallah, Hadi, Peerhossaini, Hassan, DeGroot, Christopher, and Jarrahi, Mojtaba. (2021). Motility response to hydrodynamic stress during the growth cycle in active fluid suspensions. Journal of Fluids Engineering 143.7.

[27] Monteil, Dominique T., et al. (2013). Disposable 600-mL orbitally shaken bioreactor for mammalian cell cultivation in suspension. Biochemical engineering journal 76: 6-12.

[28] Mehdizadeh Allaf, Malihe, et al. (2020). Physical and Rheological Properties of Active Fluids Under Shear Stress: Suspensions of *Synechocystis*. Fluids Engineering Division Summer Meeting. Vol. 83723. American Society of Mechanical Engineers, USA.

[29] Saini, Dinesh Kumar, Sunil Pabbi, and Pratyoosh Shukla. (2018). Cyanobacterial pigments: perspectives and biotechnological approaches. Food and chemical toxicology 120: 616-624.

[30] Safari, Reza, Zeynab Raftani Amiri, and Reza Esmaeilzadeh Kenari. (2020). Antioxidant and antibacterial activities of C-phycocyanin from common name Spirulina platensis. Iranian journal of fisheries sciences 19.4: 1911-1927.

[31] Ajala, Sheriff Olalekan, and Matthew L. Alexander.(2020). Evaluating the effects of agitation by shaking, stirring and air sparging on growth and accumulation of biochemical compounds in microalgae cells. Biofuels: 1-11.

[32] Ojo, E. O., Hadiza Auta, Frank Baganz, and G. J. Lye. (2014). Engineering characterization of a shaken, single-use photobioreactor for early-stage microalgae cultivation using *Chlorella sorokiniana*. Bioresource technology 173: 367-375

Chapter 4

4 Investigation of *Synechocystis* sp. CPCC 534 Motility during Different Stages of the Growth Period in Active Fluids[3]

The motility behavior of suspended microorganisms plays an essential role in the properties of active fluids. Despite the important progress in our understanding of microorganisms' motility in recent years, there are still several open questions about the dynamics of cell motility in active suspensions. Of special interest is the relationship between cell motility and age. In this study, cyanobacterium *Synechocystis* sp. CPCC 534 was used as the model microorganism, and the cell trajectories were tracked for 78 days during the cell growth period. Results showed that the length of cell trajectories had substantially increased from the exponential growth phase to the stationary phase and had declined at the end of the stationary phase. Similar trends were observed for the cells' mean squared displacement (MSD), the time-dependent diffusion coefficient of cell suspensions, and the cell displacement probability density function (PDF). These results suggest that the cellular age of microorganisms has a significant effect on various metrics of cell motility and, therefore, can impact the transport properties of active suspensions.

4.1 Introduction

Suspensions of photosynthetic microorganisms are often described as "living" or "active" fluids. Active fluids contain a collection of cells, or active particles, suspended in a fluid medium, where the cells can convert chemical nutrients into mechanical energy to drive the flow. In an environment with uniform nutrient distribution, cells move in a random walk pattern, with high-motility "run" periods separated by low-motility "tumble" periods [1,2]. However, in the presence of gradients in nutrient or light distribution, cells move preferentially in the direction opposite to the gradient (i.e., from low to high availability of

---

[3] Published in Processes 2023, 11(5), 1492; https://doi.org/10.3390/pr11051492

nutrients/light). These processes are called chemotaxis and phototaxis for movements driven by nutrients and light, respectively [1,3,4].

Fluid flow, cell motility, microbe biokinetics, and radiative transport are among the important parameters in designing and optimizing photobioreactors used for cell growth in active fluids [5–8]. Among these factors, motility is one of the major ones in providing favorable conditions for microorganisms' nutrient uptake and light harvesting and, therefore, enhancing biomass growth [9–11]. Moreover, motility plays a vital role in the formation of biofilms. In the initial period of biofilm formation, bacteria proceed toward and adhere to wet solid surfaces. This adhesion allows for bacterial surface colonization and creates protective biofilms. It is essential to understand the motility of the microorganisms to identify the adhesion rate and the subsequent colonization process [12–15].

In a study by Shoesmith [16], a simple quantitative method was applied to measure the motility of *Pseudomonas viscosa*, *Bacillus brevis,* and *Escherichia coli* by counting the number of bacteria passing through a small aperture during a certain period of time. The results revealed that bacterial motility is proportional to the concentration and the mean velocity of cells in the suspension. In another study by Kim [17], the impact of motility on the diffusivity of two bacteria: *Pseudomonas aeruginosa*, a motile cell, and *Klebsiella pneumoniae*, a non-motile cell, was investigated through capillary tubes. It was found that the rate of diffusion of motile cells was 1000 times faster, and the diffusion coefficient was 2.3 times higher compared to non-motile bacteria. Arora et al. [18] carried out experiments in an agitated bioreactor to examine the motility behavior of *E. Coli* as a function of its growth dynamics. They observed that the microorganisms' motility was reduced by increasing the number of cells in the culture. This was concluded to be a result of a reduction in the "running" phase of the motility pattern. In a recent study by Fadlallah et al. [19], the motility behavior of active fluids (suspensions of *Chlamydomonas reinhardtii* and *Synechocystis* sp.) was studied under different intensities of hydrodynamic shear stress for 15 days. Their results revealed that hydrodynamic shear stress had a considerable effect on the motility of *C. reinhardtii* during the exponential growth period and enhanced the cellular swimming velocity of microorganism cells. On the other hand, *Synechocystis* did

not exhibit any specific trend during the growth cycle and showed higher resistance to shear stress. This could be explained by the lack of flagella in *Synechocystis* and/or its small size in comparison to *C. reinhardtii* [19].

In bacterial cultures, once the cells have adapted themselves to the new environment, they move from the lag phase (where they are largely dormant) into an exponential growth phase. The exponential phase continues until the linear growth phase is reached, wherein the cell growth is reduced due to shading or nutrient depletion. At the end of the linear growth phase, bacteria enter the stationary phase in which the number of cell divisions balances with cell death, and the population of microorganisms remains constant in time. As nutrients deplete and waste materials inside the medium rise, the microorganism cells lose the ability to perform metabolic functions, and then the number of dead cells continues to increase and eventually exceeds that of live cells (decline/death phase) [20,21].

To the best of the authors' knowledge, most previous studies have emphasized the motility of various microorganisms for a short time period during the cell's exponential growth phase [19,22]. In this study, the motility of *Synechocystis* sp. CPCC 534 was used as a model organism to study the impacts of cell age on motility over longer periods of time (i.e., up to 78 days), going far beyond the exponential and stationary growth phases. For this purpose, the cell transport parameters such as cell velocity, mean squared displacement (MSD), time-dependent diffusion coefficient D (t), and displacement probability density function (PDF) were calculated [23]. To accomplish this, bacteria trajectories were extracted from the video footage recorded on an inverted video microscope. The average swimming velocity over a given time period was then calculated and correlated with the age of bacteria obtained from the growth curve [19]. These findings have practical implications for biomass and sustainable resource engineering, particularly with regard to designing bioreactors for mobile microorganisms, facilitating the movement of microorganisms in photobioreactors, and regulating the development of biofilms [19,23].

The model microorganism used in this study, *Synechocystis* sp., is a strain of unicellular, non-nitrogen-fixing freshwater cyanobacteria that acquires its energy for movement through photosynthesis [3,24,25]. It is one of the most prevalent microorganisms for

studying the fundamental phenomena in bacterial flows for two important reasons: its availability and capability to have both phototrophic growths by oxygenic photosynthesis during light periods and heterotrophic growth by glycolysis and oxidative phosphorylation during dark periods [26–28]. Such bacteria are naturally motile, and they can move toward favorable environmental conditions (such as light, nutrients, and temperature) or move away from unfavorable ones by using a variety of motility machinery components such as pili [18,29,30].

4.2 Materials and Methods

4.2.1 Culture Conditions

Synechocystis sp. CPCC 534 wild type was obtained from the Canadian Phycological Culture Center (Waterloo, Canada). The stock culture was maintained and grown in BG11 medium [31] at 20 ± 1 °C. Suspensions were exposed to a photon flux of 50 ± 5 μmole.m^{-2}.s^{-1} with a light cycle of 12/12 h. The initial experimental concentration of *Synechocystis* sp. in the media was adjusted to 1×10^7 cells.mL^{-1}. To provide a homogeneous environment for the cell growth and to prevent cell sedimentation inside the photobioreactor, a magnetic stirrer (VWR Canada) with stirring bars of 7.9 mm diameter and 19.8 mm length at 360 rpm rotation speed was employed. To control environmental conditions, the photobioreactors were placed in a fully controlled incubator (PHCbi) [24,32].

4.2.2 Experimental Protocol

Experiments were carried out in triplicate and were performed in 125 mL Pyrex flask photobioreactors. A Spectronic 200E spectrophotometer was used to measure the optical density (OD) of *Synechocystis* sp. CPCC 534 suspensions daily at 750 nm wavelength as a proxy for cell growth. The wavelength of maximal absorption for chlorophyll-a was found to be at 670 nm and for chlorophyll-b at 652 nm. To calculate the reference values, the intensity of the transmitted light at 750 nm was measured. The absorption at 750 nm results only from chlorophyll-free structures in the cells. A calibration curve was used to calculate the number of *Synechocystis* sp. cells per milliliter in a sample solution. Therefore, a dilution series of *Synechocystis* sp. CPCC 534, cultivated at the same

environmental growth conditions, were prepared, and the optical density and the cell density (number of cells.mL^{-1}) were measured using the Spectronic 200E spectrophotometer (Thermo Fisher Scientific, CA) and a Hausser Scientific hemocytometer, respectively [24,32].

4.2.3 Calculation of *Synechocystis* sp. Growth Rate (*r*) and Doubling Time (*k*)

The growth rate (*r*) of the *Synechocystis* sp. cells was estimated through the logarithmic growth phase by Equation (1) [33].

$$r = \frac{ln\ N_t - ln\ N_0}{\Delta t} \tag{1}$$

where N_0 is the number of cells at the beginning of an observation period, N_t is the cell population at time t, and Δt is the duration of the observation period ($t_t - t_0$).

The growth rate (*r*) is used to evaluate the number of cell divisions per day, known as doubling per day (*k*), by Equation (2) [33].

$$k = \frac{r}{ln2} = \frac{r}{0.6931} \tag{2}$$

4.2.4 Video Microscopy and Image Acquisition

An aliquot of 40 µL of suspension sample was placed in the cavity of a concave slide, covered with a glass coverslip, and finally sealed with grease to form a micro slide. To observe and record cell displacement in the closed micro slide, it was placed with its glass coverslip side on the stage of an inverted optical Olympus IX83 video microscope equipped with a 40X magnification lens and a CCD camera. The bacteria settled on the flat side of the micro slide after about 30 min. Then the cells' movement in the sample was recorded in "vsi" format for 50 min at a rate of one frame per second. The resolution of the CCD camera was 325 nm per pixel [1,23].

4.2.5 Analysis of Cell Dynamics

The recorded video footage was post-processed with Fiji ImageJ software (1.53c, Wayne Rasband) to acquire binary images. The binary video footage in "tif" format was then used

for particle tracking [34] using MATLAB Version: 9.11.0.2207237 (R2021b) (Natick, Massachusetts, USA). Cell tracking was carried out in three steps: first, all cells' x and y positions were extracted from the recorded video footage, frame by frame, to determine cell trajectories. Then, cell motility was estimated from the average cell velocity by eliminating the non-motile cells (or other debris) in the calculations. Finally, the mean squared displacement (MSD), diffusion coefficient, and displacement probability density function (PDF) were calculated to evaluate the dynamics of *Synechocystis* sp. CPCC 534 [35].

4.2.6 Statistical Analysis

For the statistical analysis, the "statsmodels" package in Python was used with 95% confidence intervals, and $p < 0.05$ was evaluated as significant [36].

4.3 Results and Discussion

4.3.1 Calibration Curve

The calibration curve was established by plotting the OD versus the number of *Synechocystis* sp. CPCC 534 cells, as is shown in Figure 4-1. The concentration of *Synechocystis* sp. CPCC 534 in all subsequent experiments was determined using the equation derived from the calibration curve (Figure 4-1) [24].
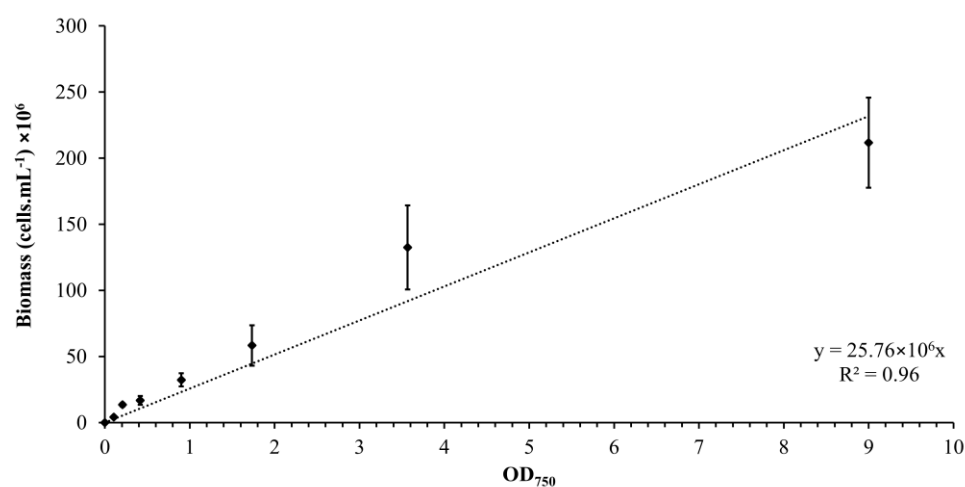
Figure 4-1:Calibration curve relating the OD750 to the biomass concentration for *Synechocystis* sp. CPCC 534 suspensions (n = 3 ± SD).

4.3.2 Growth Curve

The growth curve, Figure 4-2, represents the variation of live *Synechocystis* sp. CPCC 534 cells number during a 78-day growth period. In the present culture, *Synechocystis* sp. cells immediately moved to the exponential (log) growth phase and reached the linear phase after eight days. The transition from the exponential to linear phase is evident from the slope change in the growth curve [35].
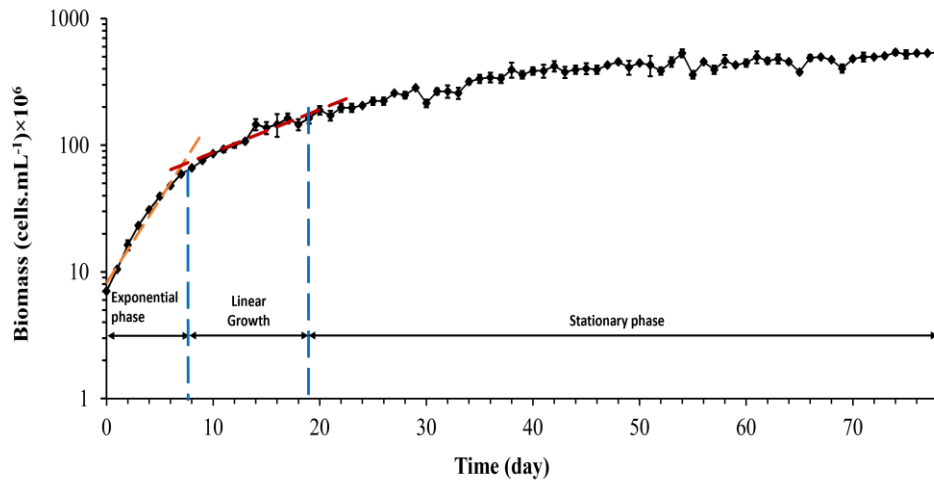

Figure 4-2:Curve of *Synechocystis* sp. CPCC 534 (n = 3 ± SD). The blue dashed lines show the end of each growth phase in this experiment.

The growth rate and doubling per day calculated during the exponential growth phase were 0.3 ± 0.01 d^{-1} and 0.43 ± 0.015 d^{-1}, respectively. The growth rate equation for both the exponential phase and linear phase, respectively, are:

$$\ln(C_{biomass}) = \ln(8 \times 10^6) + 0.3d \tag{3}$$

$$\ln(C_{biomass}) = \ln(4 \times 10^7) + 0.08d \tag{4}$$

where $C_{biomass}$ is the biomass concentration, and d is the time in days.

4.3.3 Cell Motion

For cell tracking, the concentration of microorganisms in the suspension was set to 10^7 cells.mL^{-1} and video microscope images were recorded for 50 min. Figures 4-3 to 4-5 show

the trajectories of the population of *Synechocystis* sp. CPCC 534 at (Figure 4-3) the beginning (on the first day) of the exponential growth phase, (Figure 4-4) the end of the exponential phase, and (Figure 4-5) the end of the stationary phase (at day 1, day 17, and day 78, respectively). The duration of all trajectories displayed in Figures 4–5 is 50 min. The results show the length of cell trajectories had increased noticeably during the exponential phase compared to the beginning of the exponential growth phase and the end of the stationary phase. In Figures 4-3 and 4-5, the cell trajectories mainly consist of "tumbling" movement and extend around 10 μm in space, while in Figure 4-4, cells perform more "run" movements, and the trajectories extend over 80 μm in space. This observation implies that cell motility improved with the cells' age. The decline of cell motility at the end of the stationary phase could be due to nutrient depletion in the PBR and/or the fact that most cells had reached the end of their cell life cycle, Figure 4-5 [5,32].
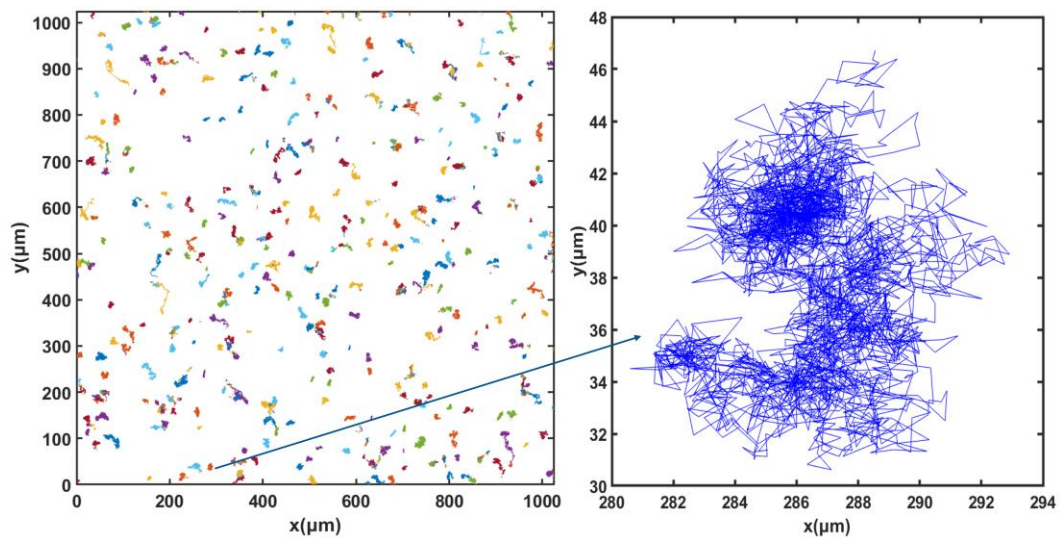

Figure 4-3:Extracted trajectories of *Synechocystis* cells from the video microscope images, recorded over 50 min, for the first day of the exponential phase, day 1.
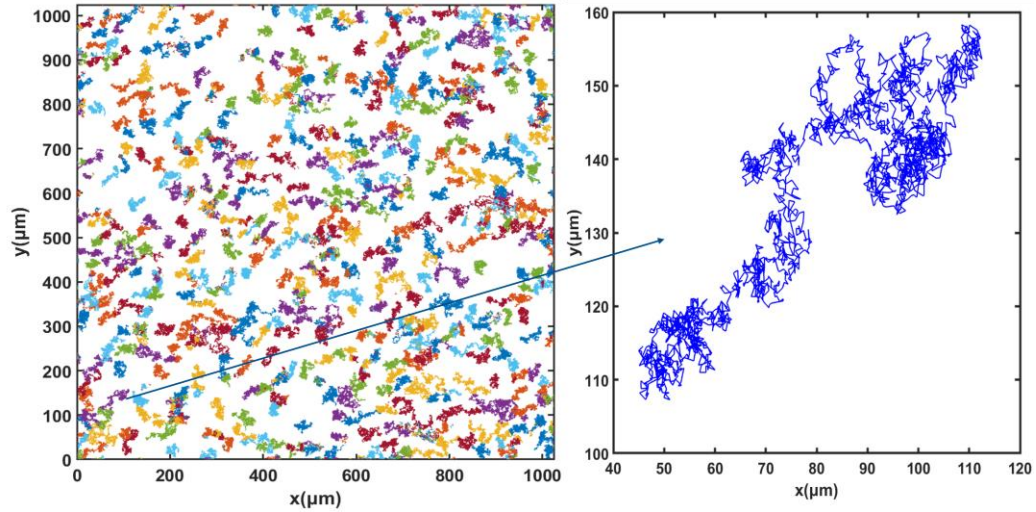
Figure 4-4: Extracted trajectories of *Synechocystis* cells from the video microscope images, recorded over 50 min, for the end of the exponential phase, day 17.
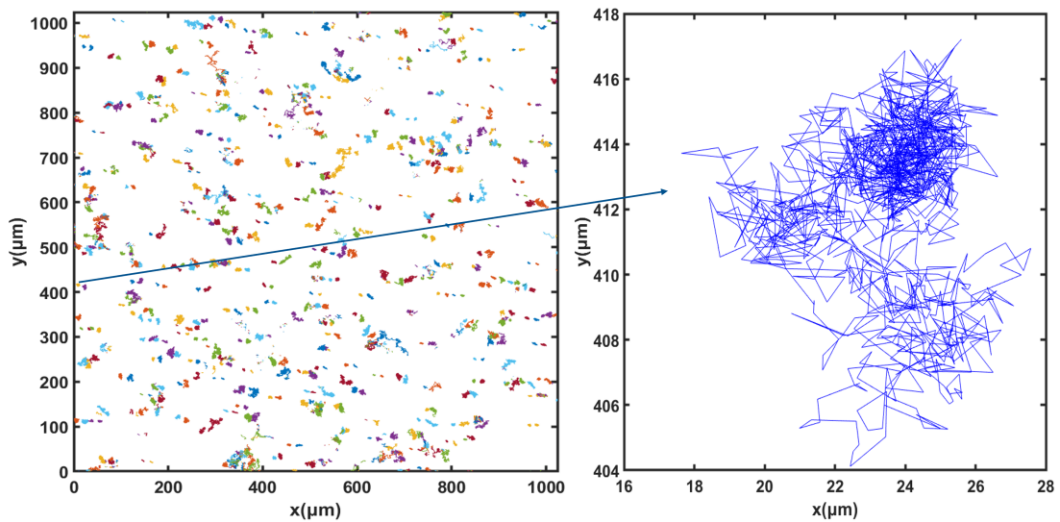

Figure 4-5:Extracted trajectories of *Synechocystis* cells from the video microscope images, recorded over 50 min, for the end of the stationary phase, day 78.

4.3.4 Evolution of Cell Motility during *Synechocystis* Growth

The instantaneous velocity of a single cell was calculated as the displacement between two consecutive frames multiplied by the acquisition framerate (one frame per second). The instantaneous velocity for each cell was then averaged over the experimental time period

to determine the average cell velocity, V_p. Finally, the average ensemble velocity was calculated as follows:

$$V_m = \frac{1}{n_p} \sum_{p=1}^{n_p} V_p \tag{5}$$

where n_p is the number of motile *Synechocystis* cells present in the recorded video [19]. The measurement time for each experimental run was 50 min, and cell concentrations for all experiments were constant (10^7 cells.mL^{-1}). In Figure 4-6, the average velocity of *Synechocystis* sp. cell is plotted as a function of time for 78 days of observation. The growth curve corresponding to the same observation period is also superposed on the average velocity curve. It is observed that the cells' average velocity increases with time during the exponential and linear growth periods and starts to decline monotonously from the beginning of the stationary growth phase.
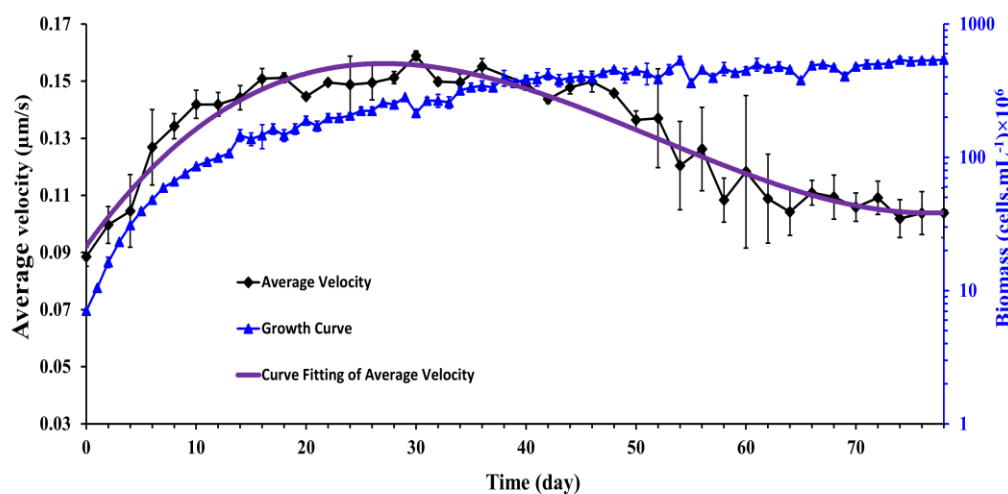

Figure 4-6:Time history of the average velocity of *Synechocystis* cells. The purple line was fitted to a non-linear third-order polynomial model. (n = 3 ± SD).

This observation suggests cell motility was directly correlated with cell growth and cell aging attenuated cell motility. Of special interest is the observation in the stationary growth region where the motility of the cells decays with time. The question arises whether the aged cells give birth to fewer motile cells or whether other factors, such as self-shading or

nutrient depletion, caused this reduction in cell motility. We could not address this question due to experimental limitations, but it would be an interesting topic for future study.

A similar pattern of results was observed by Fadlallah et al. [19] where they cultured *C. reinhardtii* at 22 ± 1 °C with a photon flux of 70 ± 5 µmole.m^{-2}.s^{-1} and a stirring rate of 360 rpm for 15 days. Their results showed the mean velocity of *C. reinhardtii* improved noticeably during the exponential phase while the average velocity oscillated randomly around a constant value in the stationary phase. In this experiment, however, the authors did not observe the decay of cell motility, perhaps because the experiments were not followed a long time enough in the stationary growth phase to verify the motility decay as was conducted in the present work.

These velocity data were fitted to a non-linear third-order polynomial model in the form:

$$V_m = a_1 d^3 + a_2 d^2 + a_3 \cdot d + a_4 \qquad (6)$$

The model parameters were determined using the "statsmodels" package in Python. The parameter values and their 95% confidence intervals (given in brackets) are:

- $a_1 = 8.36 \times 10^{-7}$ (6.44×10^{-7} to 1.03×10^{-6})
- $a_2 = -1.31 \times 10^{-4}$ (-1.54×10^{-4} to -1.09×10^{-4})
- $a_3 = 5.30 \times 10^{-3}$ (4.53×10^{-3} to 6.06×10^{-3})
- $a_4 = 9.25 \times 10^{-2}$ (8.57×10^{-2} to 9.92×10^{-2})

All parameters were found to be statistically significant ($p < 0.05$). It should be noted that Equation (6) is obtained specifically for *Synechocystis* cells under the given growth conditions. Its generality needs to be studied in future work.

4.3.5 Dynamics of Cell Motion during Growth

The mean squared displacement (MSD) as a function of experimental time is used to describe the dynamics and the nature of cell motion. After determining cell trajectories, the MSD was computed to analyze the cell transport parameters, such as cell diffusion in its surrounding environment. Figure 4-7 shows the mean squared displacement of *Synechocystis* sp. CPCC 534 increases linearly with time over a 3000 s observation time, confirming Fickian diffusion behavior. A similar pattern was also found by Vourc'h et al. [23], who studied the surface diffusion of *Synechocystis* sp. PCC 6803 during the early

stages of cell contact with a solid surface in diluted suspension. The maximum value of the MSD was estimated from Figure 4-7 and plotted in Figure 4-8 as a function of time. Due to the improvement in the cell motility, the MSD_{max} increased linearly during the exponential and linear growth phases, followed by an almost constant value up to day 44. Then the MSD_{max} declined progressively in the stationary range and roughly leveled off until the end of this period.
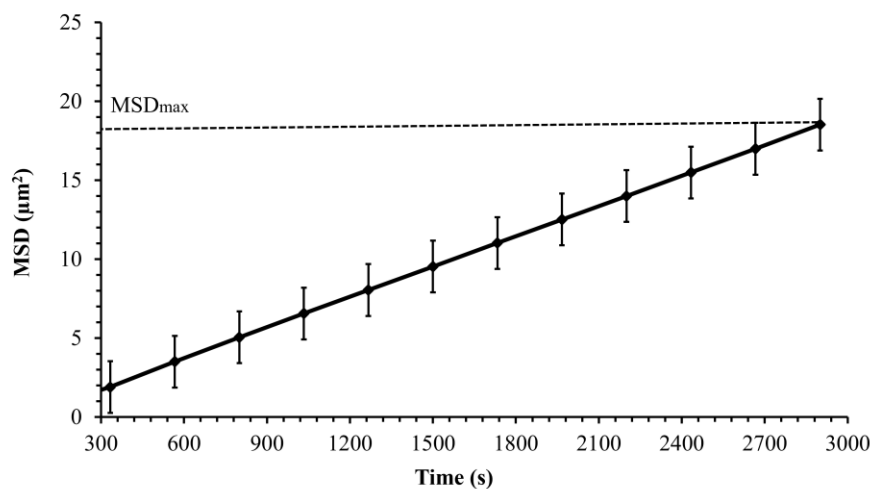

Figure 4-7:The MSD variation of *Synechocystis* sp. CPCC 534 versus time for a single experiment during 50 min observation period (n = 3 ± SD). Data were fitted to a non-linear third-order polynomial model.
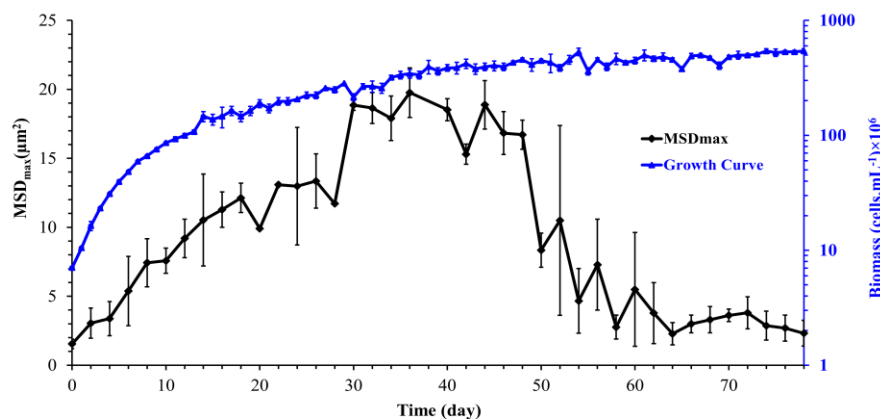

Figure 4-8:Variation of the maximum mean squared displacement (MSDmax) with time during *Synechocystis* sp. CPCC 534 growth (n = 3 ± SD).

To assess the details of the temporal evolution of the motility during an observation period, we divide the 50 min duration of the recording into 12 temporal windows centered around time t. We denote δ, the time elapsed between two successive values of t. Inside each window centered on t, we compute MSD(t,D) as the MSD computed for a time interval Δ as:

$$MSD(t, \Delta) = \frac{1}{N_t} \sum_{i=1}^{N_t} \frac{1}{\delta - \Delta} \sum_{t'=t-\frac{\delta}{2}+\frac{\Delta}{2}}^{t+\frac{\delta}{2}-\frac{\Delta}{2}} \left[X_i \left(t + \frac{\Delta}{2} \right) - X_i \left(t - \frac{\Delta}{2} \right) \right]^2 \tag{7}$$

where N_t is the number of trajectories recorded on the temporal window.

For most applications, one would need to know the behavior of the diffusion coefficient as a function of time. As $MSD(t, \Delta)$ is proportional to Δ inside each temporal window centered around t, this enables the derivation of a time-dependent diffusion coefficient $D(t)$ such as:

$$D(t) = \frac{MSD(t, \Delta)}{4\Delta} \tag{8}$$

Figure 4-9 shows a slow decrease in the diffusion coefficient with time reaching a constant value asymptotically after 3000 s. A time-dependent diffusion coefficient was also observed in [23] and was related to the secretion of EPS by *Synechocystis* cells. As was shown in the previous section, the *Synechocystis* motility is age-dependent, and therefore, it is expected that the diffusion coefficient is age-dependent as well. Thus, the instantaneous diffusion coefficient becomes concomitantly time and age-dependent, a fact that makes its dynamics quite complex. However, the long-term diffusion coefficient is of special interest in most practical applications. The long-term diffusion coefficient obtained from the experiments carried out for each point on the growth curve is plotted in Figure 4-10 for the whole growth period of *Synechocystis* sp. CPCC 534. Based on Figure 4-10, it followed the same pattern as the MSD$_{max}$ profile, confirming that cell motility dominates the diffusion dynamics of *Synechocystis* sp. CPCC 534.
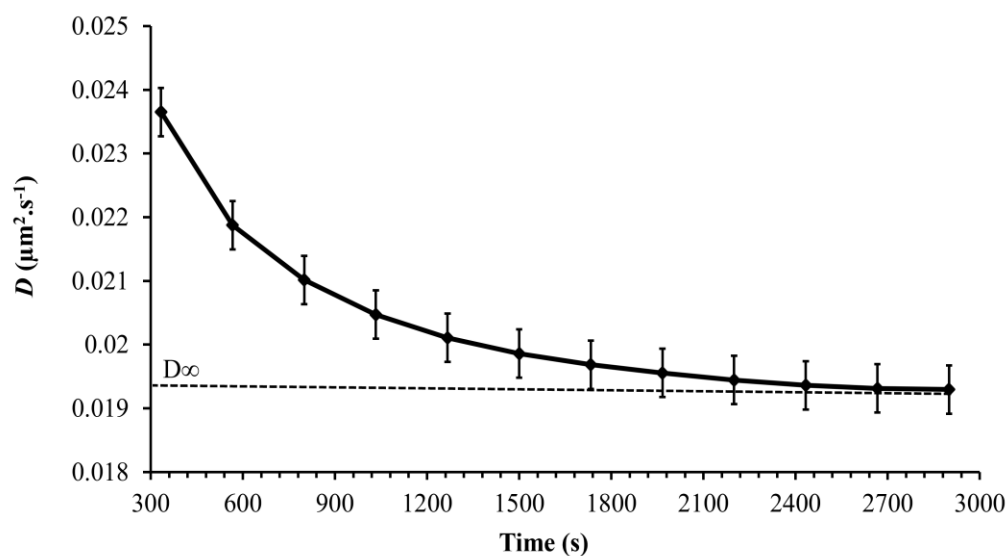
Figure 4-9: Variation, during 50 min observation time, of the time-dependent diffusion coefficient of *Synechocystis* sp. CPCC 534 (n = 3 ± SD).
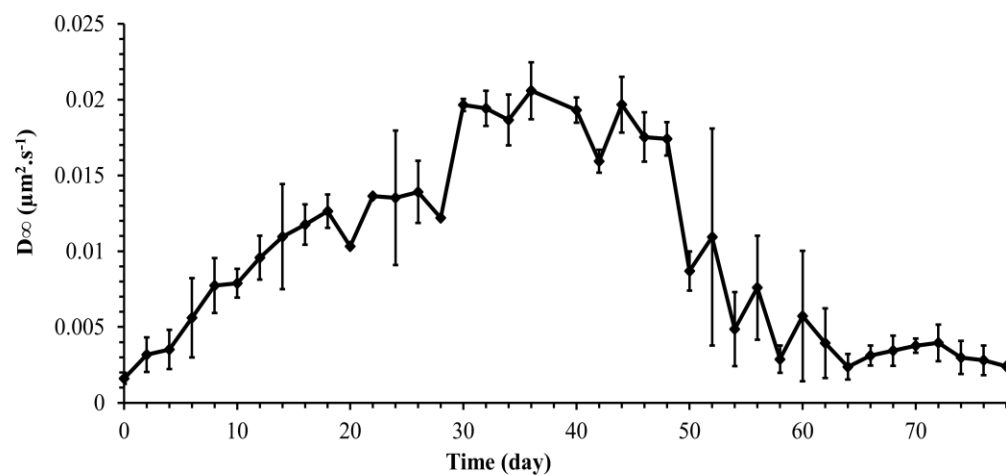

Figure 4-10: Variation of long-term diffusion coefficient (D∞) during the growth period of *Synechocystis* sp. CPCC 534 (n = 3 ± SD).

4.3.6 Probability Density Function (PDF)

In active suspensions, the probability density function (PDF) of cell displacements is usually non-Gaussian; or is a combination of a Gaussian distribution for long time intervals

and an exponential distribution for short time intervals [37]. Figure 4-11 plots the PDFs along the x-axis for various time intervals at (a) the beginning of the exponential growth phase, (b) the end of the exponential growth phase, and (c) the end of the stationary phase. The PDF distributions are symmetrical and zero-centered and show a smooth transition from exponential to a Gaussian distribution with passing time. The central part of the PDF relates to the low motility (tumble) part of cell trajectories, while the tails indicate the higher cell motility (run) parts [38]. Figure 4-11a shows that the PDF consists of two parts: a sharp central part and wide tails. The central part of the PDFs for each observation time corresponds to the non-diffusive behavior of *Synechocystis* sp. CPCC 534 (tumble), and their maximum values decline with the passage of time as the motility of cells increases. The tail of each displacement distribution broadened as time passed, implying that the diffusive behavior of cyanobacteria tends to be Gaussian at longer times. The difference between Figure 4-11a, b indicates that the tail of each displacement distribution had been expanded noticeably from the beginning of the exponential growth phase to the end of this phase, signifying that cell motility had increased as cells matured. However, the PDF was remarkably narrowed at the end of the stationary phase, Figure 4-11c, when cells aged, and their motility declined and was dominated by tumbling motion.
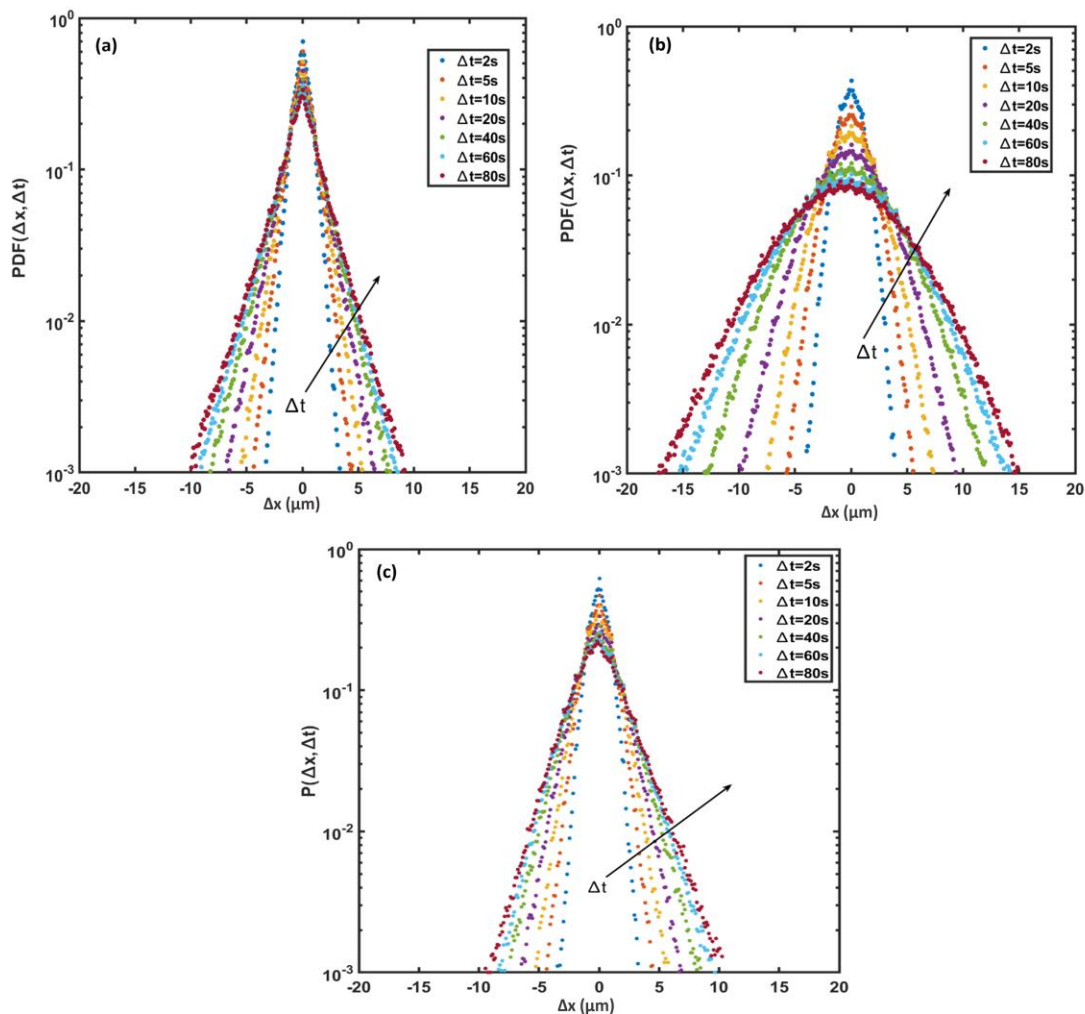
Figure 4-11:Displacement probability density function (PDF) along the x-axis for Synechocystis sp. CPCC 534 cell trajectories (a) beginning of the exponential growth phase, (b) end of the exponential growth phase, and (c) end of the stationary phase. Ar

4.4 Conclusions

The motility of wild-type *Synechocystis* sp. CPCC 534 was investigated during its complete growth cycle for 78 days. This rather long observation time, new in the literature, was aimed at investigating the correlation between the cell growth phase and cell motility evolution during the whole growth cycle, from the exponential to the decay phase.

The results revealed a direct correlation between cell motility and the cell growth phase: cell motility increased with time during the exponential linear growth phases. It declined

all through the stationary phase before reaching a constant value asymptotically. The mean squared distance traveled by cells at different stages of growth followed a trend similar to that of the cell motility time-variation, as was expected.

The instantaneous diffusion coefficient of *Synechocystis* at all growth states decreased with time and asymptotically reached a constant value. This type of time dependence for diffusion coefficient has already been observed [23] and has been shown experimentally to be due to the secretion of exopolysaccharides by *Synechsystis* cells [5]. However, the present work revealed that the long-term diffusion coefficient is also directly correlated with the growth state of the cells and follows the same time evolution as that of the MSD.

On the other hand, the PDF of the cell displacement confirmed the close correlation between the cell motility and its growth state; at the beginning of the exponential phase, the PDFs were of exponential type, revealing the non-diffusive behavior of the cells. The tail of each displacement distribution then broadened as time passed, implying the diffusive behavior of *Synechsystis* cells, and tended to Gaussian at longer times. The results of this study find their application in the prediction of biofilm formation on photobioreactor walls.

4.5 References

[1] Vourc'h, T., Léopoldès, J., & Peerhossaini, H. (2020). Light control of the diffusion coefficient of active fluids. Journal of Fluids Engineering, 142(3), 031109.

[2] Dickison, M., Ghaleeh, M., Milady, S., Wen, L. T., & Al Qubeissi, M. (2020). Investigation into the aerodynamic performance of a concept sports car. Journal of Applied Fluid Mechanics, 13(2), 583-601.

[3] Saintillan, D. (2018). Rheology of active fluids. Annual Review of Fluid Mechanics, 50, 563-592.

[4] Dervaux, J., Capellazzi Resta, M., & Brunet, P. (2017). Light-controlled flows in active fluids. Nature Physics, 13(3), 306-312.

[5] Mehdizadeh Allaf, M., & Peerhossaini, H. (2022). Cyanobacteria: Model microorganisms and beyond. Microorganisms, 10(4), 696.

[6] Ortiz, A., Díez-Montero, R., García, J., Khalil, N., & Uggetti, E. (2022). Advanced biokinetic and hydrodynamic modelling to support and optimize the design of full-

scale high rate algal ponds. Computational and structural biotechnology journal, 20, 386-398.

[7] Solimeno, A., Parker, L., Lundquist, T., & García, J. (2017). Integral microalgae-bacteria model (BIO_ALGAE): Application to wastewater high rate algal ponds. Science of the total environment, 601, 646-657.

[8] Hadiyanto, H., Elmore, S., Van Gerven, T., & Stankiewicz, A. (2013). Hydrodynamic evaluations in high rate algae pond (HRAP) design. Chemical Engineering Journal, 217, 231-239.

[9] Palma, V., Gutiérrez, M. S., Vargas, O., Parthasarathy, R., & Navarrete, P. (2022). Methods to evaluate bacterial motility and its role in bacterial–host interactions. Microorganisms, 10(3), 563.

[10] Lauffenburger, D., Aris, R., & Keller, K. (1982). Effects of cell motility and chemotaxis on microbial population growth. Biophysical journal, 40(3), 209-219.

[11] Sunda, W. G., Graneli, E., & Gobler, C. J. (2006). Positive feedback and the development and persistence of ecosystem disruptive algal blooms 1. Journal of Phycology, 42(5), 963-974.

[12] Vissers, T., Koumakis, N., Hermes, M., Brown, A. T., Schwarz-Linek, J., Dawson, A., & Poon, W. C. (2019). Dynamical analysis of bacteria in microscopy movies. PLoS One, 14(6), e0217823.

[13] Wood, T. K., González Barrios, A. F., Herzberg, M., & Lee, J. (2006). Motility influences biofilm architecture in Escherichia coli. Applied microbiology and biotechnology, 72, 361-367.

[14] Karimi, A., Karig, D., Kumar, A., & Ardekani, A. M. (2015). Interplay of physical mechanisms and biofilm processes: review of microfluidic methods. Lab on a Chip, 15(1), 23-42.

[15] Muhammad, M. H., Idris, A. L., Fan, X., Guo, Y., Yu, Y., Jin, X., ... & Huang, T. (2020). Beyond risk: bacterial biofilms and their regulating approaches. Frontiers in microbiology, 11, 928.

[16] Shoesmith, J. G. (1960). The measurement of bacterial motility. Microbiology, 22(2), 528-535.

[17] Kim, Y. C. (1996). Diffusivity of bacteria. Korean Journal of Chemical Engineering, 13, 282-287.

[18] Arora, S., Bhat, V., & Mittal, A. (2007). Correlating single cell motility with population growth dynamics for flagellated bacteria. Biotechnology and bioengineering, 97(6), 1644-1649.

[19] Fadlallah, H., Peerhossaini, H., De Groot, C., & Jarrahi, M. (2021). Motility Response to Hydrodynamic Stress During the Growth Cycle in Active Fluid Suspensions. Journal of Fluids Engineering, 143(7), 074501.

[20] Bertrand, R. L. (2019). Lag phase is a dynamic, organized, adaptive, and evolvable period that prepares bacteria for cell division. Journal of bacteriology, 201(7), 10-1128.

[21] Himeoka, Y., & Kaneko, K. (2017). Theory for transitions between exponential and stationary phases: universal laws for lag time. Physical Review X, 7(2), 021049.

[22] Jin, D., Kotar, J., Silvester, E., Leptos, K. C., & Croze, O. A. (2020). Diurnal variations in the motility of populations of biflagellate microalgae. Biophysical Journal, 119(10), 2055-2062.

[23] Vourc'h, T., Peerhossaini, H., Léopoldès, J., Méjean, A., Chauvat, F., & Cassier-Chauvat, C. (2018). Slowdown of surface diffusion during early stages of bacterial colonization. Physical Review E, 97(3), 032407.

[24] Samadi, Z., Mehdizadeh Allaf, M., Saifi, R., De Groot, C. T., & Peerhossaini, H. (2022). Effects of turbulent mixing and orbitally shaking on cell growth and biomass production in active fluids. AJBSR, 15, 396-404.

[25] Mueller, T. J., Welsh, E. A., Pakrasi, H. B., & Maranas, C. D. (2016). Identifying regulatory changes to facilitate nitrogen fixation in the nondiazotroph *Synechocystis* sp. PCC 6803. ACS synthetic biology, 5(3), 250-258.

[26] Ikeuchi, M., & Tabata, S. (2001). *Synechocystis* sp. PCC 6803—a useful tool in the study of the genetics of cyanobacteria. Photosynthesis research, 70, 73-83.

[27] Muth-Pawlak, D., Kreula, S., Gollan, P. J., Huokko, T., Allahverdiyeva, Y., & Aro, E. M. (2022). Patterning of the Autotrophic, Mixotrophic, and Heterotrophic Proteomes of Oxygen-Evolving Cyanobacterium *Synechocystis* sp. PCC 6803. Frontiers in Microbiology, 13, 891895.

[28] Knoop, H., Gründel, M., Zilliges, Y., Lehmann, R., Hoffmann, S., Lockau, W., & Steuer, R. (2013). Flux balance analysis of cyanobacterial metabolism: the metabolic network of *Synechocystis* sp. PCC 6803. PLoS computational biology, 9(6), e1003081.

[29] Chau, R. M. W., Bhaya, D., & Huang, K. C. (2017). Emergent phototactic responses of cyanobacteria under complex light regimes. MBio, 8(2), 10-1128.

[30] Conradi, F. D., Mullineaux, C. W., & Wilde, A. (2020). The role of the cyanobacterial type IV pilus machinery in finding and maintaining a favourable environment. Life, 10(11), 252.

[31] Rippka, R., Deruelles, J., Waterbury, J. B., Herdman, M., & Stanier, R. Y. (1979). Generic assignments, strain histories and properties of pure cultures of cyanobacteria. Microbiology, 111(1), 1-61.

[32] Mehdizadeh Allaf, M., Habib, Z., de Bruyn, J. R., DeGroot, C. T., & Peerhossaini, H. (2022). Rheological and Biophysical Properties of Living Fluids Under Shear: Active Suspensions of *Synechocystis* sp. CPCC 534. Journal of Fluids Engineering, 144(2), 021208.

[33] Everroad, R. C., & Wingard, L. M. (2005). A. Michelle Wood. Algal culturing techniques, 269.

[34] Berg, H.; Darnton, N.; Jaffe, N. (2003). Object Tracking Software; Rowland Institute at Harvard University: Cambridge, MA, USA.

[35] Samadi, Z., Mehdizadeh Allaf, M., Vourc'h, T., DeGroot, C. T., & Peerhossaini, H. (2022, August). Are Active Fluids Age-Dependent?. In Fluids Engineering Division Summer Meeting (Vol. 85833, p. V001T03A037). American Society of Mechanical Engineers.

[36] Nikonovas, T., Spessa, A., Doerr, S. H., Clay, G. D., & Mezbahuddin, S. (2020). Near-complete loss of fire-resistant primary tropical forest cover in Sumatra and Kalimantan. Communications Earth & Environment, 1(1), 65.

[37] Soni, G. V., Ali, B. J., Hatwalne, Y., & Shivashankar, G. V. (2003). Single particle tracking of correlated bacterial dynamics. Biophysical journal, 84(4), 2634-2637.

[38] Berg, H. C., & Brown, D. A. (1974). Chemotaxis in *Escherichia* coli analyzed by three-dimensional tracking. In Chemotaxis: Its Biology and Biochemistry (Vol. 19, pp. 55-78). Karger Publishers.

<div align="center">Chapter 5</div>

5 The Investigation of Active Fluids' Behavior in the Y-Shaped Microchannel[4]

Suspensions of photosynthetic microorganisms as "living", or "active" fluids play a crucial role in many biological, medical, and engineering applications. *Synechocystis* sp., a unicellular species of cyanobacteria, was suspended in a fluid medium (BG11) to constitute the working active fluid in this study. A bifurcating microchannel with a rectangular cross-section was designed and fabricated using Polydimethylsiloxane (PDMS) to investigate the flow characteristics of this active fluid. A micro-pump was used to introduce the fluid at a specific flow rate into the microchannel. A high magnification inverted optical video microscope captured the cells' behavior at a channel plane. The recorded video images were processed using a particle-image-velocimetry algorithm available in PIVlab to obtain the flow patterns. Streamwise and cross-stream components of velocity, known as u and v components respectively, were extracted separately to determine the interaction between the flow velocity, microchannel, and cyanobacteria motility. The results show that by comparing the average flow velocities of active and passive fluids at various flow rates, it becomes evident that the passive fluid exhibits a higher average velocity than the active fluid. This disparity can be explained by the small motion of active fluids caused by their run and tumble motion. Despite this difference, both fluids exhibit same trends in their velocity quantities, which increase in magnitude as the Reynolds number rises.

5.1 Introduction

Cyanobacteria, also known as blue-green algae, are widespread in nature. In the oceans, they play a crucial role in producing a significant amount of oxygen and consuming carbon dioxide. In addition, cyanobacteria are a basic constituent of marine food webs [1]. Using cyanobacteria to produce bioenergy and valuable bio-compounds has become an area of

---

[4] Accepted at ASME Conference, 2023

increasing interest therefore, the development of engineered cyanobacteria has received significant attention in the past two decades.

Micro swimmers including cyanobacteria are elements of active fluids that are capable of self-propelling in liquid media [2]. The properties of active fluids are fundamentally different from passive fluids. In passive fluids, the gradients of pressure, velocity, or temperature are driving forces for the flow, while in active fluids, such as bacterial suspensions, chemicals and/or light trigger cellular molecular motors to accomplish metabolic functions and navigate in the media, leading to a directed movement. Therefore, microorganisms in active fluids can create complicated and spontaneous fluid motions in the absence of external gradients. However, the presence of external gradients can alter these spontaneous motions, a topic that requires further investigation [3, 4]. Active fluids present astonishing physical phenomena over a wide range of scales, from the diffusion and motility of microorganisms to the large-scale colonization of media. Thus, studying the hydrodynamical properties of active fluids is vital due to their direct and indirect impacts on the environment, human lives, and their enormous uses in industries, medical, food, and energy areas [5]. One of the most common single-cell model organisms widely used for genetic and physiological studies of photosynthesis and energy is a unicellular freshwater cyanobacterium known as *Synechocystis* [6].

The behaviors of active fluids have been extensively studied in various situations. Vourc'h et al. [7] examined the surface diffusion of *Synechocystis* sp. during incipient stages of bacterial colonization contact with a glass surface in the dilute regime. The study by Elgeti and Gompper [8] focused on the performance of self-propelled nano-rods and micro-rods enclosed between two parallel solid walls in three dimensions. Teeffelen et al [9] investigated the Brownian dynamics of a circle swimmer in a circular confinement with a Petri dish and ring-shaped geometries and calculated the average position, and the swimmer's steady-state characteristics. In another study by Angelani et al. [10], the chance of having rectified movement of active particles was analyzed in the presence of asymmetric periodic potentials. Of special interest is the investigation of active fluids' hydrodynamics in microfluidic devices that are applicable for observing microorganism transport in confined geometries. The ability to provide controlled conditions with

exclusive geometries and specific flow rates can help scientists understand active fluids' motility and accumulation patterns [11]. The confining walls of a channel modify the swimming behavior of active fluids. The effect of channel confinement on self-propelled colloidal rods' behavior was studied using Brownian dynamics simulations. The results demonstrated that self-propelling rods aggregated near the walls of a channel and formed clusters, where the clusters were immobile in the early stage of the process, however, at later stages, most of these clusters were dissolved and mobilized [12].

These studies presented useful insight into different aspects of the microorganisms in the surrounding walls and the presence of flow. Generally, the behavior of active fluids depends on the characteristics of the microorganism itself, its shape, and the created flow field [13]. Fluid flow modifies the swimming behaviors of bacteria as well, their attachment to surfaces, and their formation of biofilms inside confined geometries. These modifications by flow and confinement must be considered for the design and operation of the processes, which involve bacteria [14]. Therefore, the following categories of devices were designed for more accurate investigation: phospholipid vesicles, polymer vesicles, droplets, and microfluidic chips. [15]. Polydimethylsiloxane (PDMS) has emerged as the most used material for microfluidics studies due to its ability to facilitate research involving living cells, owing to its transparency, non-toxicity, and oxygen permeability [16].

Fully understanding the transport properties of active fluids through microchannels has great potential for developing and designing microfluidic devices in various applications, especially in the medical industry to control cell motility. Therefore, in this research, we studied the behavior of *Synechocystis* sp. CPCC 534 in a bifurcated microchannel with a rectangular cross-section to measure the cell motility and medium fluid velocity profile.

5.2 Materials and Methods

5.2.1 Active Fluid Cultivation

Synechocystis sp. CPCC 534, was obtained from the Canadian Phycological Culture Center (Waterloo, ON, Canada), and was grown at 20 ± 1 °C in BG11 medium. The culture grew under the light cycle of 12/12 h and photon flux of 50 ± 5 µmole. m^{-2}. s^{-1}. Cells were cultivated under controlled conditions in a fully controlled PHCbi incubator. This study

used a turbulent mixing mode to improve the cell growth rate [5]. Magnetic stirrers (VWR Canada) at 360 rpm rotation speed were used to induce turbulent mixing inside the lab photobioreactors. All experiments utilized cylindrical magnetic stirring bars of 7.9 mm diameter and 19.8 mm length.

5.2.2 Microchannel Device

To carry out the experiments, a PDMS microchannel was designed and fabricated (Figure 5-1 I), which was utilized to measure the cell motility and velocity profile of *Synechocystis* sp. CPCC 534 suspensions. AutoCAD software was used to design the master (Figure 5-1 II) and then it was fabricated at Western Nano-fab. SYLGARD184 Silicone Elastomer Kit (Dow Corning Corporation, Midland, MI) was used to make the PDMS. The stiffness was adjusted by changing the mass ratio of the base to the curing agent to 10:1. After mixing the base and curing agent and degassing the mixture, it was poured into a mould and then baked in the oven at 80 °C for 1 hour and 45 minutes. After baking the PDMS, it was removed from the mould and then the cleaned PDMS microchannel was affixed on the top of a slide using 80 °C heat for an hour.
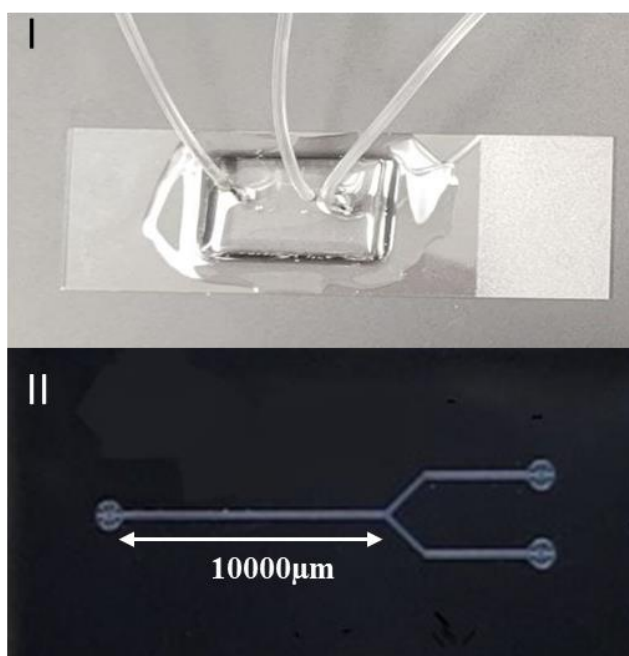

Figure 5-1:(I) A photograph of the Microchannel. (II) Schematic of Master for Microchannel Fabrication

5.2.3 Video Microscopy and Image Acquisition

To generate the flow, *Synechocystis* sp. suspension was injected by a kdScientific micropump into the sterilized PDMS microfluidic device. Then the motion of the cells was recorded using the Olympus IX83 inverted microscope equipped with a 20X magnification lens and a CCD camera. The motion of the cells within the flow was captured in "vsi" format at a rate of 50 frames per second for a duration of 10 seconds.

5.2.4 Analysis of Cell Dynamics

The obtained videos for active and passive (dead cells) fluids were analyzed using MATLAB PIVlab 2.62 (particle image velocimetry (PIV)) [17]. To investigate the interplay between the flow velocity and cyanobacteria's mobility, streamwise and cross-stream components of velocity, identified as u and v components respectively, were obtained.

5.3 Results and Discussion

Experiments were performed using the live *Synechocystis* sp. bacteria (active fluid) and dead *Synechocystis* sp. bacteria (passive fluid) at the fixed flow rate (Q=250 nl/min). The instantaneous snapshots are shown in Figures 5-2 I and II for live and dead bacteria, respectively. The bulk flow was observed to be laminar with no signification collision between the bacterial cells other than forming clusters (due to the stickiness of the secreted polysaccharide by the bacterial cells). Colonization of the bacteria was observed around the bifurcation point C (Figure 5-3 I, point C) as the flow velocity near this point was lower due to a larger channel cross-section, and formation of a stagnation point. Figures 5-3 to 5-5 show the (image-processed) velocity magnitudes ($\sqrt{u^2 + v^2}$), u components, and v components of the flow together with the velocity vector superimposed in each plot. For both fluids, we could not detect no-slip conditions on the wall mainly due to the low resolution of the PIV system. The live bacteria tended to accumulate close to the wall for colonization and biofilm formation (Figure 5-3 I). The fluids experienced lower velocities near the bifurcation point C and near the inner walls of the bifurcation branches (Figure 5-3 I, walls 2A and 3B) which implies that colonization and bio-film formation most likely

occurred in these sections if the flow was allowed for sufficient time. The dead bacterial particles experienced a higher velocity in the main branch compared to the live bacteria.

For the analysis of the subsequent plots, we define Reynolds number as $Re = \frac{V_{avg}D_h}{\nu}$, where V_{avg} is the average fluid velocity, D_h is the hydraulic diameter, and ν is assumed to be the kinematic viscosity of water (since the bulk medium fluid somewhat exhibits approximate properties of water). For the current nominal flow rate 250 nl/min, we have Re = 0.074, and the entry length to get a fully developed flow $L_{entry} = 0.06D_hRe = 0.3552$ μm. Since the length of the main branch up to the bifurcation point is 10,000 μm which is far greater than the L_{entry}, hence the flow is considered fully developed.

The u-velocity component (Figures 5-4) dominated the bulk flow, and the v-velocity (Figure 5-5) was negligible in the main branch, which confirms the bulk flow is fully developed in the main branch, but the bifurcating branches (sections 2 and 3) attained v-velocity because of flow splitting and channel geometry angular causing the flow two dimensions.

Figure 5-6 shows the instantaneous wall normal vorticity ($\eta = \frac{\partial v}{\partial x} - \frac{\partial u}{\partial y}$), the maximum vorticity occurs in the bifurcation points of the wall 1A and 1B, denoted by points D and E, respectively for both active and passive fluids. Core fluids in the main branch 1 and branches 2 and 3 show little or zero vorticity.
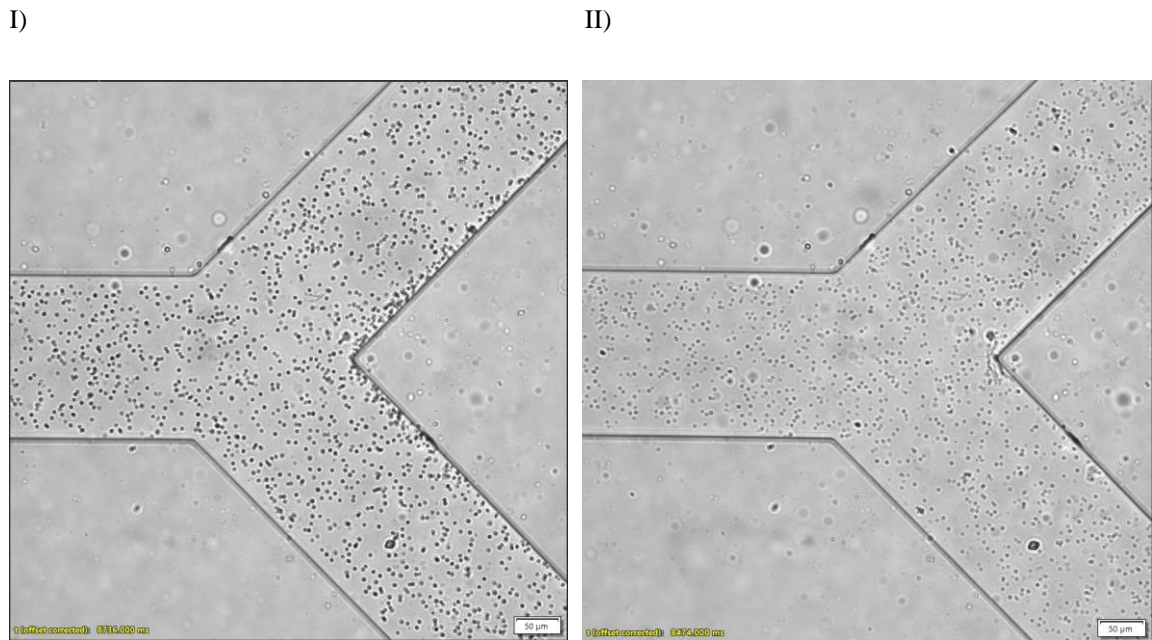
I)   II)

Figure 5-2: Snapshot of active fluid (I) and passive fluid (II) at Q=250 nl/min.

I)   II)

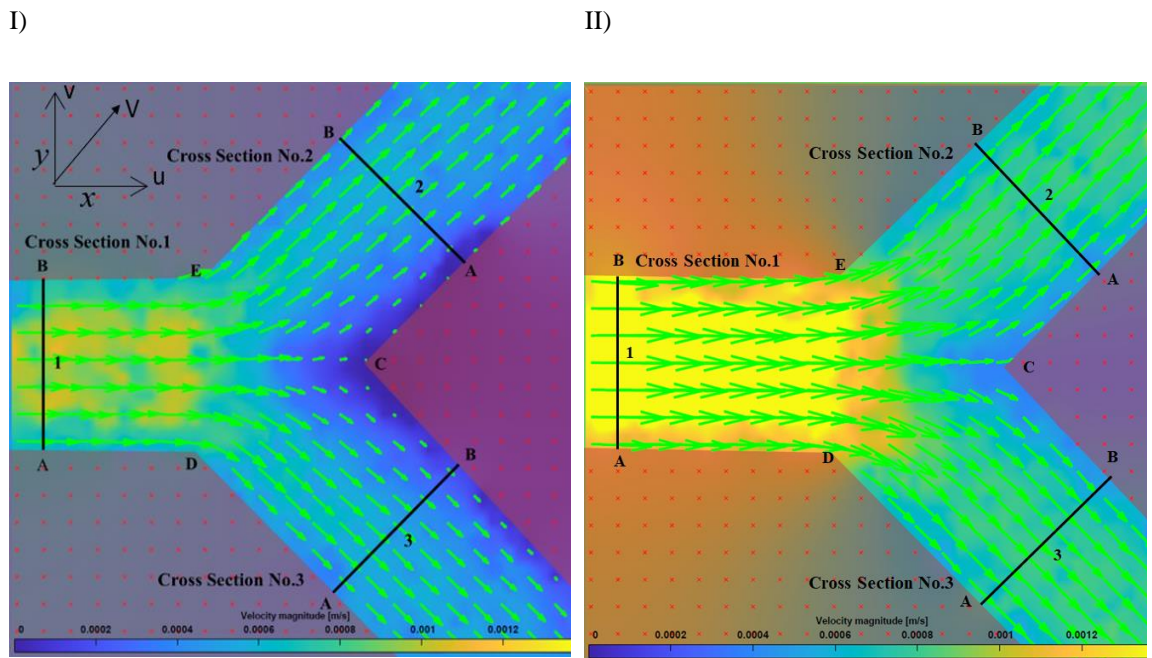Figure 5-3:Instantaneous velocity magnitude contour of active fluid (I) and passive (II) and velocity vector.
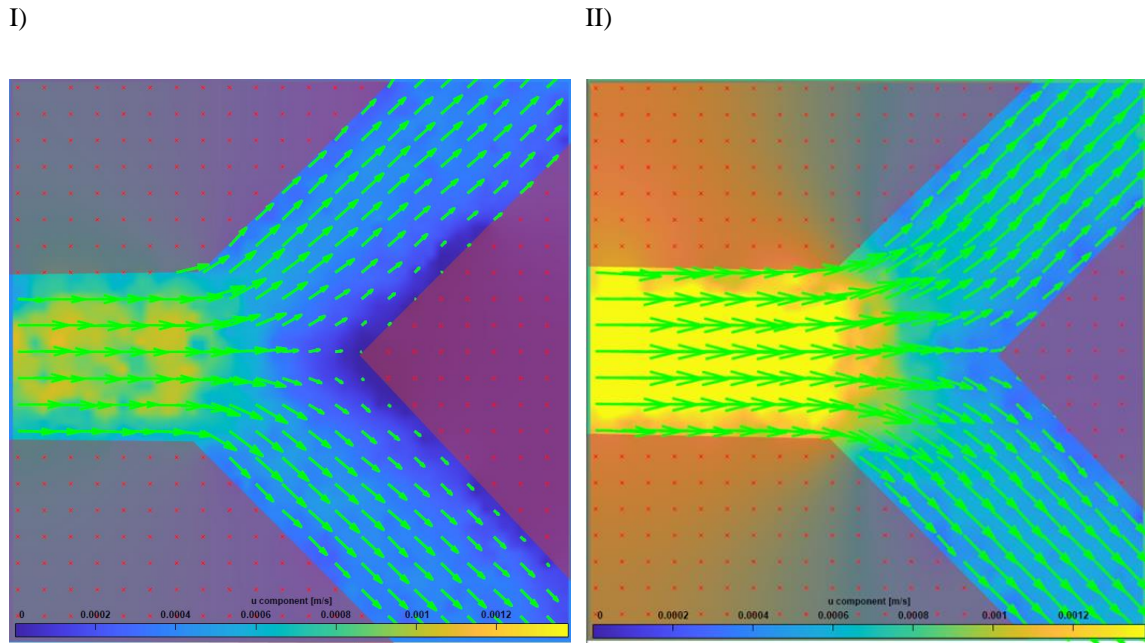
I)   II)

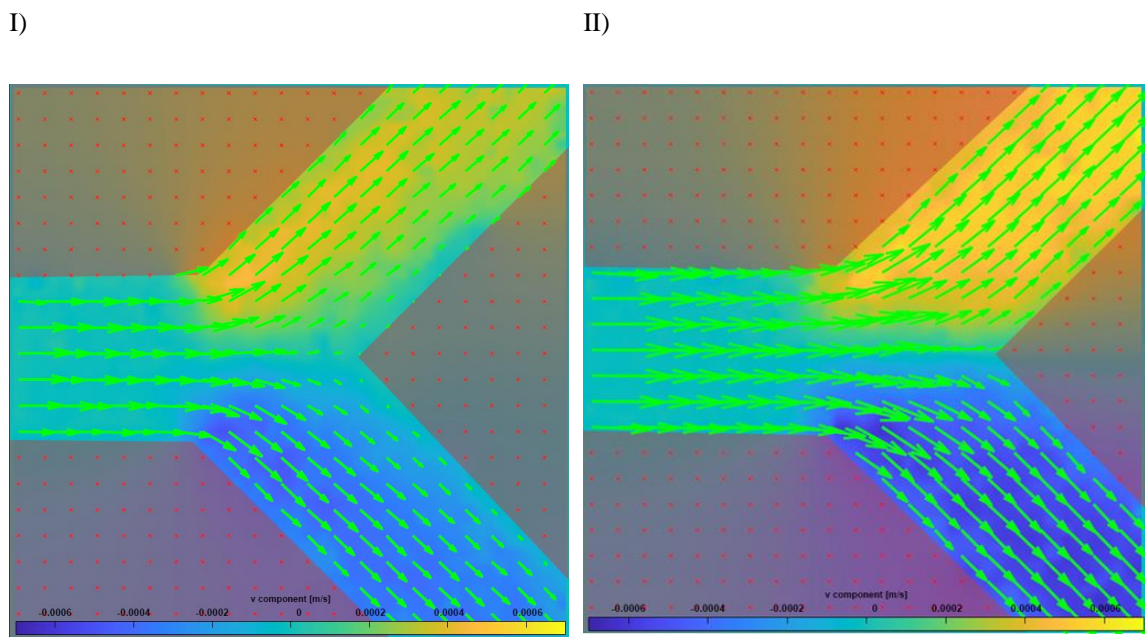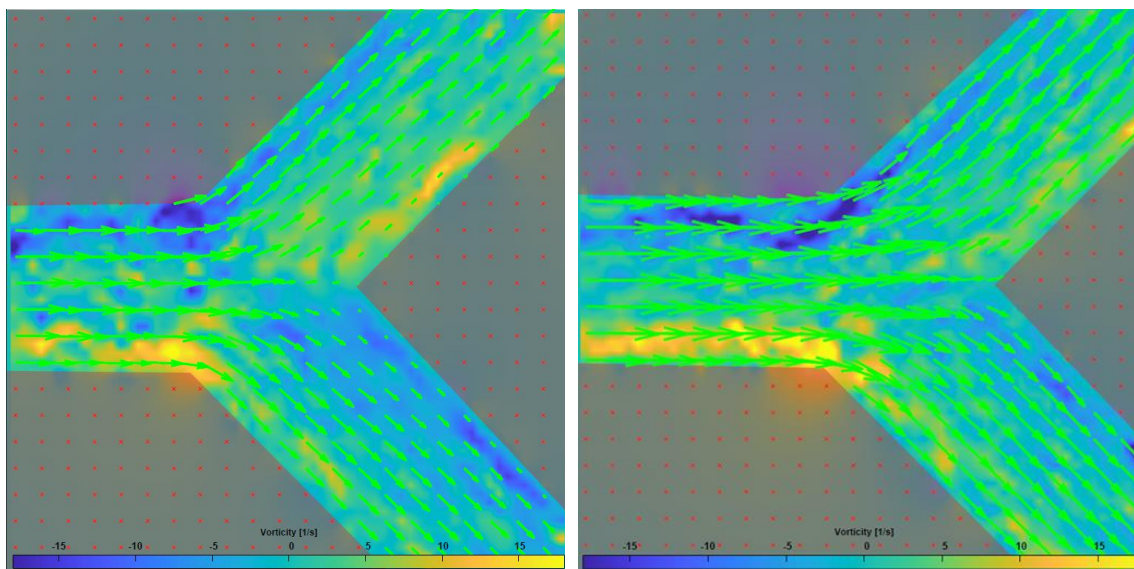Figure 5-4:Instantaneous u-velocity contour of active fluid (I) and passive (II) and velocity vector

I)   II)

Figure 5-5:Instantaneous v-velocity contour of active fluid (I) and passive fluid (II) and velocity vector.

I)   II)

Figure 5-6:Instantaneous vorticity contour of active fluid (I) and passive fluid (II) and velocity vector.

Profiles for the velocity magnitude, vorticity, u, and v components of the flow field for both fluids (active and passive) are plotted in figures 5-7 to 5-10 at three different cross-sections of the bifurcating microchannel (Figure 5-3 shows locations of the cross-section). It is noted that in these figures, due to the lack of sufficient resolution at walls, we were unable to resolve velocities very close to the wall [19], consequently, we eliminate 30 µm from each near-wall region and focus our attention on the core regions of the channel. The velocity profiles obtained from the velocity magnitude and the u-velocity (except v-component) of the main branch (section 1) exhibit almost flat profiles, although the bulk flow in fully developed in the core region of the channel and should follow the parabolic Hagen-Poiseuille profile. This can be attributed either to the fact the flow is preparing for the bifurcation at section 1 or the nature of the fluids is close to non-Newtonian. The motile bacteria show very little spanwise-wise (v) movement. In the bifurcating branches (sections 2 and 3). The zones between the centerline and the outer wall (wall B for branch 2 and wall A for branch 3), in both active and passive fluid flows experience higher velocity compared to the other half-width of the respective branch due to the centrifugal force developed because of streamline curvature (precursor of Dean flow) . This effect was more visible in the active fluid flows.
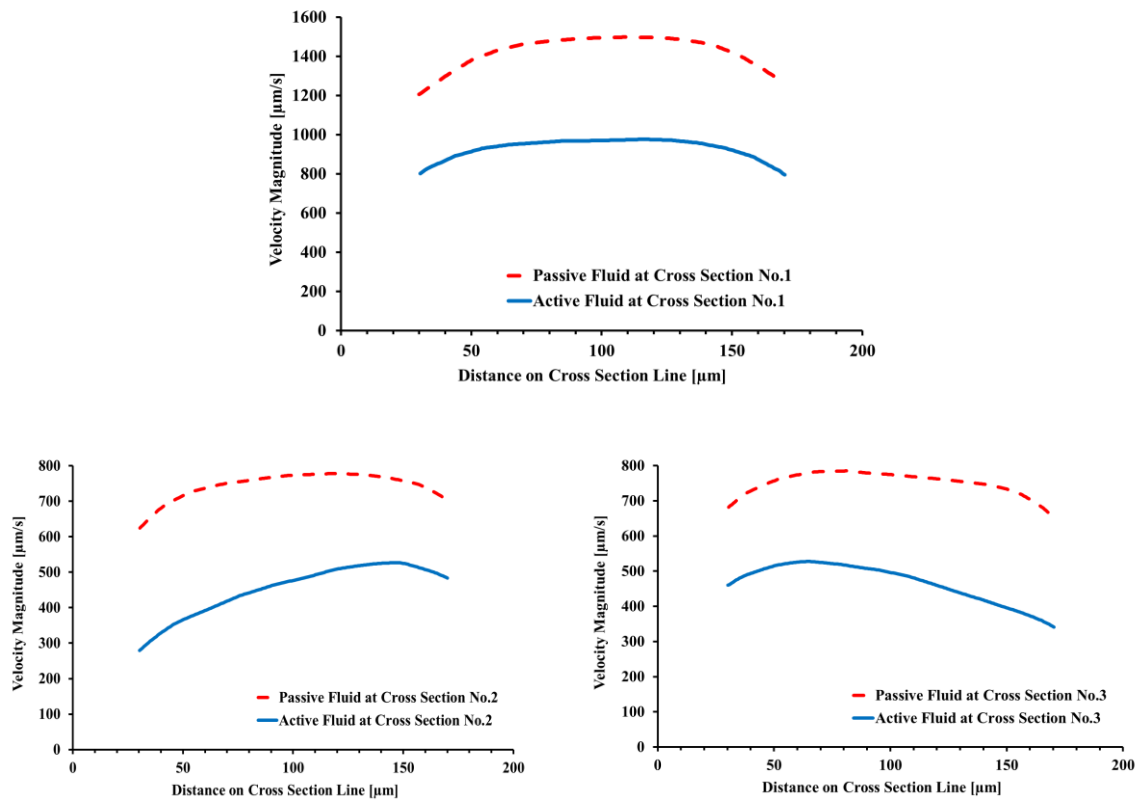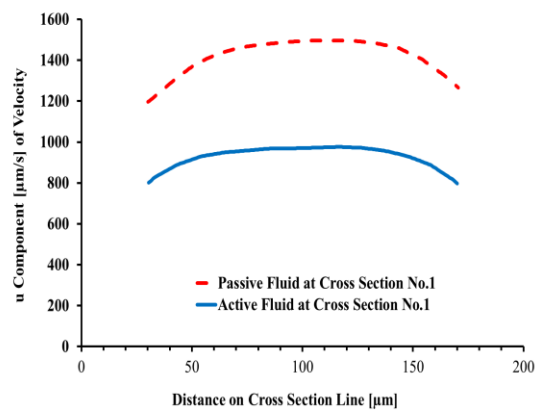
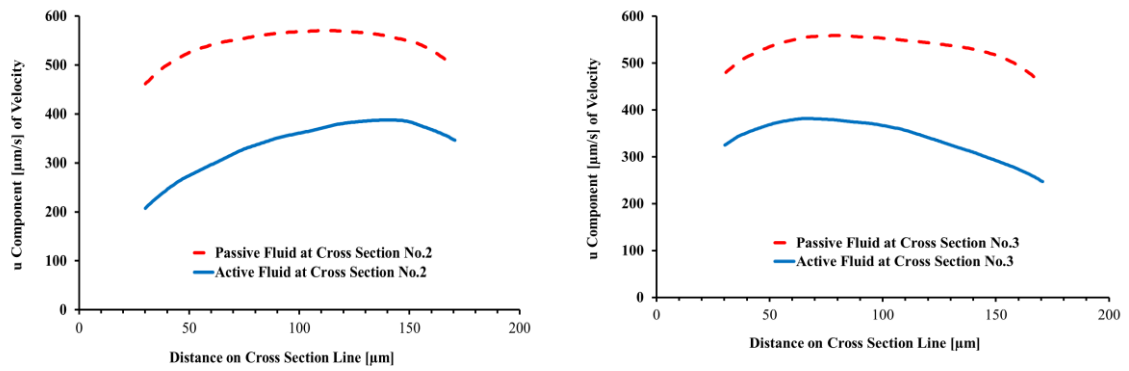Figure 5-7:Time-averaged velocity magnitude profile of active fluid and passive fluid at different cross sections.

Figure 5-8:Time-averaged u component of the velocity profile for active fluid and passive fluid at different cross sections.
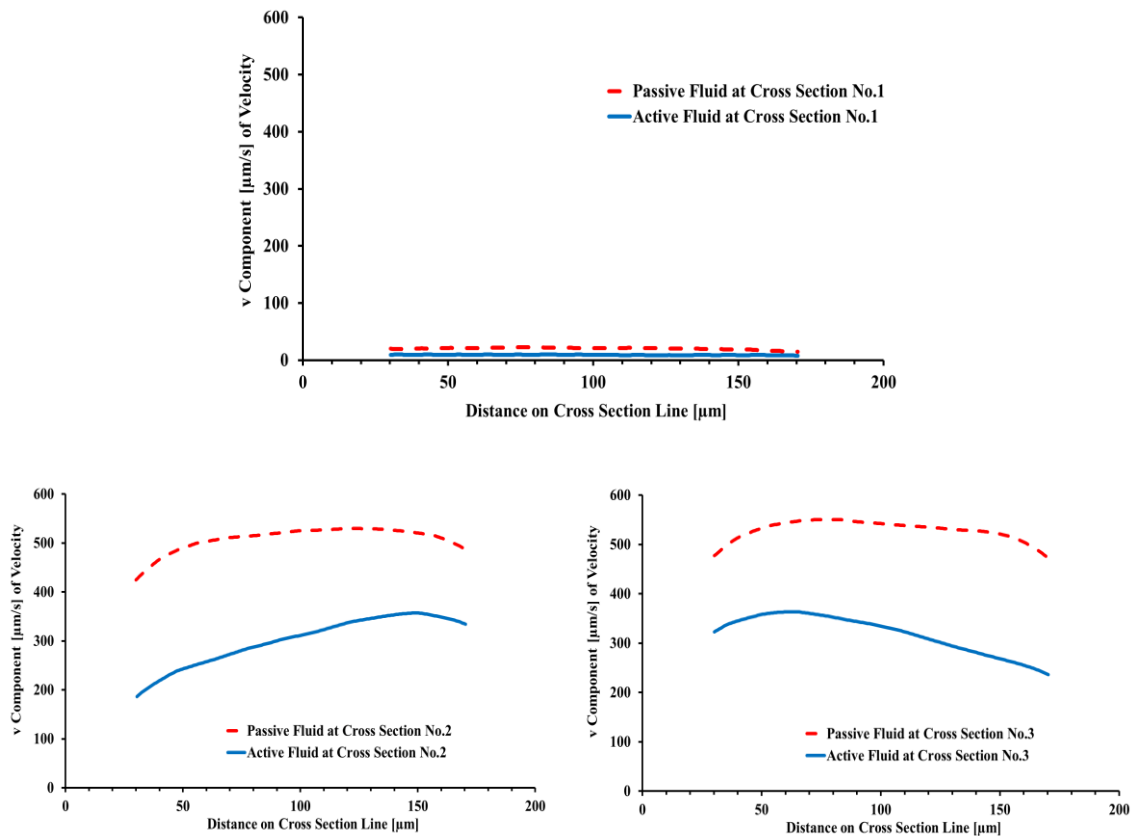

Figure 5-9:Time-averaged v component of the velocity profile for active fluid and passive fluid at different cross sections.
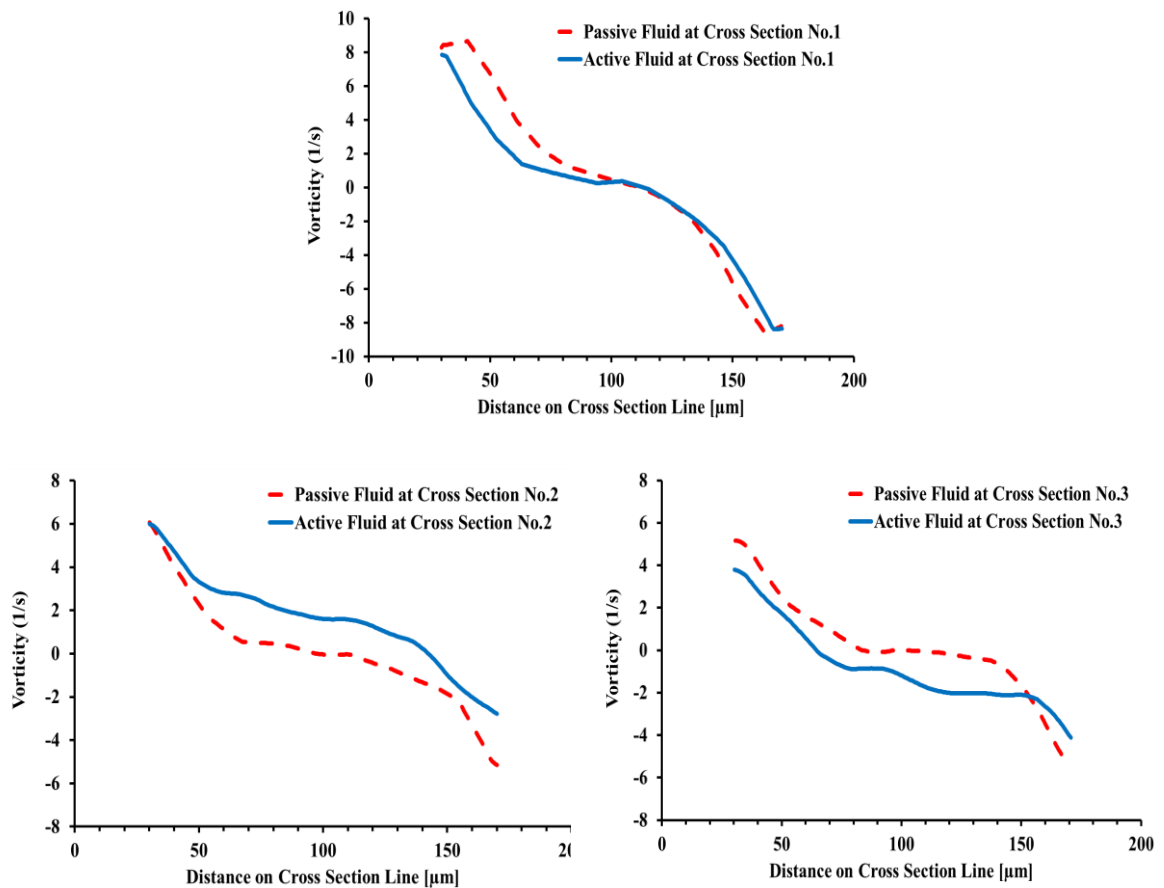
Figure 5-10:Time-averaged vorticity profile for active fluid and passive fluid at different cross sections.

Time averaged vorticity is plotted in Figure 5-10. It shows that for active fluids the core of branch 1 exhibits almost zero vorticity (time-averaged) and almost flat profile, and the core of branch 2 exhibits positive vorticity whereas the core of branch 3 exhibits negative vorticity. For passive fluids, the core of branch 1 has almost zero vorticity. Overall, it suggests that active fluid particles in the core of the channel spin in opposite directions in both branch 2 and branch 3, whereas the passive fluid particles in the core of the channel are almost spin-less.
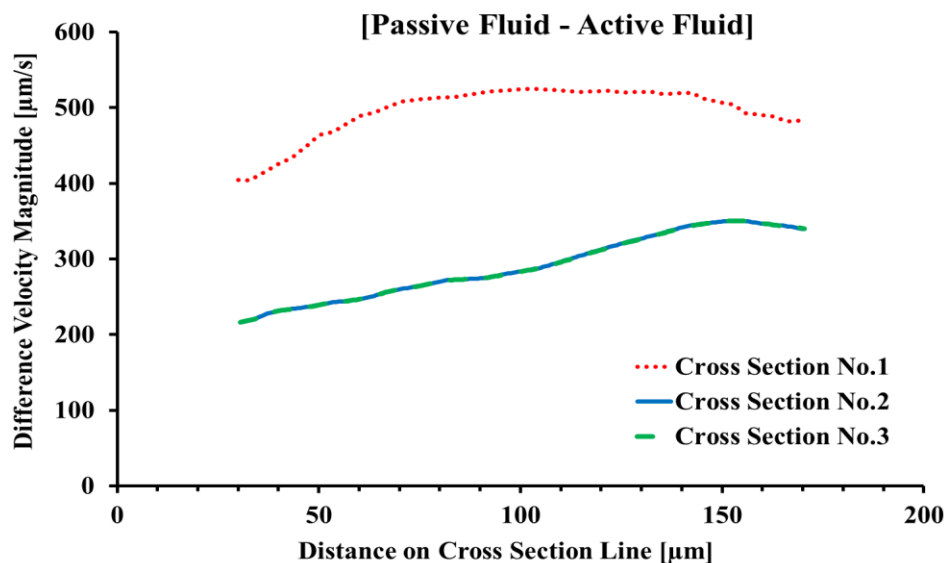
Figure 5-11: Difference velocity magnitude profile of active fluid and passive fluid at three different cross-sections

We construct Figure 5-11 by subtracting the velocity magnitude of active fluid from that of the passive fluid to obtain the possible contribution of motility in the cell overall velocity. From Figures 5-7 to 5-9 and 5-11, it is evident that dead bacteria (passive fluid) experience overall higher velocity than live bacteria (active fluid). In other words, the live bacteria show a sort of resistance to the mean flow causing a slowing down of the bulk flow. This resistance could be attributed to a tendency that *Synechocystis* cells swim in the opposite direction of the bulk flow. This tendency has been observed with *Chlamydomonas reimhardtii* (a flagella microorganism) exposed to a pulsating flow [20, 21]. However, *Synechocystis* does not have any flagella that assists in swimming by providing the required thrust like a propeller. Nevertheless, it has type IV pili which assists in generating motion by its extrusion and retraction. This process is efficient mostly on or near solid surfaces [22, 23]. Thus, it suggests that *Synochocystis* does not like to swim or does not know how to swim but can perform a random-walk motion known as "runs," with intermediate low motility periods called "tumbles" [18]. In our view, it could be the "tumbles" behavior of *Synechocystis* that leads to develop a tendency of "not-to-flow" with the same pace as of the bulk flow providing resistance to the bulk flow.

We considered mass flow continuity before and after the bifurcation to ascertain the accuracy of experiments and the veracity of the image processing. The mass continuity

translates here as, $Q_1=Q_2+Q_3$, where Q_1 is the flow rate at the main branch, Q_2 is the flow rate at branch No.2 and Q_3 is the flow rate at branch No.3. To account the geometric configuration, we define flow rate $Q = \int \vec{V}.\hat{n}\, dA$, with $\vec{V}.\hat{n} = un_x + vn_y$, where, A is the cross-sectional area, $\hat{n}$ is the unit vector normal to the surface.

For steady flow and the same size at all cross sections in Figure 5-3 I, the average velocity at cross-section No. 1 (855.14 µm/s) was equal to the sum of the average velocity at cross-sections No.2 (412.28 µm/s) and No.3 (413.6 µm/s) with relative error equal to 3.4 % in case of active fluid. For passive fluid, the average velocity at cross-section No. 1 (1343.33 µm/s) is equal to the sum of the average velocities at cross-sections No.2 (698.25µm/s) and No.3 (703.68 µm/s) with relative error equal to 4.36 %.

Variations of the time-averaged velocity magnitude, u components of the flow velocity and vorticity for both fluids (active and passive) for the main branch at cross section No. 1 were calculated at different Reynolds numbers. The results are shown in figures 5-12 to 5-14. The same figures also show the variations of the quantities as a function of nominal flow rate of the micro-pump. It is evident that for the passive fluids the velocity magnitude and u-velocity both are observed to be higher than those of active fluids in the above figures. This difference can be attributed to the minimal motion of active fluids resulting from their run and tumble motion. The velocity quantities show similar trends for both fluids, with increasing their magnitudes with the increase of Reynolds number. Active fluid velocity shows a linear increase, but the passive fluid shows a quasi-linear trend and with the increase of Reynolds number the difference in magnitudes of velocity quantities reduces. These figures also confirm that the bulk flow in the case of active fluid slows down (compared to the passive fluid flow) at all Reynolds numbers considered in this study.

Variations of the time-averaged vorticity as a function of Reynolds number shown in Figure 5-14 dictates that the fluid particles for active and passive fluids spin in opposite-wise as the vorticity of active fluid particles are mostly negative, and the vorticity of the passive fluid particles are mostly positive. Overall, with the increase of the Reynolds number both live and dead bacterial particles gradually achieve zero vorticity, suggesting that, at a high enough Reynolds number this difference disappears.
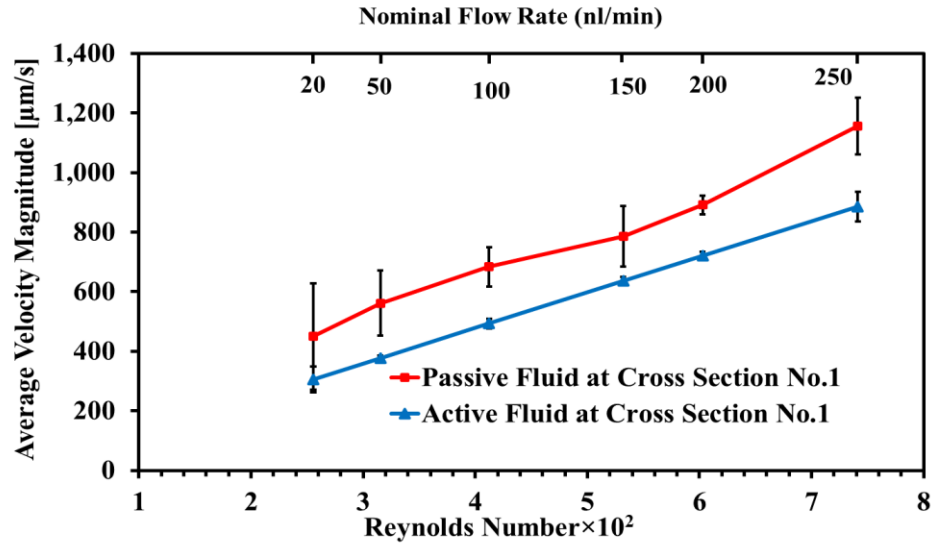
Figure 5-12: Time-averaged velocity magnitude profile of active fluid and passive fluid at different Reynolds numbers
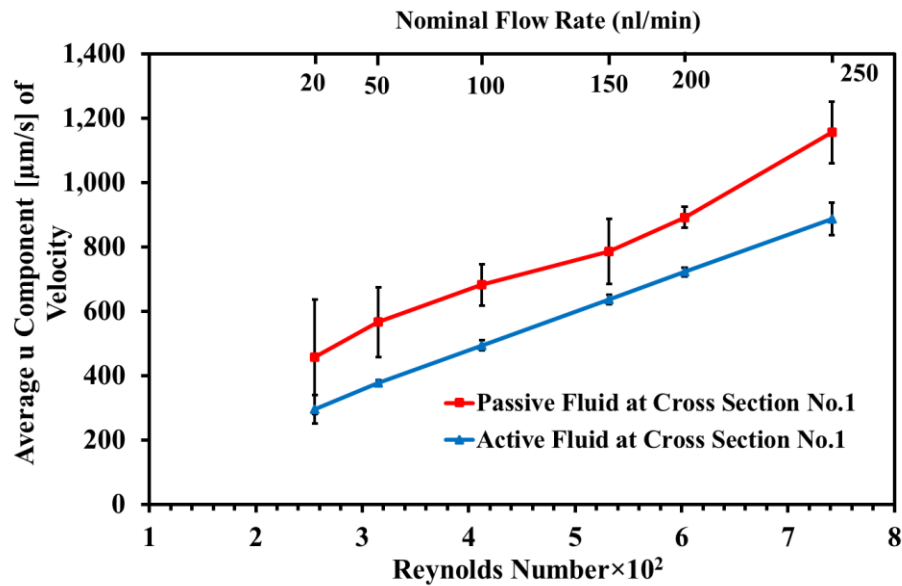

Figure 5-13: Time-averaged u components of the flow velocity profile of active fluid and passive fluid at different Reynolds numbers
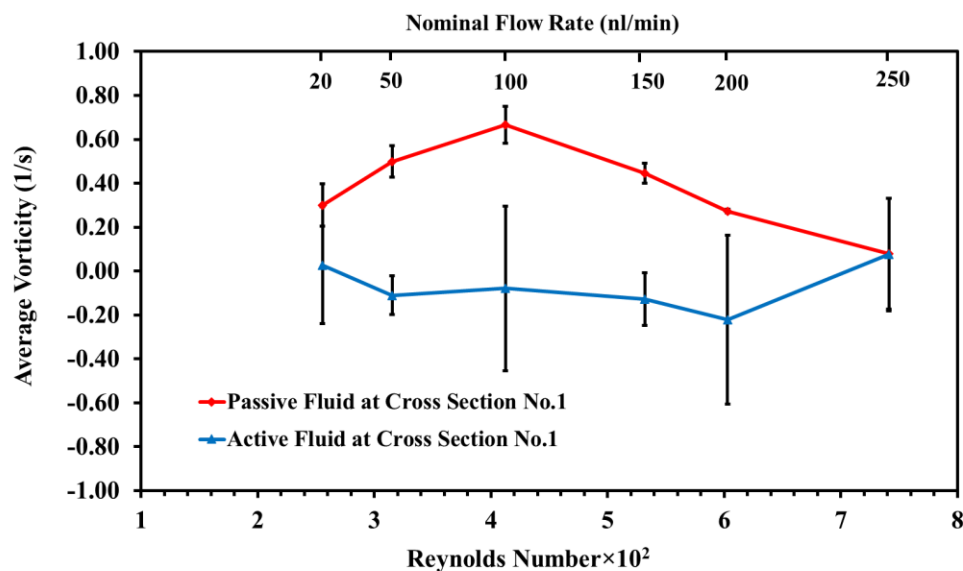
Figure 5-14: Time-averaged vorticity profile of active fluid and passive fluid at different Reynolds numbers

5.4 Concluding Remarks

Flows of suspension fluid containing live *Synechocystis* sp. bacteria (active fluid) and dead *Synechocystis* sp. bacteria (passive fluid) at different flow rates in a bifurcating microchannel were investigated experimentally. Below we summarize the following remarks gained from the current analysis:

(I)   It is identified that the inner walls (wall A for branch 2 and wall B for branch 3) of the branches could be prone to bacterial colonization, and, thus, biofilm formation. Since many biological arterial systems mimic bifurcating micro-channel, the formation of biofilm on the diseased arterial wall is therefore of utmost importance to understand which branch is prone to bacterial colonization and eventual clogging of the branch.

(II)   The active fluid (live *Synechocystis* sp bacteria) slows down the bulk flow in the channel. This could have a significant consequence if this type of bacterium is used as a micro-robot for drug delivery in the diseased arterial wall. This is the first time this phenomenon has been reported and needs further confirmation by future studies.

(III)   The analysis of the average flow velocity for active and passive fluids reveals that the average velocity for passive fluid is more than that of active fluid at the different flow rates.

(IV)   Slowing down of the bulk flow by live *Synechocystis* sp bacteria is observed for all Reynolds numbers considered in this study, and at high-enough Reynolds number live *Synechocystis* sp bacteria, we believe, undergo hibernation or long tumble periods.

Synechocystis cells exhibit a random-walk pattern, characterized by intervals of high motility known as "runs," which are intermittently broken by low motility periods called "tumbles" [18]. The certainty of this fact, that this type of movement enables them to swim against the flow, particularly under low flow rate conditions, requires further investigations at different flow rates. Hence, for future work, experiments should be focused on a range of low flow rates. Similar studies have been carried out for suspensions of *Chlamydomonas reimhardtii*, revealing a net effect of cell motility on the flow [20, 21]. However, one should bear in mind that *Chlamydomonas reimhardtii* is a highly motile flagella microorganism, this is not the case with *Synechsystis*. The low motility of *Synechsystis* makes it difficult to assess the effect of cell motility on the base (continuous phase) flow.

5.5 References

[1] Schuergers, N., Lenn, T., Kampmann, R., Meissner, M. V., Esteves, T., Temerinac-Ott, M., Korvink, J., Lowe, A., Mullineaux, C., & Wilde, A. (2016). Cyanobacteria use micro-optics to sense light direction. Elife, 5, e12620.

[2] Yuan, J. (2015). Microswimmers and microfluidics: Understanding and manipulating the locomotion of undulatory microswimmers. The University of Pennsylvania.

[3] Vourc'h, T., Léopoldès, J., & Peerhossaini, H. (2020). Light control of the diffusion coefficient of active fluids. Journal of Fluids Engineering, 142(3).

[4] Samadi, Z., Mehdizadeh Allaf, M., Saifi, R., De Groot, C. T., & Peerhossaini, H. (2022). Effects of turbulent mixing and orbitally shaking on cell growth and biomass production in active fluids. AJBSR, 15, 396-404.

[5] Samadi, Z., Mehdizadeh Allaf, M., Vourc'h, T., DeGroot, C. T., & Peerhossaini, H. (2022, August). Are Active Fluids Age-Dependent?. In Fluids Engineering Division Summer Meeting (Vol. 85833, p. V001T03A037). American Society of Mechanical Engineers.

[6] Mehdizadeh Allaf, M., & Peerhossaini, H. (2022). Cyanobacteria: Model microorganisms and beyond. Microorganisms, 10(4), 696.

[7] Vourc'h, T., Peerhossaini, H., Léopoldès, J., Méjean, A., Chauvat, F., & Cassier-Chauvat, C. (2018). Slowdown of surface diffusion during early stages of bacterial colonization. Physical Review E, 97(3), 032407.

[8] Elgeti, J., & Gompper, G. (2009). Self-propelled rods near surfaces. EPL (Europhysics Letters), 85(3), 38002.

[9] van Teeffelen, S., Zimmermann, U., & Löwen, H. (2009). Clockwise-directional circle swimmer moves counter-clockwise in Petri dish-and ring-like confinements. Soft Matter, 5(22), 4510-4519.

[10] Angelani, L., Costanzo, A., & Di Leonardo, R. (2011). Active ratchets. EPL (Europhysics Letters), 96(6), 68002.

[11] Liljenstolpe, M. (2022). Bacterial Reconcentration in Irregular Microchannels.

[12] Wensink, H. H., & Löwen, H. (2008). Aggregation of self-propelled colloidal rods near confining walls. Physical Review E, 78(3), 031409.

[13] Qi, K., Annepu, H., Gompper, G., & Winkler, R. G. (2020). Rheotaxis of spheroidal squirmers in microchannel flow: Interplay of shape, hydrodynamics, active stress, and thermal fluctuations. Physical Review Research, 2(3), 033275.

[14] Conrad, J. C., & Poling-Skutvik, R. (2018). Confined flow: consequences and implications for bacteria and biofilms. Annual review of chemical and biomolecular engineering, 9, 175-200.

[15] Du, H., Xu, W., Zhang, Z., & Han, X. (2021). Bacterial behavior in confined spaces. Frontiers in Cell and Developmental Biology, 9, 629820.

[16] Binz, M., Lee, A. P., Edwards, C., & Nicolau, D. V. (2010). Motility of bacteria in microfluidic structures. Microelectronic Engineering, 87(5-8), 810-813.

[17] Thielicke, W., & Sonntag, R. (2021). Particle Image Velocimetry for MATLAB: Accuracy and enhanced algorithms in PIVlab. Journal of Open Research Software, 9(1).

[18] Vourc'h, T., Léopoldès, J., & Peerhossaini, H. (2020). Light control of the diffusion coefficient of active fluids. Journal of Fluids Engineering, 142(3).

[19] Sheng, J., Malkiel, E., & Katz, J. (2008). Using digital holographic microscopy for simultaneous measurements of 3D near wall velocity and wall shear stress in a turbulent boundary layer. Experiments in fluids, 45, 1023-1035.

[20] Chau, H.M. ; Peerhossaini, H. ; Pashmi, E. ; Salek, M. (2020). Active control of passive and active particle distribution at the outlet of of double Y-microchannel using pulsatile flow. Journal of Fluids Engineering, 142 (1).

[21] Chau, H.M.; Peerhossaini, H. ; Jarrahi, M. (2022). Phototactic microwimmers in pulsatile flow : toward a novel harvesting method. Biomicrofluidics. 16, 054103.

[22] Lauga, E. (2016) Bacterial hydrodynamics. Ann. Rev. Fluid Mech. 48 (1), 105–135.

[23] Craig, L., Forest, K.T. and Maier, B. (2019) Type IV pili: dynamics, biophysics and functional consequences, Nature Reviews | Microbiology, 17, 429-440.

Chapter 6

6 Conclusions and Recommendations.

This chapter provides a summary of the thesis work, including the key findings of each chapter. Additionally, suggestions for potential future research are also presented.

6.1 Summary

Active fluids are fluids that contain self-propelling particles or organisms, such as bacteria, algae, and sperm cells, which can convert chemical energy into mechanical energy to drive fluid flow. Unlike passive fluids, which rely on external energy sources, active fluids have unique properties that make them an interesting subject of study. Photobioreactors are devices used to cultivate photosynthetic microorganisms, such as algae and cyanobacteria, for various applications, including biofuel production, wastewater treatment, and carbon capture. For the optimal growth of active fluid inside photobioreactors, several factors need to be taken into consideration, such as light intensity, temperature, pH, nutrient availability, and mixing conditions. The behavior of active fluid in photobioreactors is also important to understand, as it can affect the overall performance and productivity of the system.

In chapter 2, a generic numerical method for the calculation of light-scattering properties of photosynthetic microorganisms within the visible spectrum was developed to analyze the light transfer in photobioreactors. The main challenges associated with the theoretical approach are the dependency of optical properties on wavelength and the cell's biochemical composition. Also, based on previous studies, exact input data such as pigment characteristics and measured pigment content, by taking into consideration the complexity of shapes and the sizes of microorganisms, is essential for obtaining reliable theoretical models. To achieve the aims of this research, the FDTD approach was used to model the scattering properties of *Chlamydomonas reinhardtii*. Geometry was created for the homogenous cell, coated cell, and heterogeneous cell. Regarding boundary conditions, first, a PML thickness is selected equal to half of the largest wavelength in the simulations, if it does not work, PML thickness should be repeatedly doubled until the simulation is converged. The scattering field in different angular positions and scattering efficiency were calculated. The presented method provides more flexibility in terms of geometry than Mie

theory and T-matrix solutions, as it can accommodate non-homogeneous cells of arbitrary shape. The results demonstrate that accounting for non-homogeneous geometry leads to different outcomes compared to using simplified models such as homogeneous or coated spheres. However, further research is necessary to precisely determine the optical and geometric characteristics of cell organelles, including pigment absorption properties, refractive indices of each cell component, and the exact shape of the cells.

In chapter 3, the study aimed to examine the effects of two mixing techniques, namely turbulent stirring and orbitally shaking, on the growth parameters of *Synechocystis* sp. CPCC 534, in comparison to a stationary culture. For this purpose, the wild-type strain of *Synechocystis* sp. CPCC 534 was cultivated in a chemically defined liquid BG11 medium under controlled conditions in three different mixing modes. To generate turbulent mixing within the lab photobioreactors located in a fully controlled PHCbi incubator, digitally controlled magnetic stirrers from VWR Canada were employed in the turbulent stirring (TS) mode. The Orbitally shaking (OS) mode involved placing the photobioreactors within a fully controlled incubator shaker. For the Molecular Diffusion (MD) mode, the photobioreactors were maintained in stationary positions within well-controlled compartments. In all three modes, the light intensity and temperature were uniformly set at 50 ± 5 µmole.m^{-2}. s^{-1} and 20 ± 1°C, respectively. According to the findings, the growth metrics of *Synechocystis* cultures, such as growth rate, doubling per day, yield, and Chl$_a$ production, demonstrated improvement when mixing was applied, as compared to cultures without any mixing. Mixing improves microorganisms growth by preventing self-shading, breaking up boundry layers in the culture, and provide better nutrient uptake and more homogenous light and temperature distribution inside the photobioreactors. Turbulent stirring appeared to be more effective than orbitally shaking in enhancing cell growth metrics, which can be attributed to the differing fluid motion and wall shear stress distribution between the two mixing methods.

In chapter 4, the investigation focused on examining the motility of *Synechocystis* sp. CPCC 534 throughout its growth cycle. For this investigation, *Synechocystis* sp. CPCC 534 was cultured in BG11 medium, with a light cycle of 12/12 hours at a temperature of 20 ± 1 °C. An inverted video microscope, which was equipped with a 40X magnification lens

was utilized to capture the movement of *Synechocystis* sp. cells in a closed microchip during its growth period. The taken video was binarized by Fiji ImageJ software in "tif" format and then imported to MATLAB to extract all particles' x and y positions from the recorded video frame by frame. The average cell velocity was used to estimate the cell motility after eliminating non-motile cells or debris in the calculations. Subsequently, the dynamics of *Synechocystis* sp. CPCC 534 was evaluated by calculating the mean squared displacement (MSD), diffusion coefficient, and displacement probability density function (PDF). The study found a direct relationship between cell motility and the growth phase of *Synechocystis* sp. CPCC 534: the motility increased during the exponential linear growth phases and decreased during the stationary phase until reaching a constant value asymptotically. The mean squared distance traveled by cells during different stages of growth followed a pattern similar to the variation in cell motility over time. The instantaneous diffusion coefficient of *Synechocystis* sp. CPCC 534 decreased over time during all growth stages and ultimately reached a constant value asymptotically. In addition, the long-term diffusion coefficient is also linked to the growth state of the cells and demonstrates the same temporal pattern as the mean squared displacement (MSD). Cell displacement's probability density function (PDF) supported the strong link between cell motility and growth state. At the start of the exponential phase, the PDFs exhibited an exponential pattern, indicating non-diffusive cell behavior. As time progressed, the tail of each displacement distribution widened, indicating the diffusive nature of *Synechocystis* cells, and approached a Gaussian distribution at longer times. Results revealed that the average velocity, mean square displacement, long-term diffusion coefficient, and PDF are also directly correlated with the growth period of the cells. All mentioned parameters increased during exponential phases and decreased from the middle of the stationary phase and this issue might be due to self-shading or nutrient depletion, which caused this reduction in cells' activities. These findings have practical applications in forecasting biofilm formation on photobioreactor surfaces.

In chapter 5, to explore different infinitesimal flow characteristics of the active fluid, a microchannel with a rectangular cross-section that bifurcates was designed and fabricated using Polydimethylsiloxane (PDMS). The initial step towards achieving this objective involved designing the master using AutoCAD software, which was subsequently

fabricated at Western Nano-fab and then the PDMS was prepared using the SYLGARD184 Silicone Elastomer Kit. The flow of *Synechocystis* sp. suspension was injected into the sterilized PDMS microfluidic device using a micropump. The movement of the cells was subsequently recorded with a CCD camera and a 20X magnification lens-equipped inverted microscope at a rate of 50 frames per second for a duration of 10 seconds. MATLAB ParticleVlab (Particle Image Velocimetry (PIV)) was utilized to analyze the videos of both active and passive fluids at different flow rates that were acquired. The findings indicate that when comparing the average flow velocities of active and passive fluids at different flow rates, it becomes apparent that the passive fluid demonstrates a higher average velocity than the active fluid. This difference can be attributed to the limited motion of active fluids resulting from their run and tumble motion. However, both fluids still exhibit similar trends in their velocity quantities, which escalate in magnitude as the Reynolds number increases.

6.2 Recommendations for Future Work
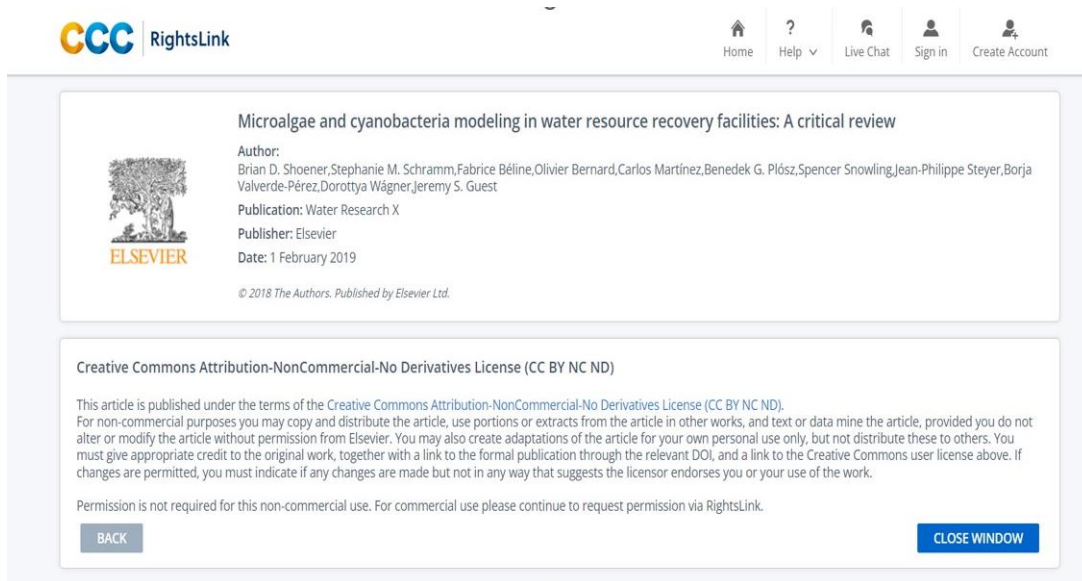
Future work concerns the analysis of optical properties of microorganisms: Scattering efficiency and absorption efficiency. The following ideas could guide the future work in this subject:

- The simulation of absorption efficiency for three different geometries: the homogeneous microorganism cell, coated microorganism cell, and the heterogeneous microorganism cell.

- The validation of the computational results obtained from the FDTD method by experimental results. Further inquiry is necessary to precisely establish the optical and geometric parameters of cell organelles, such as the pigment absorption characteristics, refractive indices of individual cell components, and cell shape.

- Additional research needs to be conducted to determine the optimal stirring rate that enhances growth rate, yield, doubling per day, and Chl_a, for both turbulent stirring and orbital shaking mixing modes.

- Further investigation would be necessary on the influence of light on the cell motility of *Synechocystis* during the growth period.

- Future experiments will be needed to be carried out on cell aggregation in a microfluidic devices under laminar flow conditions. The study will also include an assessment of diffusion and cell-cell interaction in the population of *Synechocystis* cells, with a focus on statistical analysis of the random walk.

Figures License and Permission

Permission for Figure 1-1

Permission for Figure 1-2

Curriculum Vitae

Name: Zahra Samadi

Post-secondary Education and Degrees:
Bachelor of Science, Shahid Bahonar University of Kerman
Kerman, Iran
2005-2009

Master of Science, Isfahan University of Technology (IUT
Isfahan, Iran
2009-2011

Doctor of Philosophy, The University of Western Ontario
London, Ontario, Canada
2019-2023

Honours and Awards:
Madiha Salman Memorial Scholarship in Civil and Environmental
Engineering, Western University
2023

Academic Joint Fund for Support of Graduate Student Research
Doctoral Fellowship
2023

Related Work Experience
Teaching Assistant
The University of Western Ontario
2020-2023

Publications:

[1] Samadi, Z., Mehdizadeh Allaf, M., Vourc'h, T., DeGroot, C. T., & Peerhossaini, H. (2023). Investigation of Synechocystis sp. CPCC 534 Motility during Different Stages of the Growth Period in Active Fluids. Processes, 11(5), 1492. https://doi.org/10.3390/pr11051492

[2] Samadi, Z., Mehdizadeh Allaf, M., Vourc'h, T., DeGroot, C. T., & Peerhossaini, H. (2022, August). Are Active Fluids Age-Dependent? In Fluids Engineering Division Summer Meeting (Vol. 85833, p. V001T03A037). American Society of Mechanical Engineers. DOI:10.32393/csme.2020.14

[3]   Samadi, Z., Mehdizadeh-Allaf, M., Saifi, R., De Groot, C. T., & Peerhossaini, H. (2022). Effects Of Turbulent Mixing Versus Orbitally Shaking on Cell Growth In Active Fluids. Canadian Society for Mechanical Engineering International Congress 2022, https://doi.org/10.7939/r3-9j8n-s472

[4]   Samadi, Z., Mehdizadeh Allaf, M., Saifi, R., De Groot, C. T., & Peerhossaini, H. (2022). Effects of turbulent mixing and orbitally shaking on cell growth and biomass production in active fluids. American Journal of Biomedical Science & Research, 15, 396-404. DOI: 10.34297/AJBSR.2022.15.002129

[5]   Samadi, Z., Johlin, E., DeGroot, C., & Peerhossaini, H. (2021, August). Modelling optical properties of algae using the finite-difference time domain method. In Fluids Engineering Division Summer Meeting (Vol. 85307, p. V003T05A016). American Society of Mechanical Engineers. https://doi.org/10.1115/FEDSM2021-66314

[6]   Mehdizadeh Allaf, M., Habibi, Z., Samadi, Z., DeGroot, C. T., Rehmann, L., de Bruyn, J. R., & Peerhossaini, H. (2020, July). Physical and Rheological Properties of Active Fluids Under Shear Stress: Suspensions of *Synechocystis*. In Fluids Engineering Division Summer Meeting (Vol. 83723, p. V002T03A026). American Society of Mechanical Engineers. https://doi.org/10.1115/FEDSM2020-20104

[7]   Samadi, Z., Haghshenasfard, M., & Moheb, A. (2014). CO_2 absorption using nanofluids in a wetted-wall column with external magnetic field. Chemical Engineering & Technology, 37(3), 462-470 . https://doi.org/10.1002/ceat.201300339